The Effect of Operating Conditions on Gas Holdup and Mixing in Tower Fermenters

by

Jalaleddin Shayegan Salek

being a thesis submitted in support of an application for the Degree of Doctor of Philosophy in the Department of Chemical Engineering, University of Aston in Birmingham.

June 1974

SUMMARY

The design and operation of bubble columns is a subject which has recently received a great deal of attention, since applications of such equipment are increasing. Recent work has shown that there is a real possibility of utilizing bubble columns in aerobic systems used for fermentations.

At present there is a considerable body of knowledge about the various parameters affecting design and operation of bubble columns. Unfortunately much of the research work carried out has been concerned with small diameter columns and operating conditions not applicable to those suitable for fermentation purposes. The discrepancies in the data published by different researchers also suggest the need for further investigations.

The object of this research was to attempt to coordinate previous knowledge about flow patterns in bubble columns with fresh data obtained in a wider range of column geometries and using operating conditions applicable to fermentation processes.

Gas holdup was investigated thoroughly under different operating conditions in air-water systems. A number of fermentation media were also used as the liquid phase. It was found that apart from superficial gas velocity which is the governing factor in air-water systems, other liquid phase properties have a marked effect on gas holdup within the range of operating conditions used. Indeed it was noticed that these effects could, in some cases, dominate the effects of other operating parameters.

Mixing studies in the liquid phase have also been carried out. A steady-state tracer injection method was used and concentration profiles were measured over the length of the columns. Although the axially dispersed plug-flow model was used to calculate the dispersion coefficients, attempts have been made to look for better models. It is suggested that

a series of stirred tanks with back-mixed flow provides an appropriate alternative. Variation of dispersion coefficients with superficial gas velocity showed a similar trend to that of gas holdup in the case of air-water systems.

It is concluded that the research has opened up a new approach to the behaviour of such systems with the possibility of accounting for mixing effects in the axial as well as the radial direction.

List of Contents

List of Figures

List of Tables

Acknowledgments

The author wishes to express his thanks to:

1. The University of Aston in Birmingham for financial assistance in the form of a Research Studentship.
2. Professor G V Jeffreys and all the Staff of the Chemical Engineering Department for their assistance.
3. Dr E L Smith for his guidance and friendly supervision throughout the project.
4. Mr M Fidgett for his discussion and help on mathematical modelling of bubble columns.
5. Mr M.R Shayegan for his assistance in presenting the diagrams.
6. Staff in Communication Media for photographic assistance.
7. Dr R N Greenshields, Dr G N Morris, Dr A James, Mr A Dowen, Mr S Coote, Mr S Pannell, Mr R Spensley and Mr R Cocker, Members of the group for their discussions.
8. Mrs Deeley for typing the thesis.

1. Introduction

Work on tower fermentation systems and their applications originated as a joint project between the Departments of Chemical Engineering (Dr. E.L.Smith) and Biological Sciences (Dr. R.N. Greenshields) of the University of Aston in Birmingham and the Czechoslovack Academy of Sciences, Institute of Microbiology (Dr. Z. Sterbacek). The microbiologists and biochemists in the group are mostly concerned with the applications of tower fermenters, in particular beer and alcohol fermentations, and biomass - and metabolite - production using moulds and bacteria. The engineering aspects of the research, that is to say design, scale-up and operation of tower fermenters for both aerobic and anaerobic processes, have been carried out mainly in the author's Department. The link between the biologists and the engineers has been sustained through regular meetings of the group.

The overall engineering research programme has been divided into the following sub-projects:

1. Properties of suspensions of micro-organisms;
2. Behaviour of single bubbles in suspensions of micro-organisms;
3. Behaviour of bubble swarms in tower fermenters;
4. Properties of microbial aggregates and their behaviour in tower fermenters;
5. Mass- and heat-transfer studies in gas-liquid-solid systems in towers, and
6. Development of mathematical models to aid in the design, scale-up and operation of tower.

The author's research was concerned with meeting some of the

objectives of sub-project 3. It should be noted that preliminary studies in this area were undertaken by Downie [7].

At the outset, it was intended that initial studies with air-water systems would be followed by research with aerated microbial suspensions. After completing a series of gas holdup measurements over a range of air and water flow-rates, it became clear that the behaviour of the apparently simple air-water system was not easy to understand, particularly at high temperatures. In addition, an extensive literature survey (see Section 2.1) indicated that there was a lack of consistent information about the effects of temperature, dissolved salts and microbial suspensions on gas holdup. Indeed, although a substantial number of papers have been published in this field during the course of the work, it is clear that our understanding of the behaviour of bubble columns is still imprecise.

In the first part of the work (see Section 2) sufficient data were collected to evaluate the effects of column geometry, distributor design, gas and liquid flow-rates and liquid phase properties on gas holdup in tower fermenters. This information has since been of considerable value in designing and operating towers for specific fermentations.

Mixing studies, originally planned to be the main area of activity, occupied the second stage of the programme (see Section 3). To begin with the unsteady-state tracer technique used by Downie was studied critically, and qualitative results, based on visual observations, were obtained using various tracer techniques. It was found that the unsteady-state tracer method could lead to both experimental and computational errors. Consequently, Downie's results were re-examined in an attempt to reduce some of the

computational error. At the same time mixing studies were made by introducing a steady flow of tracer into the top of the columns. Both the axial and radial concentration profiles of tracer were obtained over the range of air and water flow-rates of interest.

The final stage of the work was mainly devoted to an analysis of all the experimental data with the object of obtaining a better understanding of bubble column behaviour. Published work with other multi-phase systems, in particular liquid-liquid and gas-solid systems was also reviewed (see Section 3.1.)

Although the axially dispersed plug flow model was used to obtain the dispersion coefficients, there is still doubt about its validity. Attempts were made to develop a more suitable model to account for the mixing phenomena, but point measurements of gas hold-up and velocity are probably required before real progress can be made.

2. Gas Holdup Studies

2.1. Literature Survey

2.1.1. Introduction

Gas holdup in a bubble column characterises the retention of the bubbles within the liquid. It is an important parameter because it is used with other data, for calculating mixing coefficients, mass transfer coefficients and chemical reaction rates.

Gas hold up, ϵ, can be defined simply as

$$\epsilon = (\text{total volume}) - (\text{liquid volume at rest})/(\text{total volume})$$

$$= (V_{TOT} - V_L)/V_{TOT} \qquad (2.1)$$

ϵ can be identified as gas holdup or fractional gas holdup or average gas holdup, while the point or local volumetric gas fraction (void fraction) may be defined as the probability that gas will exist at a particular point in the flow field at a particular time. For a system with steady time-averaged properties this probability can be evaluated by averaging measurements at any point over a suitable time interval. If, in addition, the flow field is homogeneous,implying that the time-averaged properties are space-independent, one can replace the time average by a space average over some suitable volume.

2.1.2. Gas Holdup Measurement Techniques

Average gas holdup has been measured by a number of investigators using different techniques. The most common and simple way, which has been widely used[1-4] is to introduce quick-acting valves on the gas and liquid feed. A quick shutoff, either manually or automatically, can then be used to trap the flowing gas-liquid mixtures. After the mixture has been allowed

to separate, the average gas holdup can be determined by noting the volume of both phases. Fig.2-1 illustrates the different stages of separation of the two phases.

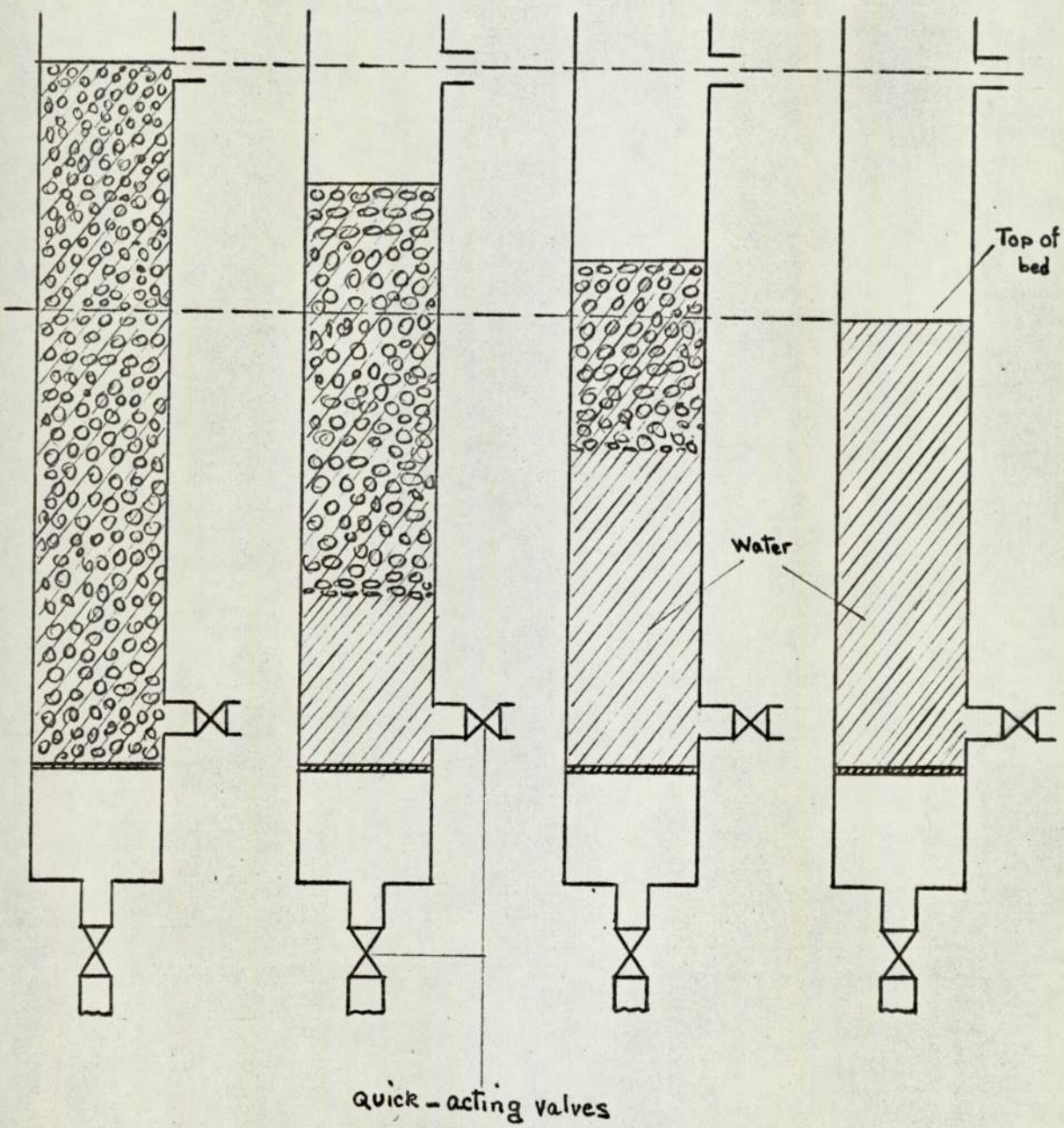

Fig 2-1 Stages in the Collapse of a Bed of Bubbles

Average gas holdup can also be determined by measuring the pressure at one or several points in the column. Reith et alia[5], Towell et alia[6] and Downie[7] used this method to evaluate both the average gas holdup over the whole column and the axial distribution of holdup. By assuming that the upward movement of the bubbles is due only to buoyancy, Reith et alia[5] showed that the following relationship exists between the fluid level in the manometer tubes, h, the position of the measuring points, x and the local gas fraction ε at x:

$$\varepsilon = \frac{dh}{dx} \qquad (2.2)$$

The local gas fraction at x is, therefore equal to the slope of the measured h - x plot.

Another way to measure the average gas holdup is to use radial attenuation methods[8]. Such measurements are based on the fact that one phase absorbs more radiation than the other. By measuring the amount of attenuation from a suitable source, the relative amounts of each phase can be determined.

Neal and Bankoff[9] used a high resolution resistivity probe for determination of local void properties in gas-liquid flow. Their measurements were based on the fact that the liquid phase is a better conductor of electricity than the gas.

2.1.3. Methods for Gas Holdup Correlation

The Lockhart-Martinelli Correlation and Modifications

One of the earliest holdup correlations is the well known Lockhart-Martinelli[10] correlation. This is based on certain limiting assumptions, although the resulting correlations have been applied to all regions of two-phase flow, both by the originators

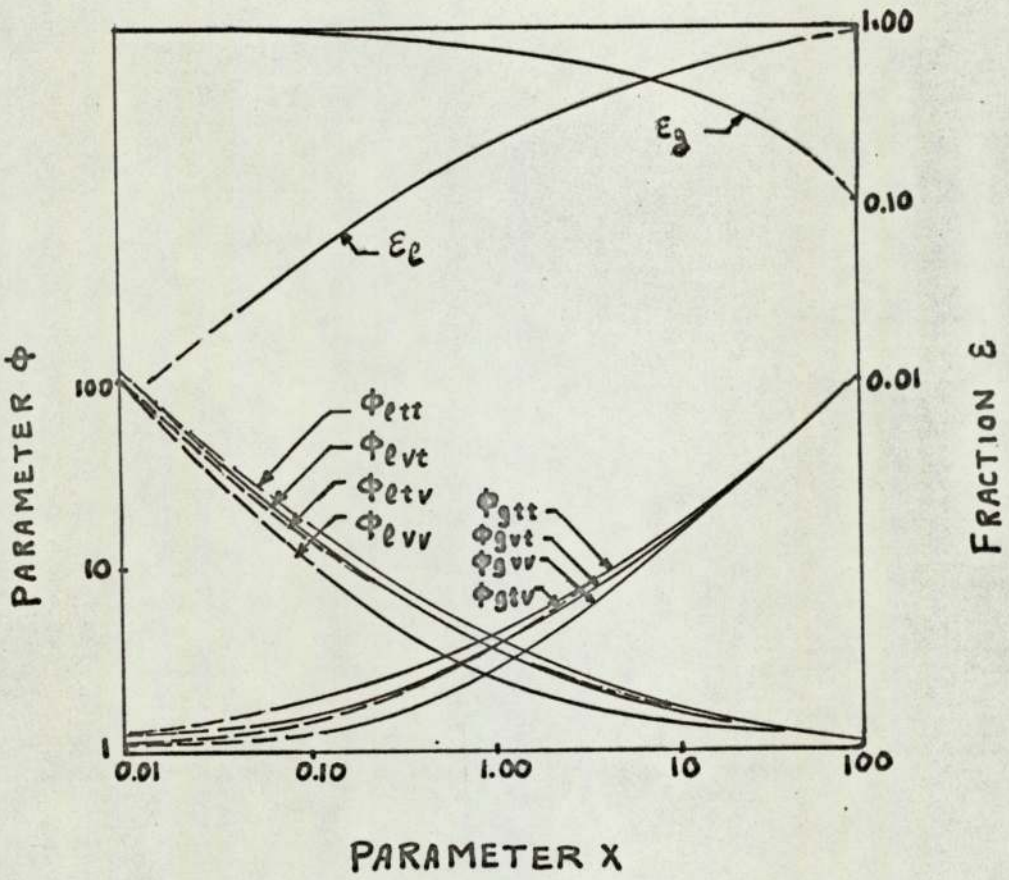

Fig 2.2. Pressure Drop Correlation of Lockhart and Martinelli for Frictional Pressure Losses in Horizontal cocurrent Flow.

and by many other investigators. The correlation is presented as a plot of an empirical function, ϕ , against a parameter, X , with one curve representing each of the four flow regimes (turbulent-turbulent, viscous-turbulent, turbulent-viscous and viscous-viscous flow). The correlating quantities are defined as

$$\phi_g^2 = \frac{(\Delta P/\Delta z)_{TP}}{(\Delta P/\Delta z)_g} \quad \text{or} \quad \phi_l^2 = \frac{(\Delta P/\Delta z)_{TP}}{(\Delta P/\Delta z)_l} \tag{2.3}$$

and

$$X^2 = \frac{(\Delta P/\Delta z)_l}{(\Delta P/\Delta z)_g} \tag{2.4}$$

In the above expressions the quantities $(\Delta P/\Delta z)_l$ or $(\Delta P/\Delta z)_g$ are calculated from conventional single phase correlations on the basis that the liquid or gas is flowing in the pipe alone. Lockhart and Martinelli have given the appropriate expressions for x^2 and the relationships among ϕ_g , ϕ_l , ε_g and ε_l for the various flow regimes. The relationships are shown graphically in Fig.2.2.

The Lockhart-Martinelli correlation has been modified by several investigators. Chisholm and Laird [11] accounted for tube roughness in the turbulent-turbulent regime using the basic equation:

$$\phi^2 = 1 + \frac{21}{X} + \frac{1}{X^2} \tag{2.5}$$

Hughmark and Pressburg[2] statistically analysed their own and other data for vertical flow. They found that when the Lockhart-Martinelli parameter, x, was estimated from the empirical equation:

$$X = (G_g / G_\ell)^{0.9} (\mu_\ell^{0.19} \gamma^{0.205} \rho_g^{0.7}) / (G_g^{0.435} \rho_\ell^{0.72}) \quad (2.6)$$

gas holdup could be predicted with an average deviation of ±0.083 for air and a variety of liquids in columns of diameters from 1.0 to 5.9 cm.

Scott[12], in his review, mentions a modification due to Davis involving the introduction of the Froude Number into the Lockhart-Martinelli parameter, x: this provides a description of gravitational and inertial forces so that the model can be applied to vertical flow. The revised parameter, x, is defined empirically for turbulent-turbulent flow as:

$$X = 0.19 \left(\frac{G_\ell}{G_g}\right)^{0.9} \left(\frac{\rho_g}{\rho_\ell}\right)^{0.5} \left(\frac{\mu_\ell}{\mu_g}\right)^{0.1} \left(\frac{u}{d_c g}\right)^{0.185} \quad (2.7)$$

Hughmark & Pressburg[2] have correlated data for vertical two-phase flow with the slip velocity, u_s, in a plot of $(\Delta P_{TP} - \Delta P_\ell)/\Delta z$ against v_s, obtaining a family of curves having as a parameter

$$\Psi = 1/\mu_\ell^{0.147} \gamma^{0.194} (G_\ell + G_g)^{0.07} \quad (2.8)$$

The quantity Ψ was determined by a statistical correlation of numerous data obtained by these workers as well as others.

The Bankoff Model and Modifications

Bankoff[13] proposed a model for horizontal bubbly-flow in which power law distributions are assumed for the gas holdup and liquid velocity-profile. Effects of buoyancy are neglected and the gas velocity at any radial point is assumed to be equal to the liquid velocity at that point. The result for the average slip ratio, η,

is

$$\eta = \frac{\text{average } u_{sg}}{\text{average } u_{s\ell}} = \frac{1-\varepsilon}{K-\varepsilon} \tag{2.9}$$

where K is a flow parameter found by Bankoff to range from 0.6 to 1.0. This equation can be solved for the average gas holdup to give

$$\varepsilon = \frac{K Q_g}{Q_g + Q_\ell} \tag{2.10}$$

A modification of this model to allow its use in upward flow is described by Bankoff and Nassos[14]. The assumptions are the same as in the model for horizontal flow, except that the average gas velocity in upward flow is assumed to be equal to the same function of the average liquid velocity as in horizontal flow plus a contribution due to buoyancy. From this, the slip ratio becomes:

$$\eta = \frac{1-\varepsilon}{K-\varepsilon}\left\{1 + K_1\left[\frac{\rho_\ell - \rho_g}{\rho_\ell u_{s\ell}^2}\cdot g d_c\right]^{1/2}\right\} \tag{2.11}$$

It is interesting to compare the results obtained by Bankoff with the analysis of slug flow given by Nicklin et alia[15]. They derived the following expression for the velocity of the bubbles:

$$u_{bs} = 1.2\left(\frac{Q_g + Q_\ell}{A_c}\right) = \frac{Q_g}{\varepsilon A_c} \tag{2.12}$$

or

$$\varepsilon = \frac{0.83 Q_g}{Q_g + Q_\ell} \tag{2.13}$$

a result practically identical to that of Bankoff.

Hughmark[16] has extended this approach to obtain an empirical correlation covering wide ranges of data for air-water systems in vertical flow. Esentially the correlation involves using Eq.(2.10) with a variable value of the coefficient K. This coefficient was expressed by Hughmark as a function of the mixture Reynolds Number, Froude Number and liquid volume-fraction:

$$K = f\,\frac{(N_{Re})^{1/6}\,(N_{Fr})^{1/8}}{(1-\varepsilon)^{1/4}} \qquad (2.14)$$

Brown et alia[17] have developed another model for predicting average gas holdup using Bankoff's flow parameter. The model accounts for the radial distributions of void fraction and liquid velocity.

In the case of bubbly flow:

$$\varepsilon = \frac{Q_g}{\left(Q_g + Q_\ell \frac{1-\varepsilon}{K-\varepsilon} \pm u_{bs}(1-\varepsilon)A_c\right)} \qquad 0.75<K<1.0 \quad (2.15)$$

and for slug flow:

$$\varepsilon = \frac{Q_g}{\left(Q_g + Q_\ell \frac{1-\varepsilon}{K-K_2\varepsilon} \pm u_{bs}(1-\varepsilon)A_c\right)} \qquad 0.5<K<1.0 \quad (2.16)$$

These equations give the average gas holdup in terms of the gas-flow rate, the liquid flow-rate and the bubble rise velocity. The model accounts for the effect of buoyancy in vertical flow and can be used to predict gas holdup in upward and downward vertical flow

situations. For horizontal flow with a zero slip velocity the model reduces to the Bankoff model.

Relationships with Superficial Gas Velocity and Bubble Rise Velocity

A number of workers have correlated gas holdup with bubble rise velocity and superficial gas velocity and obtained relatively simple equations.

Fair[18], in his review, has proposed the following equation for bubbly flow:

$$\varepsilon = \frac{\alpha}{u_{bs} + u_{s\ell}/(1-\varepsilon)} u_{sg} \qquad (2.17)$$

The factor α accounts for departure from true, unhindered or unaided vertical rise of bubbles and can for very small columns (<7.5 cm) be influenced by wall effects. Fair calculated the numerical value of α for different systems. For open vessels with diameters less than 7.5 cm the value is 2.5 and with diameters greater than 30.5 cm the value is 0.7. Equation (2.17) gives reasonable results for low values of superficial gas and liquid velocities: with no net liquid flow it reduces to:

$$u_{sg} = \frac{1}{\alpha} \varepsilon . u_{bs} \qquad (2.18)$$

Turner[19] suggested a similar equation but without factor α. His equation can be written as:

$$u_{sg} = \frac{1}{1-\varepsilon} \varepsilon u_{bs} \qquad (2.19)$$

This assumes that the slip velocity is independent of ε.

Lehrer's correlation (20):

$$\varepsilon = \frac{u_{sg}/u_{bs}}{1 + u_{sg}/u_{bs}} \qquad (2.20)$$

can be rearranged to give the same equation as that of Turner. Lehrer suggested that Mendelson's equation be used to predict the rise velocity of single bubbles.

Freedman and Davidson[21] combined the Marrucci equation, in which the dissipation of energy between the bubbles is considered, with Turner's approach and obtained:

$$u_{sg} = \frac{1}{1-\varepsilon^{5/3}} \varepsilon u_{bs} \qquad (2.21)$$

Towell et alia[6] in their analysis of bubble flow for large bubble columns obtained another expression but similar in nature:

$$u_{sg} = \frac{1}{(1-\varepsilon)(1-2\varepsilon)} \varepsilon u_{bs} \qquad (2.22)$$

This applies when $u_{s\ell} / u_{sg}$ is small (as is often the case in bubble-column reactors).

Wallis[3], and Gomezplata & Nichols[22] have also predicted gas holdup for air-water systems in small diameter towers in a similar fashion, though they used constants instead of u_{bs}. Wallis' correlation with zero liquid flow rate is:

$$u_{sg} = \frac{1}{1-\varepsilon} \varepsilon . 19.2 \qquad (2.23)$$

This gives reasonable results for values of gas holdup up to about 0.2. The correlation of Gomezplata and Nichols takes into account the effect of liquid flow-rate on gas holdup.

$$u_{sg} = \frac{1}{1-\varepsilon} \varepsilon (\beta + u_{s\ell}) \qquad (2.24)$$

β is the characteristic velocity parameter, which is 60 cm/s for upward flow and -60 cm/s for downward flow. The equation is like that of Fair (see equation (2.17)).

Mashelkar[23] in his review on bubble columns presented another correlation for air-water which again is very similar to others given above:

$$U_{sg} = \frac{1}{1-2\varepsilon} \cdot \varepsilon \cdot 30 \qquad (2.25)$$

He also made reference to a paper by Hughmark[24] covering a very wide range of column dimensions, flow conditions and system properties. Hughmark showed that the term $U_{sg} / (\frac{1}{\rho_\ell} \times \frac{72}{\gamma})^{1/3}$ can be used to correlate the published data and plotted a curve by means of which the gas holdup in an operating bubble column may be computed. Mashelkar[23] combined his equation with Hughmark's and suggested the following correlation for typical solvents:

$$\varepsilon = \frac{U_{sg}}{30 + 2\,U_{sg}} \left(\frac{1}{\rho_\ell} \times \frac{72}{\gamma}\right)^{1/3} \qquad (2.26)$$

Although taking into account variations in density and surface tension, this equation neglects viscosity, an important variable.

A Generalised Approach

Bhaga & Weber[25] in their recent survey considered holdup in vertical two- and three-phase flow. In the case of gas-liquid flow they derived the following equation:

$$\frac{\langle U_{sg} \rangle}{\langle \varepsilon \rangle \langle 1-\varepsilon \rangle^{n+1}} = C_2 \frac{\langle U_{sg} + U_{s\ell} \rangle}{\langle 1-\varepsilon \rangle^{n+1}} + K_2' U_\infty \qquad (2.27)$$

where C_2 = distribution parameter = $\dfrac{\langle \varepsilon (U_{sg} + U_{s\ell}) \rangle}{\langle \varepsilon \rangle \langle U_{sg} + U_{s\ell} \rangle}$

K_2 = terminal velocity coefficient = $\dfrac{\langle \varepsilon (1-\varepsilon)^{n+1} \rangle}{\langle \varepsilon \rangle \langle 1-\varepsilon \rangle^{n+1}}$

$\langle \quad \rangle$ = average value

n = exponent which depends on the bubble size and flow regime and can be determined experimentally.

The equation of Bhaga and Weber is in generalised form and can be reduced to those of previous investigations by either neglecting the effect of non-uniform flow and concentration profiles or assuming different values for n or both. Their experimental results are in good agreement with the model presented.

Dimensional Analysis

Kim at alia[4] in a recent paper have summarised their work on two- and three-phase fluidized beds for a relatively large two-dimensional column. They have correlated their data for liquid-gas systems by a trial and error least squares analysis and give:

$$\varepsilon = 1.02\left[(N_{Fr})_\ell \rho_g/\rho_\ell\right]^{-0.009}\left[(N_{Fr})_g \rho_\ell/\rho_g\right]^{0.036}\left[(N_{Re})_g (N_{Re})_\ell\right]^{-0.015} \qquad (2.28)$$

with standard error of estimate = 0.013

This is valid for air-water systems, $u_{sg} < 26$ cm/s and $1.5 < u_{s\ell} < 10$ cm/s.

Akita and Yoshida[26] considered all the conceivable factors which can affect the gas holdup (such as column diameter d_c, the diameter of gas inlet orifice d_o, superficial gas velocity u_{sg}, kinematic viscosity ν_ℓ and density of liquid ρ_ℓ, surface tension, and gravity g) and derived the following correlation by dimensional analysis:

$$\frac{\varepsilon}{(1-\varepsilon)^4} = 0.2\,(N_{Bo})^{1/8}\,(N_{Ga})^{1/12}\,(N_{Fr})^{1.0} \qquad (2.29)$$

where

N_{Bo} = Bond Number = $g D^3 \rho_\ell / \gamma$

N_{Ga} = Galileo Number = $g D^3 / \nu_\ell^2$

N_{Fr} = Froude Number = $u_{sg} / \sqrt{gD}$

or in simplified form:

$$\frac{\varepsilon}{(1-\varepsilon)^4} = 1.2\, g^{-7/24}\, \mu_\ell^{-1/6}\, (\gamma/\rho_\ell)^{-1/8}\, u_{sg} \qquad (2.30)$$

For air-water systems this becomes:

$$u_{sg} = \frac{17}{(1-\varepsilon)^4}\,\varepsilon \qquad (2.31)$$

2.1.4. Parameters affecting the Gas Holdup

The effects of different parameters on gas holdup have been studied by most workers. However, some of these parameters such as liquid physical properties or column geometry have received less attention. In this section the effects of gas flow-rate, liquid flow rate, column geometry, gas distribution design and liquid physical properties have been surveyed.

2.1.4.1. Effect of Gas Flow-rate

The effect of gas flow-rate on holdup is illustrated by Fig.2.3. and Fig.2.4. In Fig.2.3. although the data are for columns about 5 cm in diameter and air and water as the gas and liquid phases, the fractional gas holdups recorded by different workers are seen to vary greatly. Fig.2.4. shows gas holdups for larger columns (30.5 cm - 61 cm): the differences are again striking.

2.1.4.2. Effect of Liquid Flow-rate

Akita & Yoshida[26] recently examined the effect of liquid rate on gas holdup. They found that for sodium sulphite-air systems in a column 15.2 cm in diameter the effect is negligible for superficial liquid velocities up to 4.5 cm/s whether flow is counter-current or cocurrent. In the same range of superficial liquid velocities, Argo & Cova[28], Bischoff & Phillips[30], Kato & Nishiwaki[33], and Reith et alia[5] found that there is no marked effect of liquid flow rate on gas holdup.

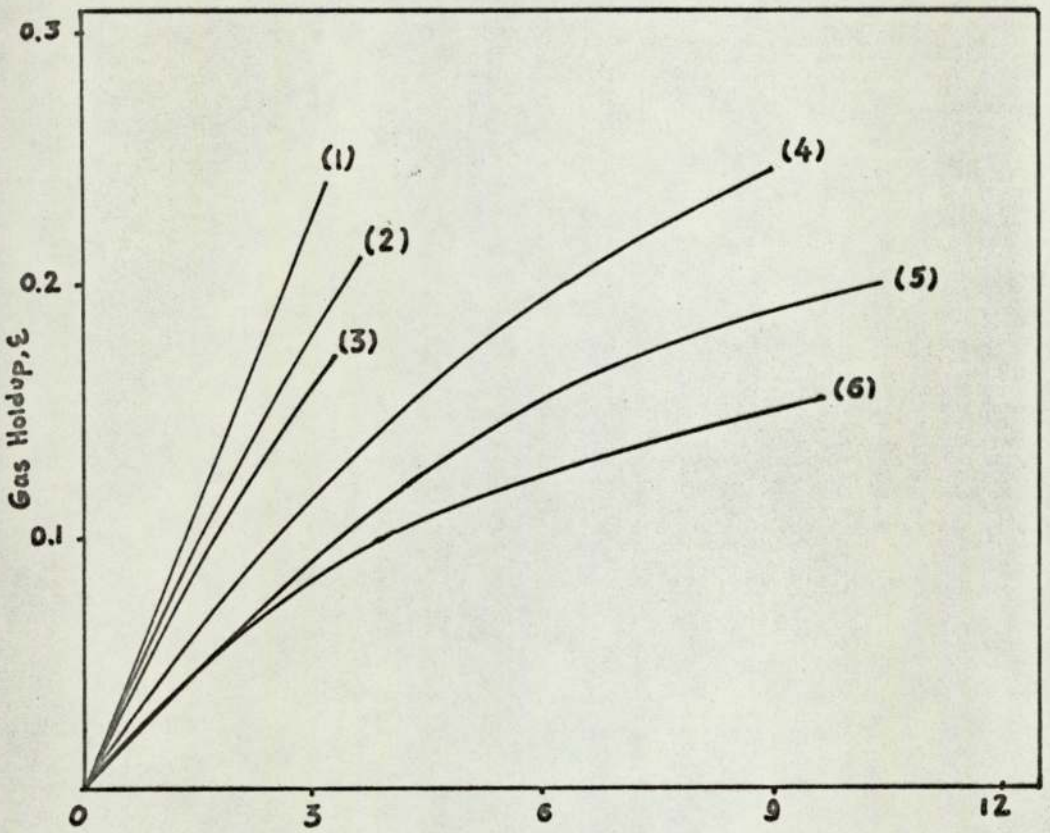

Curve no.	Name	Ref no.	Column dia. (mm)
1	Fair et alia	29	50.8
2	Bischoff and Phillips	30	50
3	Bhaga and Weber	25	38
4	Argo and Cova	28	50
5	Reith et alia	5	50.8
6	Kunugita et alia	27	50

Fig 2.3. Dependence of Average Gas Holdup on Superficial Gas Velocity for Small Bubble Columns.

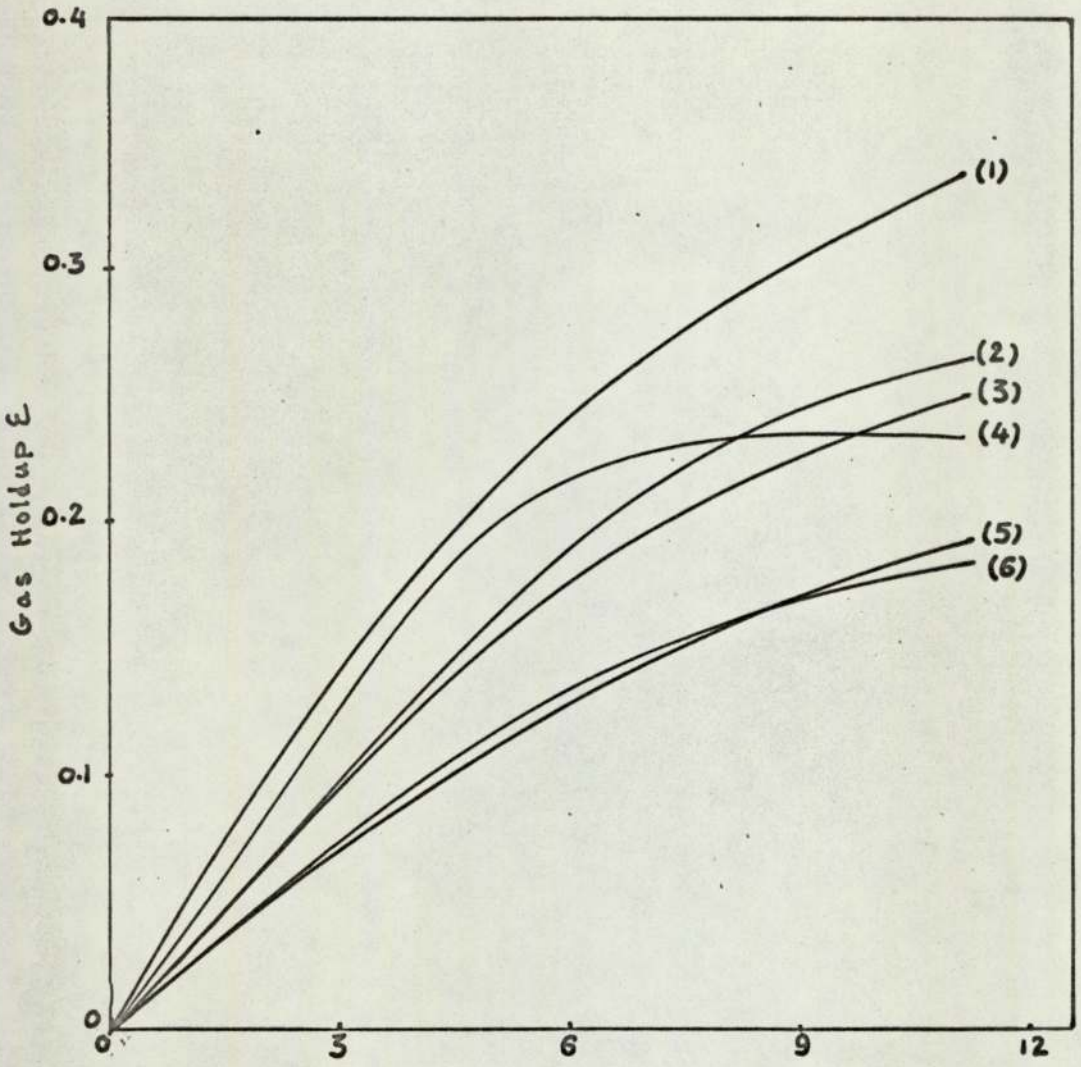

Curve no.	Name	Ref no.	Column Dia. (cm)
(1)	Argo and Cova	28	44.8
(2)	Fair et alia	29	45.7
(3)	Towell et alia	6	40.7
(4)	Freedman and Davidson	21	61.0
(5)	Yoshida and Akita	31	30.5
(6)	Ellis and Jones	32	30.5

Fig 2.4. Dependance of Average Gas Holdup on Superficial gas velocity for Large Bubble columns.

However, Kim et alia[4] found that the mean bubble size and rising velocity decreased with increasing liquid flow-rate and therefore gas holdup increased.

Østergaard & Michelson[34] reported a slight decrease in ε with increasing superficial liquid velocity.

2.1.4.3. Effect of Column Height

Yoshida & Akita[31] found that column height does not have a marked effect on gas holdup. However, they suggested for heights less than 100 cm end-effects might have an important influence on results.

Fair et alia[29] concluded that, although local values of ε can vary somewhat with height, the dependence of average gas holdup on height is not marked. This was confirmed by Bhaga & Weber[25].

Fig.2.5 shows the data of Towell et alia[6] on the effect of column height on gas holdup. Nevertheless their conclusion was that the air-rate is the only pertinent parameter as far as holdup is concerned in large bubble columns.

2.1.4.4. Effect of Column Diameter

In general most workers have found that as the column diameter is decreased the gas holdup for a given gas flow-rate increases.

Fair et alia[29] and Yoshida & Akita[31] found no effect of column diameter when this exceeded 15 cm. but a slight decrease in hold-up was reported by Yoshida & Akita for the case of a 7.5 cm column.

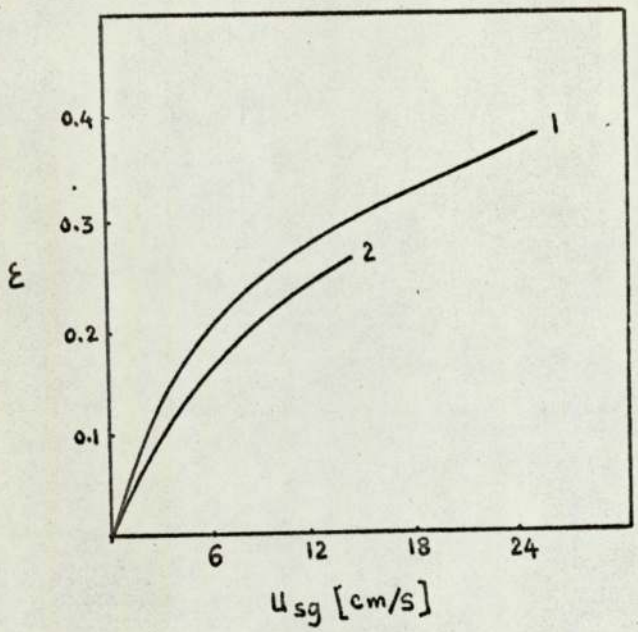

Curve No.	Col. Diameter (cm)	U_{sl} cm/s	Col. Height (cm)
1	40.6	0.71	183
2	40.6	0.71	274.5

Fig 2.5 Comparison of Gas Holdup for Different Column Heights

Shulman & Molstad[35] found that changing from a column diameter of 5 cm to one of 10 cm had no effect on gas holdup. However a slight increase was observed when using a 2.5 column diameter at a fixed gas velocity.

Reith et alia[5] observed much lower gas holdups for larger columns. Their explanation for this phenomenon was that in the larger columns the presence of random circulation patterns (eddies) causes the gas to rise in regions where the liquid is also rising.

Ellis & Jones[32] also suggest that wall-effects increase the value of gas holdups in columns less than 7.5 cm. This has been

further confirmed by Freedman & Davidson[21].

2.1.4.5. Effect of Gas Distributor Design

Different investigators have reported varying views on the effect of gas distributor design on gas holdup.

Freedman & Davidson[21] examined the influence of distributor geometry on gas holdup. It was shown that the holdup decreased from the value obtained with uniform gas distribution to a value depending on the degree of maldistribution of air at the base of the column. Some of their data are summarised in Fig.2.6.

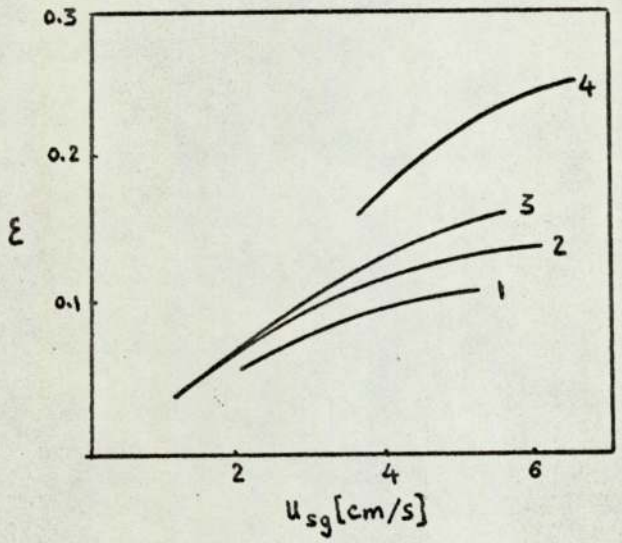

No. of curve	% Cross-section Aerated	No. of Holes	Hole Diameter (mm)
4	100	441	0.34
3	62	86	0.67
2	25	100	0.67
1	15	97	0.67

Fig 2.6. Dependance of Gas Holdup on Gas Distributor Design[21].

Towell et alia[6] found that distributor design has little effect on gas holdup. However, their so-called "two-phase distributor" gave a somewhat higher holdup at high liquid flow-rates. This was because dissipation of the energy required to pump the liquid through the two-phase orifice produced small bubbles in the region close to the distributors.

Reith et alia[5] after examining several types of air distributors - single tubes, fine gauzes and perforated plates with different numbers of holes of various diameters - reached the conclusion that the gas holdup remains unaffected by changes in orifice geometry.

Yoshida & Akita[31] also believe that fractional gas holdup is not affected by the nozzle diameter. They explained this in the following way: over the range of gas rate studied (up to 30 cm/s), gas was observed to flow out of the nozzle as a continuous jet stream and then to be split into bubbles by the turbulent motion of liquid in a zone just above the nozzle.

Kato & Nishiwaki[33] found that on decreasing the hole diameter of the gas distributor, the size of the bubbles generated decreased and gas holdup increased: also the range of linear increase of gas holdup with respect to superficial gas velocity became wide.

Aoyama et alia[36] reported that when a porous plate was used as a gas distributor ε increased almost linearly with increasing superficial gas velocity, u_{sg}, but decreased sharply at a certain value of u_{sg}. This value of u_{sg} appeared to correspond to the transition from bubble-flow to slug-flow caused by coalescence of bubbles. When a perforated plate was used as the gas distributor,

the change in the value of ε showed that the transition was gradual, as visually observed.

Ellis & Jones[32] found that perforated baffles placed inside a bubble column increased the gas holdup significantly. This was confirmed by Fair[18] who reported that when the baffles were vibrated even greater holdups could be obtained at any given superficial gas velocity. Bischoff and Phillips[30] also looked at gas holdup in a column containing a number of perforated plates. They observed that the gas holdup tended to level out at about 0.35 at a gas velocity of 18 cm/s and that the plate spacing had only a slight effect on gas holdup.

2.1.4.6. Effect of Electrolyte Solutions

Braulick et alia[37] found a significant difference in bubble dispersion in pure water and solutions of electrolytes. While the coalescence and turbulence patterns for salt solutions were the same as those observed for air dispersions in water, super-imposed on these patterns in salt solutions was a fine dispersion of microscopic bubbles. Because of the nature of the solutions with which these small bubbles were associated, Braulick et alia called them 'ionic bubbles'. Ionic bubble generation appeared to be associated with areas of intense liquid turbulence and because of their low rising velocities, these bubbles were easily carried along with the liquid eddies and served to make them visible. It is obvious that the interfacial contact areas of such ionic bubble clouds are very large and in addition the residence times are likely to be unusually long. The ionic bubble fraction could, therefore, provide a major mode for mass transfer in electrolyte solutions that would be absent

in pure liquid systems.

Fair et alia[29] also found that electrolytes can exhibit holdup values 20 to 30% higher than non-electrolyte because of the formation of very small stable bubbles with correspondingly slower rise velocities. Yoshida & Akita[26,31] also observed these very fine bubbles in electrolyte solutions and suggested that their occurrence can be explained by the electrostatic potential at the gas-liquid interface.

2.1.4.7. The Effect of Suspended Particles

Kato et alia[38] obtained gas holdup data for bubble column in which glass spheres (average diameter = 100μ) were suspended. They found that in the region of low gas velocity the gas holdup of the air-water-glass sphere system is somewhat less than that of an air-water system. They consider this to be caused by the larger rising velocity of coalesced bubbles in the presence of solid particles. In the region of high gas velocity, where large coalesced bubbles rise frequently, the effect of solid particles on gas holdup becomes gradually smaller as gas velocity increases.

Imafuki et alia[39] employed different kinds of solid particles with wider ranges of size and density - glass spheres, ion exchange resins, $FeSiO_2$ powder and Cu powder. Their results show that in the presence of solids the chance for bubbles to coalesce is much larger than in bubble columns without a solid phase. The effect of the concentration of solid particles on the value of ε was not very strong.

2.2. Experimental Programme

When examining gas holdup, all the parameters which might have an effect should be considered carefully. The literature survey indicates that the geometry of the column as well as the operating conditions and physical properties of the liquid phase are among the most important parameters. Although the range of each variable was chosen so as to meet the requirements of this particular project, effort has been made to go to extreme values to discover general trends or discontinuities in system behaviour.

2.2.1. Gas Flow-Rate

A high gas flow rate is not desirable in a fermentation. Outside the bubbly-flow regime, coalescence occurs leading to a reduction in the gas-liquid interfacial area and, as confirmed later, to only a small increase in gas holdup. In some cases, the wild movement of bubbles or slugs at high air flows may break up microbial flocs during fermentation and lead to 'washout' problems. Economy in the use of compressed air is also an important factor in process design and means that air flow rates during a fermentation must be kept to a minimum. For these reasons, attention has been concentrated on the bubbly flow regime. For air-water systems, this regime is observed up to a superficial gas velocity of about 5 cm/s. In this research experiments at figures up to 12 cm/s were carried out.

2.2.2. Liquid Flow-rate

Liquid flow-rate directly controls the output of the plant and therefore it is desirable to cover as wide a range as possible. However there are certain constraints which must be borne in mind.

System behaviour at low liquid flow-rates (corresponding to

superficial liquid velocities << 1 cm/s) is of interest since many biochemical reactions are relatively slow and in a 'once through' process long residence times may be involved. At relatively high liquid flow-rates micro-organisms are readily elutriated, making it difficult to maintain high microbial concentrations inside a column.

From the engineering point of view, it was decided to choose liquid flow-rates in the laminar, transition and turbulent regimes (based on a gas-free system). For the size of columns used superficial liquid velocities were limited to a maximum figure of about 3 cm/s.

2.2.3. Column Geometry

To assess the extent of wall effects as well as aspect ratio on gas holdup four columns were constructed having diameters of 7.8 cm, 15.2 cm, 30.5 cm and 61.0 cm. Previous work (see Section 2.1) has suggested that above about 15 cm the wall effect is not important. It was hoped that with these four columns enough information for design purposes and scale up would be obtained.

2.2.4. Design of Gas Distributor

Bubble size and bubble size distribution might be expected to have an effect on gas-holdup. This suggests that the design of gas distributor could be an important factor in the performance of bubble columns, although previous investigators have obtained conflicting results. Consequently, it was decided to investigate the effect of the more common types of gas distributor, such as porous plates and perforated plates, and then on the basis of the data obtained to decide whether any sophisticated design was justified.

2.3. Experimental Equipment

Four column diameters were used: 7.6 cm, 15.2 cm, 30.5 cm and 61.0 cm. The 7.6 cm column was an independent unit which will be described separately. The other three columns were linked to common storage tanks, liquid-phase pumping and metering systems and air-supply and metering systems.

2.3.1. The 7.6 cm Diameter Column

A general layout of the 7.6 cm column with the liquid circulation and air supply systems is given in Fig.2.7

The liquid reservoirs (1) consisted of two 43 l tanks, 38 cm in diameter by 38 cm deep. The tanks were manufactured from 10 gauge stainless steel and fitted with removable lids.

The liquid was fed to the column by means of a centrifugal pump (2), obtained from Stuart Turner Ltd., and capable of delivering 720 gallons/h against a 10 ft. head. The water flow was metered by a group of three Rotameters (3) (Metric 7F with a ceramic float; 10F and 14F both with stainless steel floats), covering flows from 0 to 8 l/min. The Rotameters were fitted with Q.V.F. valves downstream. The liquid was introduced into the column through a cross-shaped distributor, constructed from two 6 cm lengths of copper tube. Holes of 2 mm diameter were drilled at the sides and bottoms of the tubes.

The gas supply (4) was obtained from a compressed air service main via a 1.3 cm n.b.'T'. This was fed directly to a Rotameter (7P with Duralumin float) via a control valve (5), used to regulate the flow and pressure at the meter. The metering pressure was measured by the calibrated pressure gauge (6) . The gas distributor was made of a stainless steel porous plate surrounded by a U-shaped rubber

Scale 1:10 [only for Column and storage Tanks]

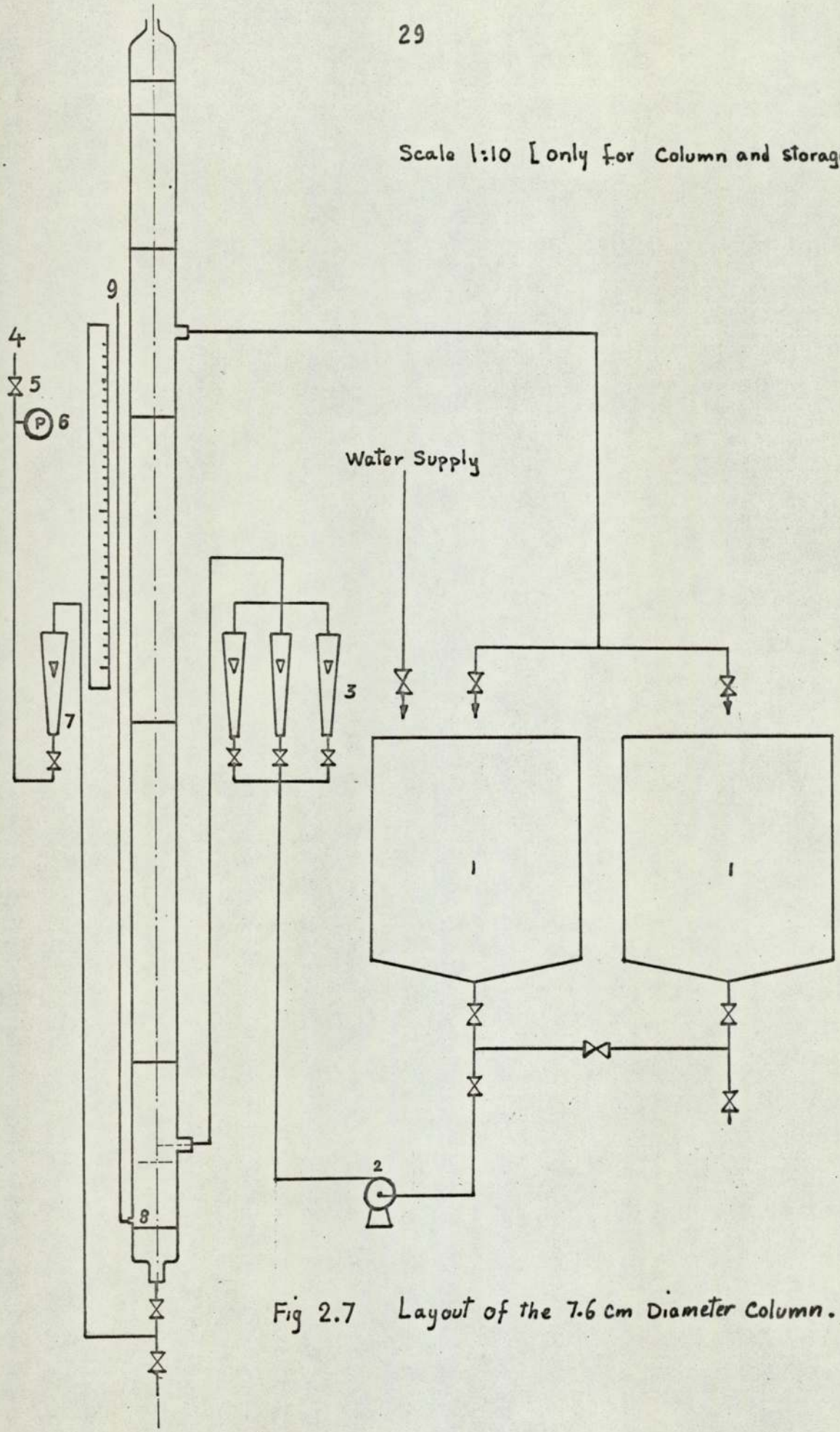

Fig 2.7 Layout of the 7.6 cm Diameter Column.

gasket and was fitted between two sections of QVF glass-pipe at the bottom of the column.

The column was made of 7.6 cm diameter Q.V.F. glassware. Two large sections, each 61 cm in length were set between two 30.5 cm sections having 2.54 cm bore side-arms for liquid inlet and outlet.

Right at the bottom of the column and very close to the gas distributor, a 6 mm hole (8) was drilled on a side-arm to take a side tube (9) (6 mm bore glass) . This was used to evaluate the pressure drop and gas holdup over the length of the column.

The overall column height from the gas distributor plate to the top was 208 cm. The distance from the gas distributor to the liquid outlet was 161 cm.

Fig.2.8 gives a general view of the 7.6 cm diameter column.

2.3.2. Equipment Common to the 15.2, 30.5 and 61.0 cm Columns

A schematic view of the liquid circulation and air supply systems is given in Fig.2.9.

The liquid reservoirs (1 and 2) consisted of two 600 l tanks, 91.5 cm in diameter by 91.5 cm deep (see Fig.2.10). The tanks were manufactured from 10-gauge stainless steel, with removable lids. Steam as well as cold-water could be introduced into one of the tanks (1) through two separate stainless steel coils (1.3 cm o.d. x 350 cm in length)(7) to control the temperature of the liquid. Compressed air could also be introduced into the bottom of the tank by means of a 1.3 cm o.d. stainless steel tube (8) fitted with two nozzles: these could be used to keep microbial suspensions well-mixed during the course of experiments.

The liquid was fed to the columns by means of two Q.V.F. centrifugal pumps (3,4). One (3) was connected to a bank of three Rota-

Fig 2.8. General View of the 7.6 cm. Diameter Column.

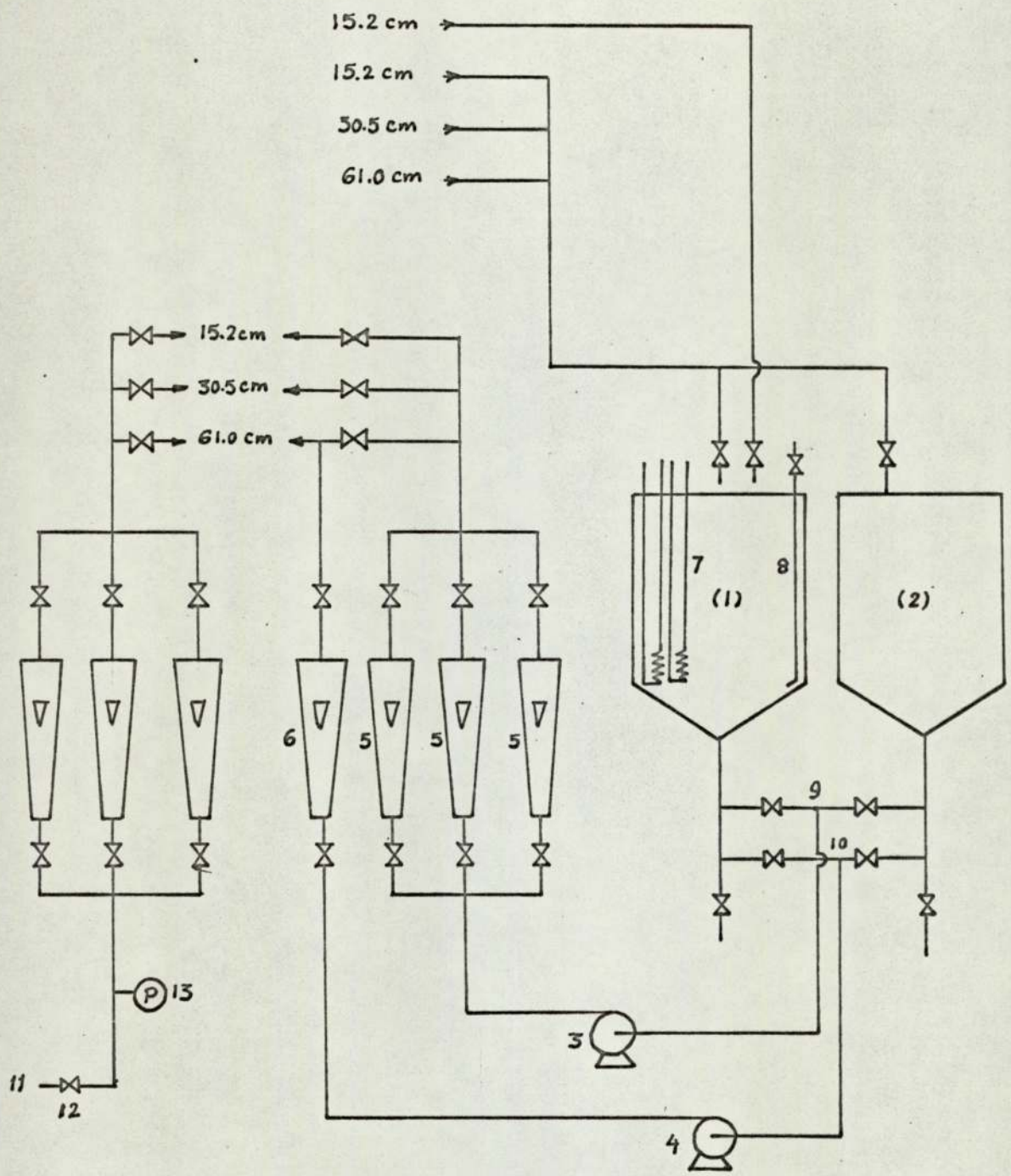

Fig 2.9. Schematic flow Diagram of equipment common to the 15.2 cm, 30.5 and 61.0 Columns.

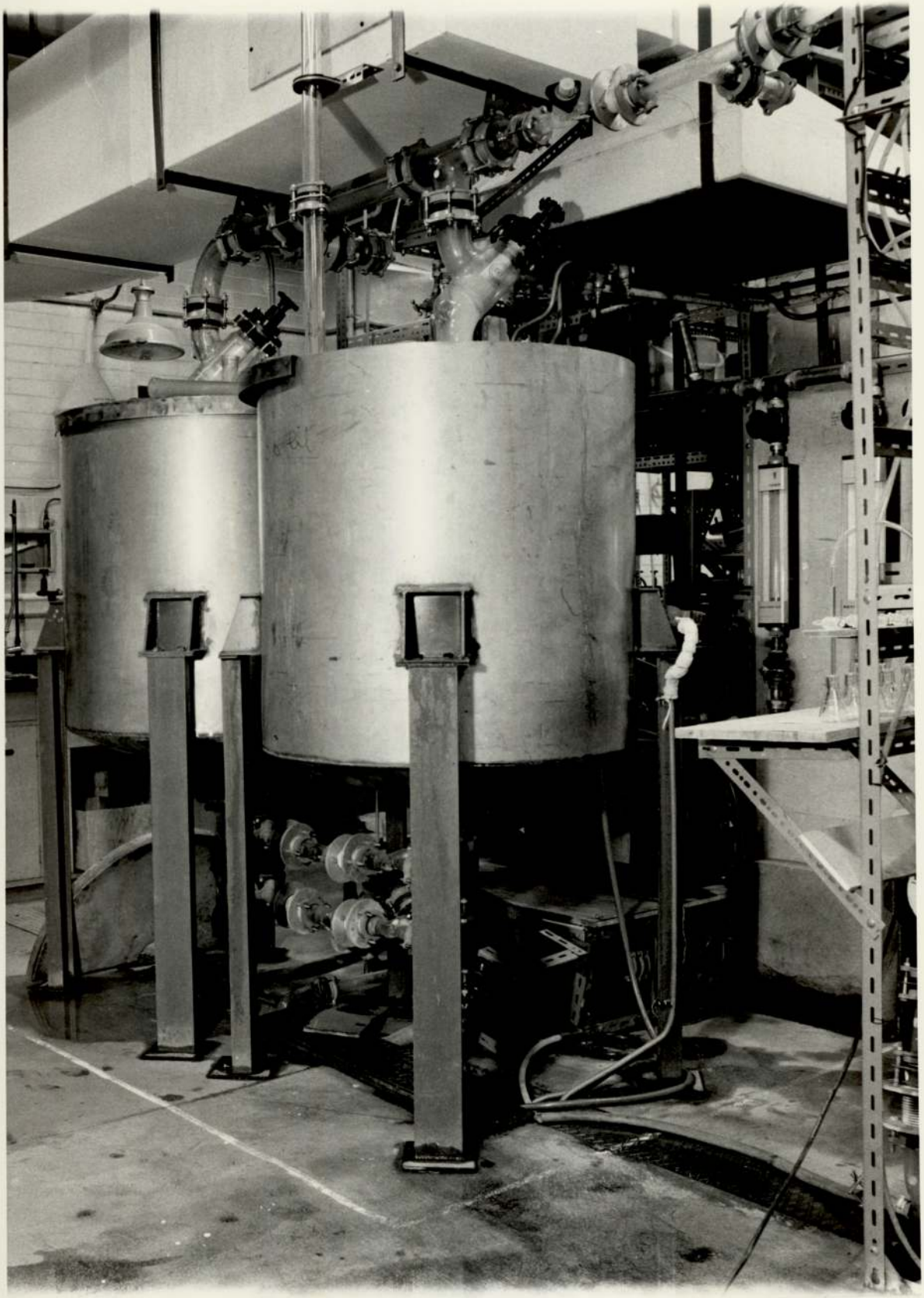

Fig 2.10. Liquid Phase Storage Tank.

meters (5) (Metric 24XG, 35G and 65G, all with stainless steel floats), each of which could be switched into the liquid feed-lines to any of the three columns. The other pump (4) was used to deliver liquid to the 61.0 cm column through a separate Rotameter (6) (47P with stainless steel float). The maximum liquid flow-rate which could be obtained from the two pumps was about 150 l/min, equivalent to a superficial liquid velocity of about 1 cm/s in the 61.0 cm column. The Rotameter lines were each fitted with P.T.F.E.-lined diaphragm valves downstream and stainless steel ball valves upstream. These two types of valves were used for flow regulation and rapid shut-off respectively. All the liquid-side pipework comprised standard 3.8 cm ($1\frac{1}{2}$") Q.V.F. glassware and valves or 2.54 cm o.d. stainless steel tubing fitted with suitable couplings.

The gas supply (11) was obtained from a compressed air service main via a 2.54 cm n.b.line. This was fed directly to the metering section via a control valve (12) used to regulate flow and pressure at the meters. The metering section consisted of three Rotameters (Metric 14G, 24XG and 47XG all with Duralumin floats) enabling the flow-rate to be measured from 0 to 1000 l/min at S.T.P. The metering pressure was measured by the calibrated pressure gauge (13). The flow control was similar to that used on the liquid phase, i.e. P.T.F.E.-lined diaphragm valves downstream and ball valves upstream. From the metering section three 3.8 cm n.b.Q.V.F.lines led to the air chambers below the gas distributors in the three columns. The air chambers were made up in the same way for each column and were designed to give even gas distribution.

2.3.3. The 15.2 cm Diameter Column

This column was made up of standard lengths of Q.V.F. 15.2 (6") bore pipe (see Figs.2.11 and 2.12). The lowest section (1) comprised an unequal 'T' piece, with 3.8 cm bore side-arm which was used for entry of the liquid. Section (7) again comprised a 'T' piece with 5.1 cm bore side-arm for the liquid off-take: the side-arm bore was designed to take the highest liquid flow-rate without producing any head. The top sections of the column (8) and (9) were designed to reduce and recycle foam: any excess foam was returned through (10) to one of the storage tanks (Fig.2.7.(1)). The outlet (11) was connected to a manometer. The overall column height, from the gas distributor plate to the top of the column was 315 cm and the liquid seal was 247 cm.

The liquid distributor, which was used only for preliminary work was constructed from 1.3 cm o.d. copper tubing, brazed up and drilled: it was very similar to one used in the 30.5 cm diameter column (see Fig.2.16). The distributor ring itself (10.1 cm o.d.) was situated 4.5 cm above the gas distributor plate.

The air inlet system to the column (12) consisted of 2.5 cm n.b. mild-steel pipe, control valve(13),glass inlet section (14), reducer (15) and the distributor plate (16). The latter was clamped between the adjoining faces of the Q.V.F.sections. The air could be saturated by introducing some water into the lower part of section (14), and the temperature of the air could be controlled by wrapping the outer face of section (14) with heating tape. The amount of heat could be readily altered by a variac in the electrical circuit. The air temperature was measured by a thermometer (17) fixed inside the reducer (15).

To measure the pressure drop and gas holdup in any part of

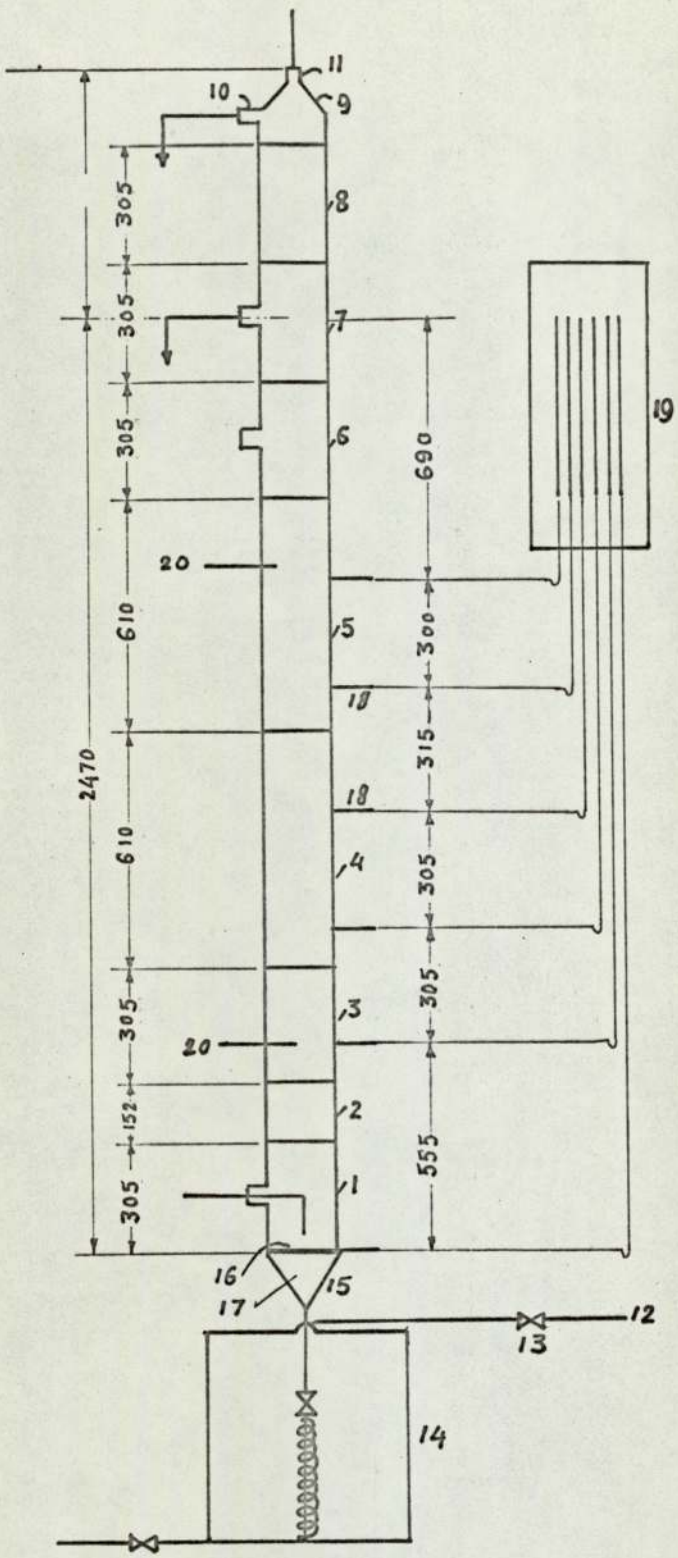

Fig 2.11. Construction of the 15.2 cm Diameter Column.

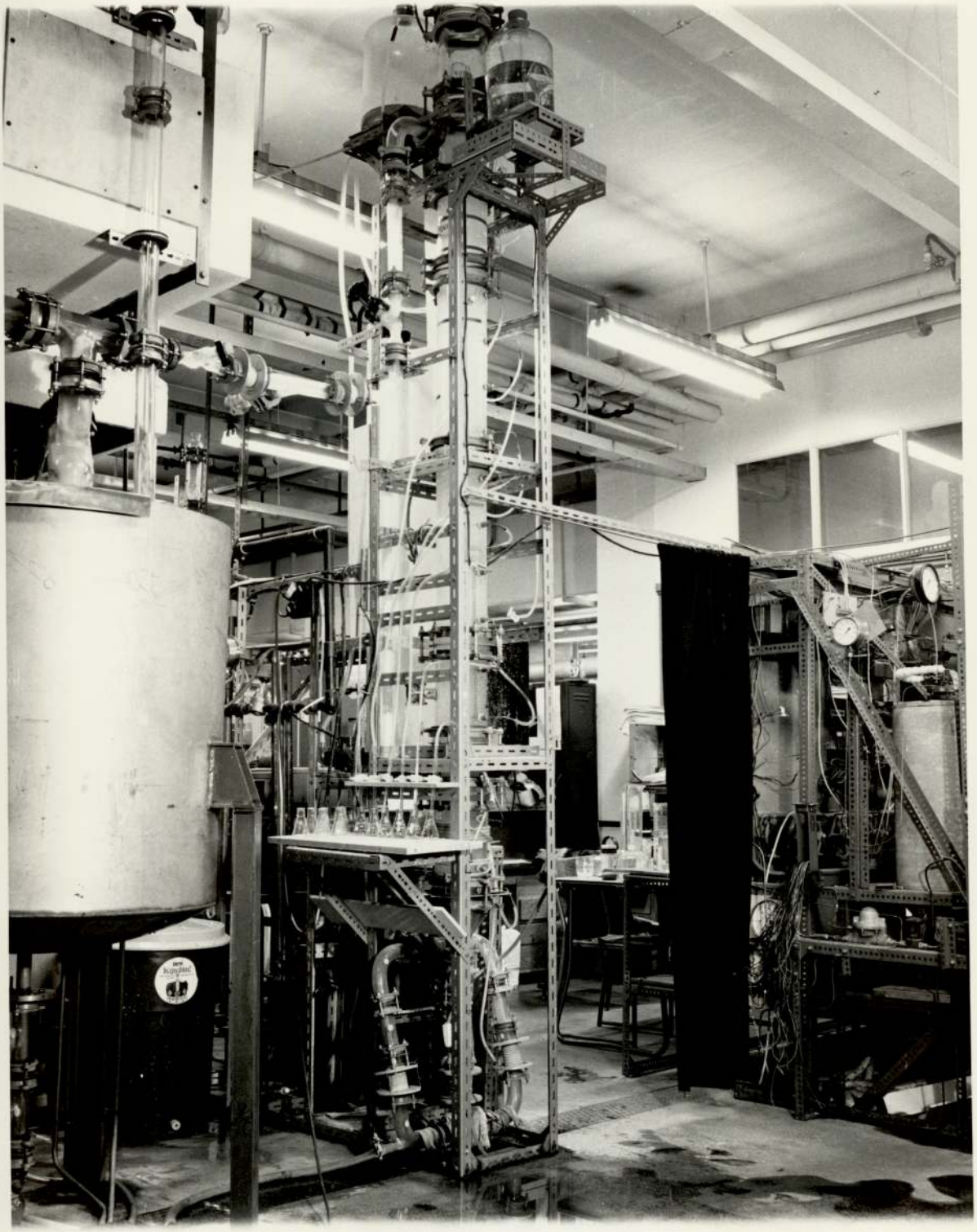

Fig 2.12. General View of the 15.2 Cm. Diameter Column.

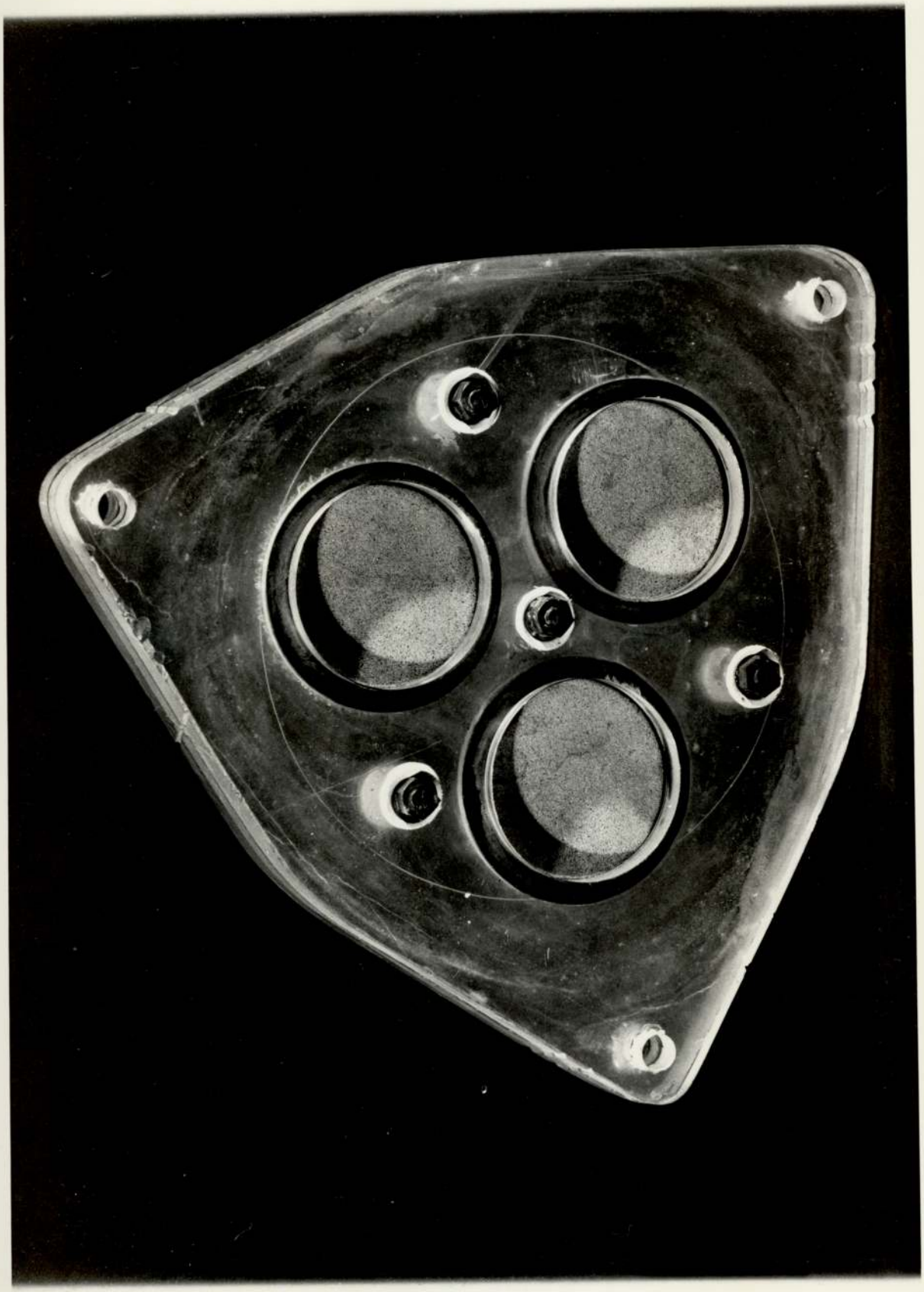

Fig 2.13. General View of the Gas Distributor for the 15.2 cm. Diameter Column.

the column, 1.3 cm diameter holes were drilled along the length of the column. The holes were supplied with fittings so that 3.2 mm o.d. stainless steel tubes could easily be inserted into the column; and these tubes were connected by means of flexible P.V.C.tubing to vertical glass tubes mounted at the top of the column (19). Beside each glass tube a self-adhesive downward scale was affixed: the zeros of these scales were at the same level as the water outlet. Thermometers (20) were fixed at two different points up the column to show the temperature.

Two gas distributors were used. One consisted of three perspex plates, cut as shown in Fig.2.13 and fitted with stainless steel sinters: the sinters themselves were clamped between the two outer perspex plates as shown in Fig.2.13. The second was a perforated plate made of aluminium, 3.2 mm thick and drilled with 55 holes of 0.75 mm diameter on a 17.4 mm triangular pitch.

2.3.4. The 30.5 cm Diameter Column

This was built up in a similar manner to the 15.2 cm column (see Figs.2.14 and 2.15). The overall height of the column was 310 cm and the liquid seal was 247 cm, the same as for the 15.2 cm column.

The liquid distributor was constructed from 2.54 cm o.d.copper tubing (see Fig.16) with a number of 4.0 mm diameter holes. The clearance between the distributor ring (22.8 cm o.d.) and the gas distributor plate was 3.8 cm.

The gas distributors used were similar in design to those employed in the 15.2 cm column. In the case of the porous plate distributor the only difference was that it contained 9 sintered metal discs instead of 3 (see Fig.2.17). The perforated plate distributor contained 162 holes of 0.75 mm diameter on a 25.4 mm triangular pitch.

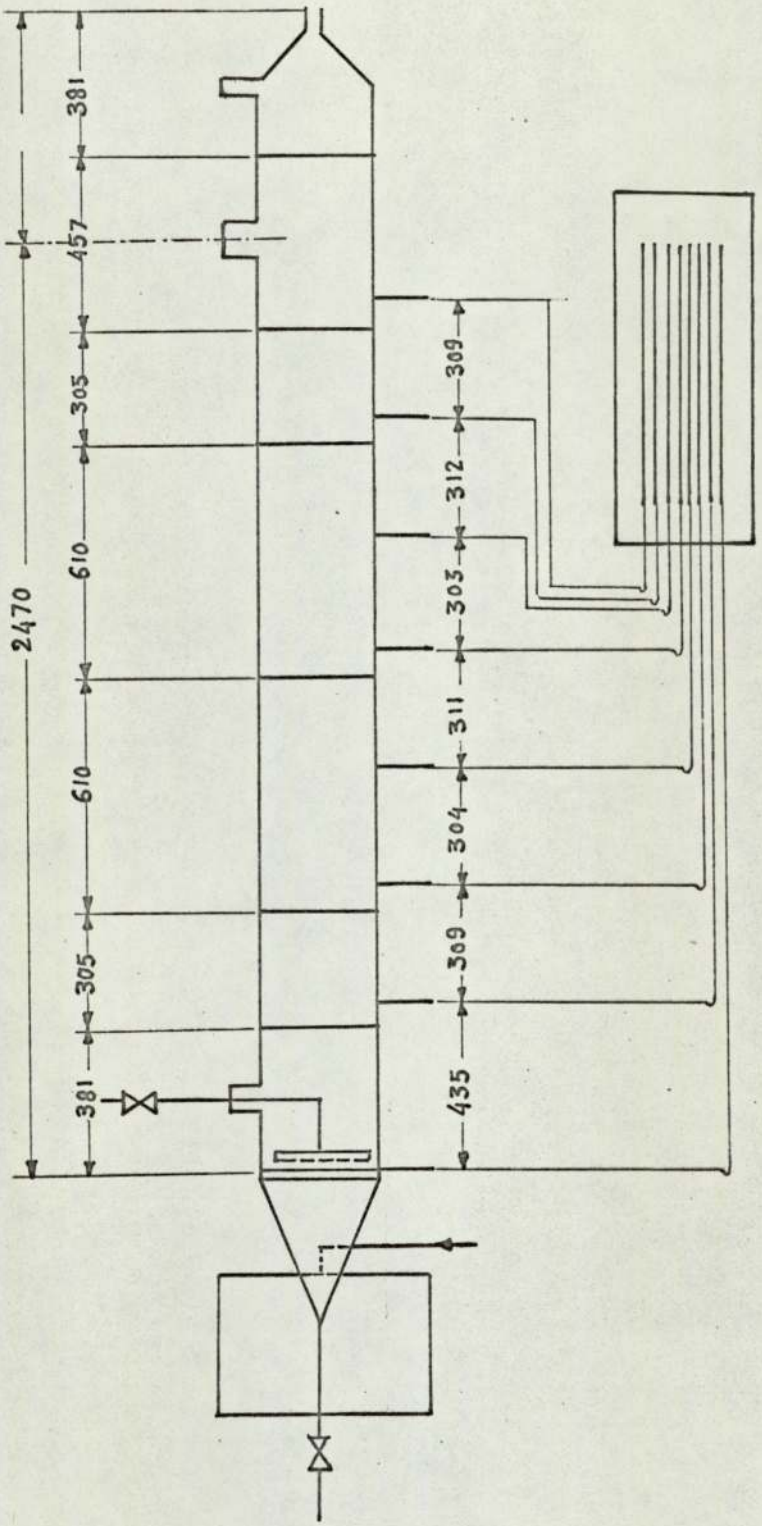

Fig 2.14. Construction of the 30.5 cm Diameter Column

Fig 2.15. General View of the 30.5 Cm. Diameter Column.

Fig 2.16. General View of the Liquid Distributor for the 30.5 Cm. Diameter Column.

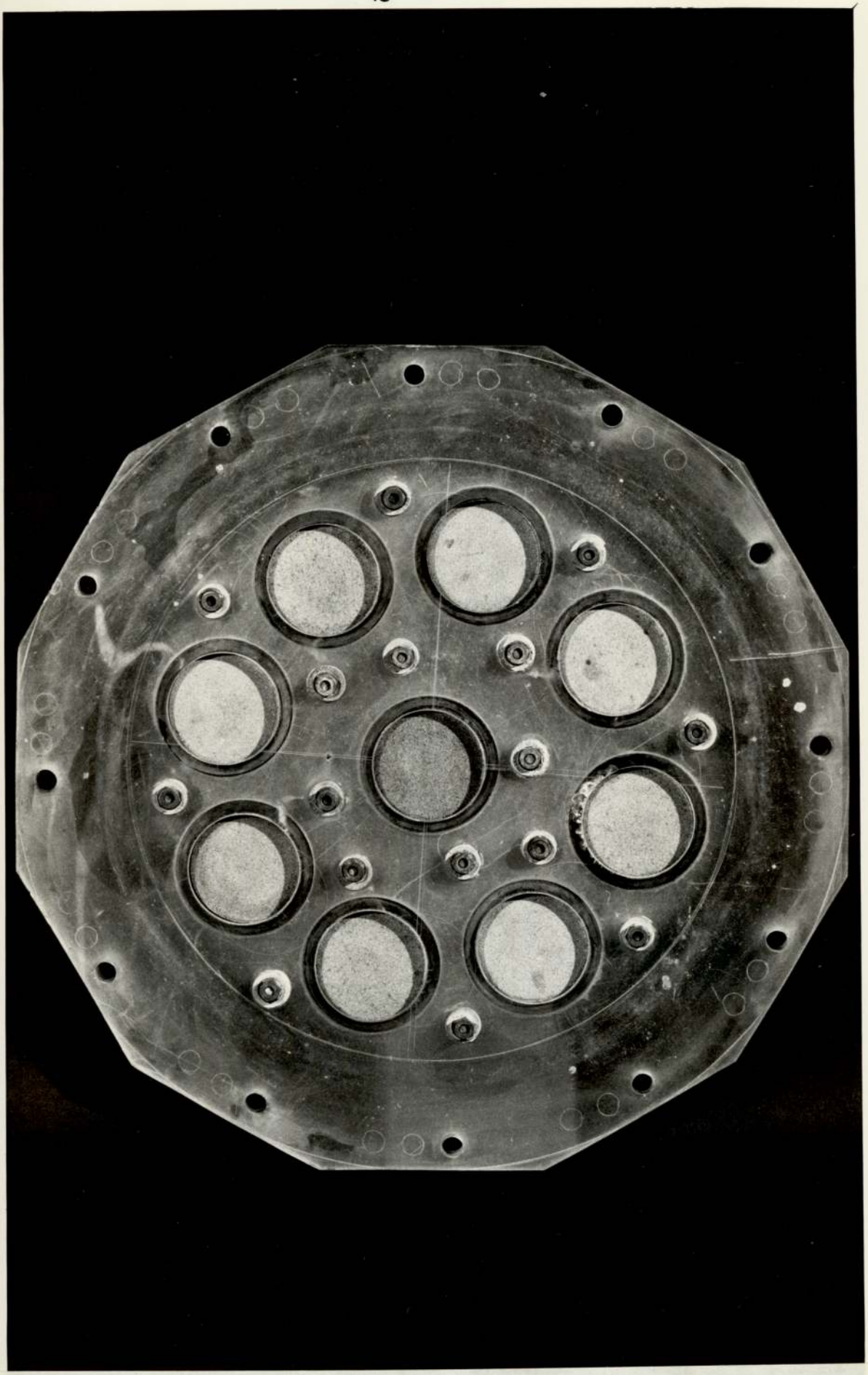

Fig 2.17. General View of the Gas Distributor for the 30.5 cm. Diameter Column.

Sampling points were drilled at 30.5 cm intervals and connected to a board of glass tubes in the same fashion as with the 15.2 cm column.

2.3.5. The 61.0 cm Diameter Column

This column was manufactured from two pieces of 10-gauge stainless steel, each 104 cm long (see Figs.2.18 and 2.19): the two sections were bolted together. The liquid inlet and outlet pipes were 7.6 cm in diameter and were connected to Q.V.F. piping and fittings of the same size.

The air inlet to the column was of the same design as those used in the two larger columns. The gas distributor consisted of 9 perforated perspex plates (10.5 cm in diameter and 3.2 mm thick), each containing 37 holes of 0.75 mm diameter on a 13 mm triangular pitch (see Fig.2.20).

To measure gas holdup, seven 9.5 mm-holes were drilled along the length of the column and into these were welded 9.5 mm o.d. stainless steel tubes: these were then connected to a board of glass tubes in the same way as for the other columns.

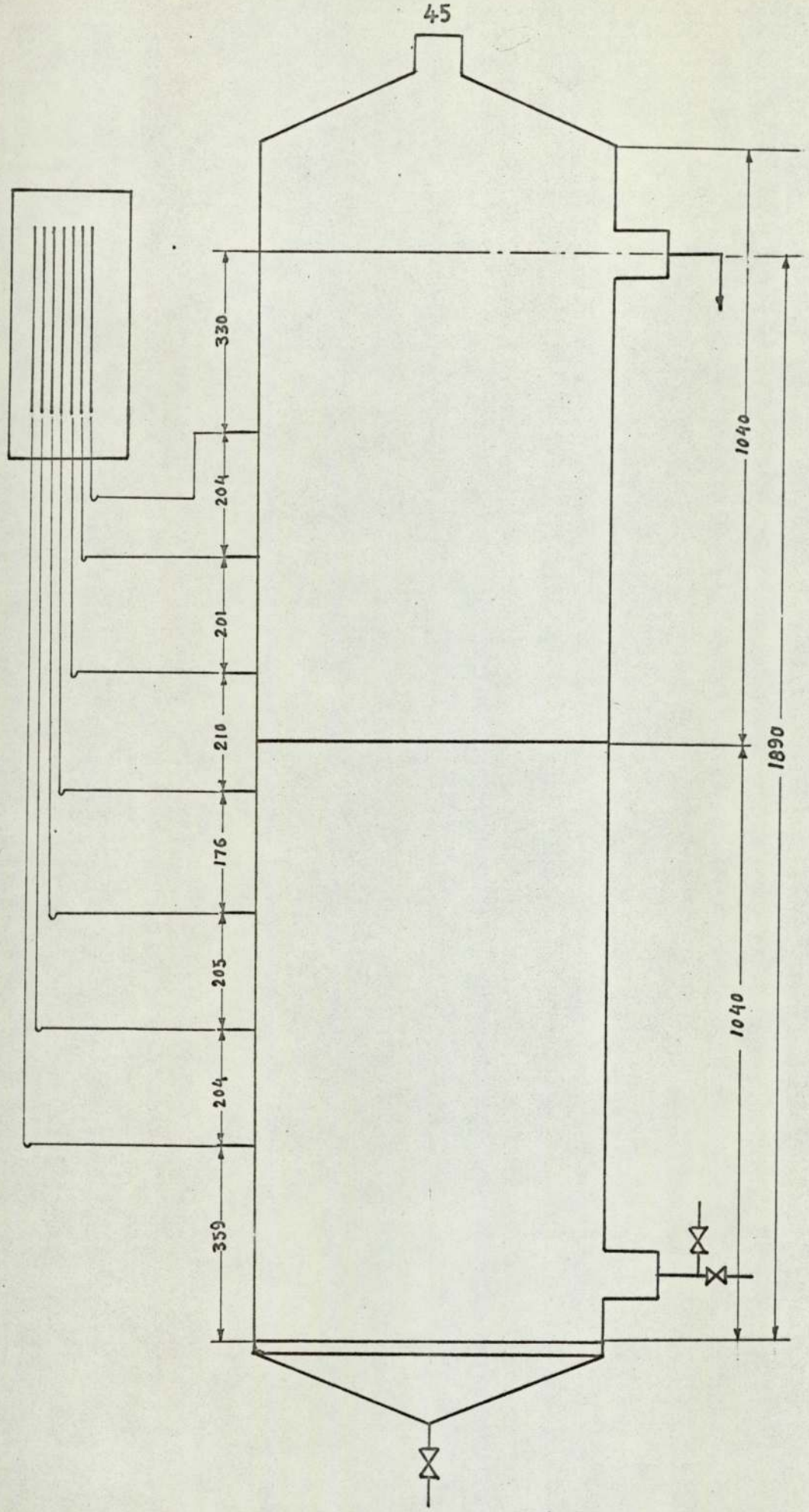

Fig 2.18. Construction of the 61.0 Cm Diameter Column.

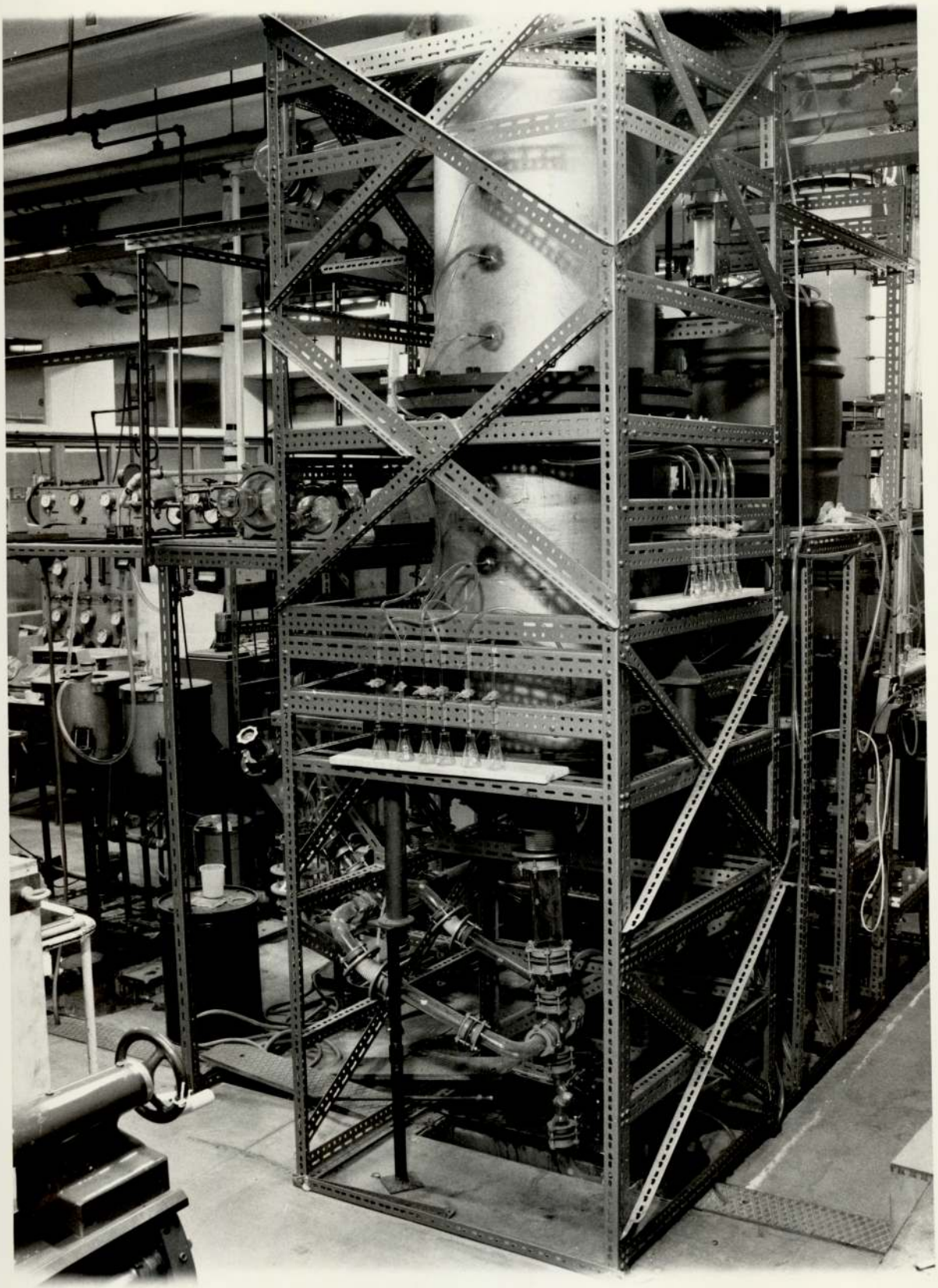

Fig 2.19. General View of the 61.0 cm. Diameter Column.

2.20. General View of the Gas Distributor for the 61.0 cm. Diameter Column.

2.4. Experimental Results

2.4.1. Comments on the Method of Measuring Gas Hold-up

Fig.2.21 shows schematically the equipment used for the measurement of gas hold-up. A and B are two manometers fixed at arbitrary points up the column - the number of these manometers varied in different columns. Δl , the difference between two liquid levels in the manometers, gives an indication of gas hold-up for the section of the column between the two manometers. This can be shown by the following simple calculation.

By definition :

$$\varepsilon = \frac{lA - l_o A}{lA} = 1 - \frac{l_o}{l} \qquad (2.32)$$

where l_o = height taken by liquid if the gas were excluded .

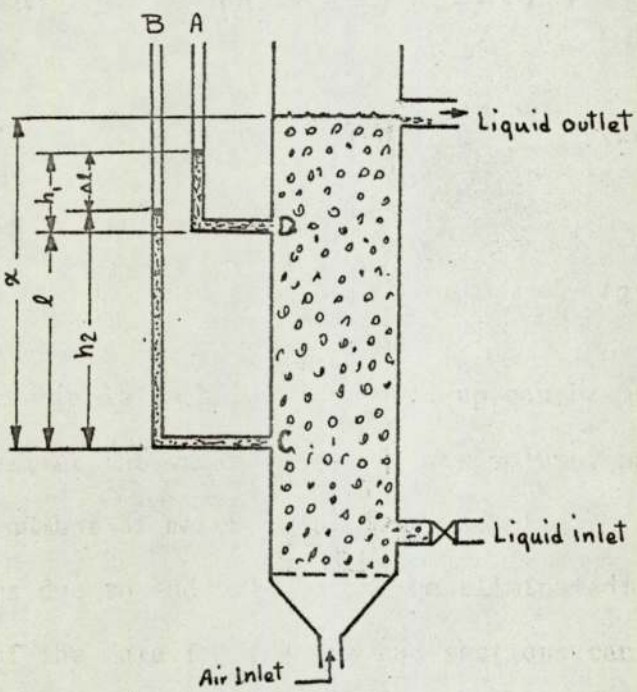

Fig 2.21 Basis for the Measurement of Gas Holdup.

If ρ_ℓ = liquid density, ρ_g = air density and

ρ = density of mixture

$$\rho = \frac{\ell_o A \rho_\ell + A(\ell - \ell_o)\rho_g}{\ell A}$$

or $$\rho = \rho_\ell - (\rho_\ell - \rho_g)(1 - \frac{\ell_o}{\ell}) \qquad (2.33)$$

Combining equations 2.32 and 2.33:

$$\varepsilon = \frac{\rho_\ell - \rho}{\rho_\ell - \rho_g} \qquad (2.34)$$

As $\rho_\ell \gg \rho_g$ equation (2.34) becomes

$$\varepsilon = \frac{\rho_\ell - \rho}{\rho_\ell} \qquad (2.35)$$

Now

Pressure at C : $P_c = \rho \alpha = \rho_\ell h_2$,

Pressure at D : $P_D = \rho(\alpha - \ell) = \rho_\ell h_1$,

and

$$\Delta P = \rho \ell = \rho_\ell (h_2 - h_1) = \rho_\ell (\ell - \Delta\ell) \; ;$$

$$\therefore \quad \frac{\Delta\ell}{\ell} = \frac{\rho_\ell - \rho}{\rho_\ell} \qquad (2.36)$$

From equations (2.34) and (2.35)

$$\varepsilon = \frac{\Delta\ell}{\ell} \qquad (2.37)$$

With this simple technique gas hold-up can be measured for any section as well as the whole length of the column, provided there are a sufficient number of manometers. One advantage of this technique is that errors due to end-effects can be eliminated: also examination of the data for the two end-sections can help in the design of the inlet and take-off systems.

For the bubbles to be formed at the gas distributor the air

pressure must exceed the bed height pressure and pressure drop across the gas distributor, i.e.

$$P > L' \rho_\ell + \Delta P_D$$

where L' = height of gas-free liquid in the column.

ΔP_D is the sum of the friction and contraction pressure-drop due to flow of gas through the pressure plate (ΔP_f) and the maximum bubble-pressure required for the formation of bubbles at the plate surface (ΔP_o) :

$$\Delta P_D = \Delta P_o + \Delta P_f \ .$$

It is well known that during formation of a bubble at a jet the pressure first increases until the bubble is a hemisphere whose radius is equal to that of the jet and thereafter decreases as the bubble grows. Such fluctuations of pressure cause a random formation of bubbles which themselves appear to move about in chaotic fashion throughout the bubble bed. Due to these random effects, pressure drop across the bubble column fluctuates to a certain extent at any point, and for this reason oscillations are observed in manometer levels at all points in the column.

To obtain simultaneous liquid levels in all manometers, it was decided to take photographs of the bank of manometers associated with each column. This is important as the calculation of gas hold-up over each column section was based on the difference between manometer levels. An average value was then found by taking two or three photographs during each run. Repeated experiments showed that the results were reproducible within ±3%. In most cases, the end-effects have been excluded from the average value of gas hold-up.

2.4.2. Results for Air-Water Systems: Effect of Column Diameter, Liquid Flow and Gas Distributor Design.

Fig. 2.22 to 2.25 show the results of gas hold-up measurements for air-water systems for the four different columns (7.6 cm, 15.2 cm, 30.5 cm, and 61.0 cm in diameter). The graphs also include the results for different gas distributors. The number of data points in each graph has been reduced in most cases because of their close proximity: for the same reason, only a few lines have been included. All the data used to plot these graphs are given in Appendix (A) - Tables 1 to 5.

Tables 6 to 8 list the manometer readings for the 15.2 cm, 30.5 cm and 61.0 cm columns. Based on these data Figs.2.26, 2.27 and 2.28 were plotted. These graphs show gas hold-up distribution over the length of each column.

2.4.3. Results from 15.2 cm Column: Effect of Temperature, Dissolved Salts and Microbial Suspensions.

The experiments to assess the effect of temperature, electrolyte solutions, fermentation media and microbial suspensions on gas hold-up were all carried out in the 15.2 cm column. The choice of column size was based on information available in the literature and from preliminary work: this suggested that for column diameters $\geq$ 15 cm wall effects are reduced to such an extent that the data obtained can be used for design and scale up purposes.

Effect of Temperature: Air-Water Systems

The effect of liquid-phase temperature was studied using water as the liquid phase. A range from 15°C to 45°C was chosen because this covers temperatures frequently used in fermentation

processes. Figs. 2.29 and 2.30 show how the temperature affected gas hold-up for $U_{sl}=0$ and $U_{sl}=1.87$. In Figs.2.31 and 2.32 temperature has been plotted on the abscissa and gas hold-up on the ordinate: these plots show more clearly the interactions between gas hold-up and temperature. Fig.2.33 shows the influence of liquid flow-rate. Detailed information is tabulated in Appendix (A) Table 9.

Effect of Dissolved Salts

The effect of electrolyte solutions was studied by measuring the gas hold-up in two KCl solutions of different concentration (1% and 4% wt/wt). Figs. 2.34 and 2.35 summarise the results of this work and Table 10 in Appendix (A) gives the detailed experimental data.

Different concentrations of sugar solutions were first used to simulate fermentation media. Fig.2.36 shows the effect of six different concentrations of sugar on gas hold-up: the data for this graph are presented in Table 11 of Appendix (A)

Experiments were then carried out using a 3% (wt/wt) solution of malt extract supplied by E.D.M.E.Limited, Mistly, Essex. The results are plotted in Fig 2.37 and listed in Table 12 of Appendix (A) . High concentrations of malt could not be used due to foaming problems.

Charging wort, supplied by Barbourne Brewery, Worcester, was also used to measure gas hold-ups at different flow-rates. Fig.2.38 shows the effect of superficial gas velocity on gas hold-up for such a system. Experimental data are given in Table 13 of Appendix (A). The physical properties of the charging wort, viz. density, surface tension and pH were measured and the data are presented in Table 20

of Appendix (A)

Effect of Microbial Suspensions

Tests were performed with suspensions of brewers' yeast, A. niger mould and vinegar-producing bacteria.

The yeast used was obtained from Ansells Brewery, Gosta Green, Birmingham: it was a non-flocculent strain of Saccharomyces cerevisiae , typical of the brewing yeasts used in the U.K. The yeast was obtained fresh from the filter-presses after fermentation and contained approximately 75% by weight of water. The suspensions were made by diluting the pressed yeast with different volumes of tap water. Dry yeast percentages as well as other physical properties of these suspensions are given in Table 14 of Appendix (A)

Figs. 2.39 and 2.40 show the effect of U_{sg} on gas hold-up for these suspensions. Experimental data used to plot these graphs are given in Table 15 of Appendix (A)

Aspergillus niger mould grown in the Department of Biological Sciences, University of Aston in Birmingham by Morris (40) was suspended in diluted molasses solution (10%) and the gas hold-up measured. The results are given in Table 16 of Appendix(A) and are plotted in Fig.2.41. It was stated that, during the course of growth of the mould, silicone was used as an antifoam agent. To study the effect of antifoam some preliminary tests were performed with air-water systems. Figs.2.46 and 2.47 show the state of the bubble column before and after adding 0.5 cc of a 25% silicone solution:30% silicone as methyl polisiloxane (Silcolapse 437, I.C.I. Stevenston, Ayrshire) was diluted by the addition of two parts of water to one part of antifoam emulsion. The data are graphed in

Figs.2.42 and listed in Table 17 in Appendix (A)

Vinegar was produced through a semi-continuous process using charging wort as a fermentation medium. The effect of superficial gas velocity on hold-up was assessed at different stages of fermentation, and the results are shown in Fig.2.43. Fig.2.44 shows how gas hold-up varied during the course of fermentation at the operational gas velocity (U_{sg}=1.89 Cm/S). Experimental results are given in Tables 18 and 19 in Appendix (A), and Table 20 gives the composition, surface tension and density of the medium as the fermentation progressed.

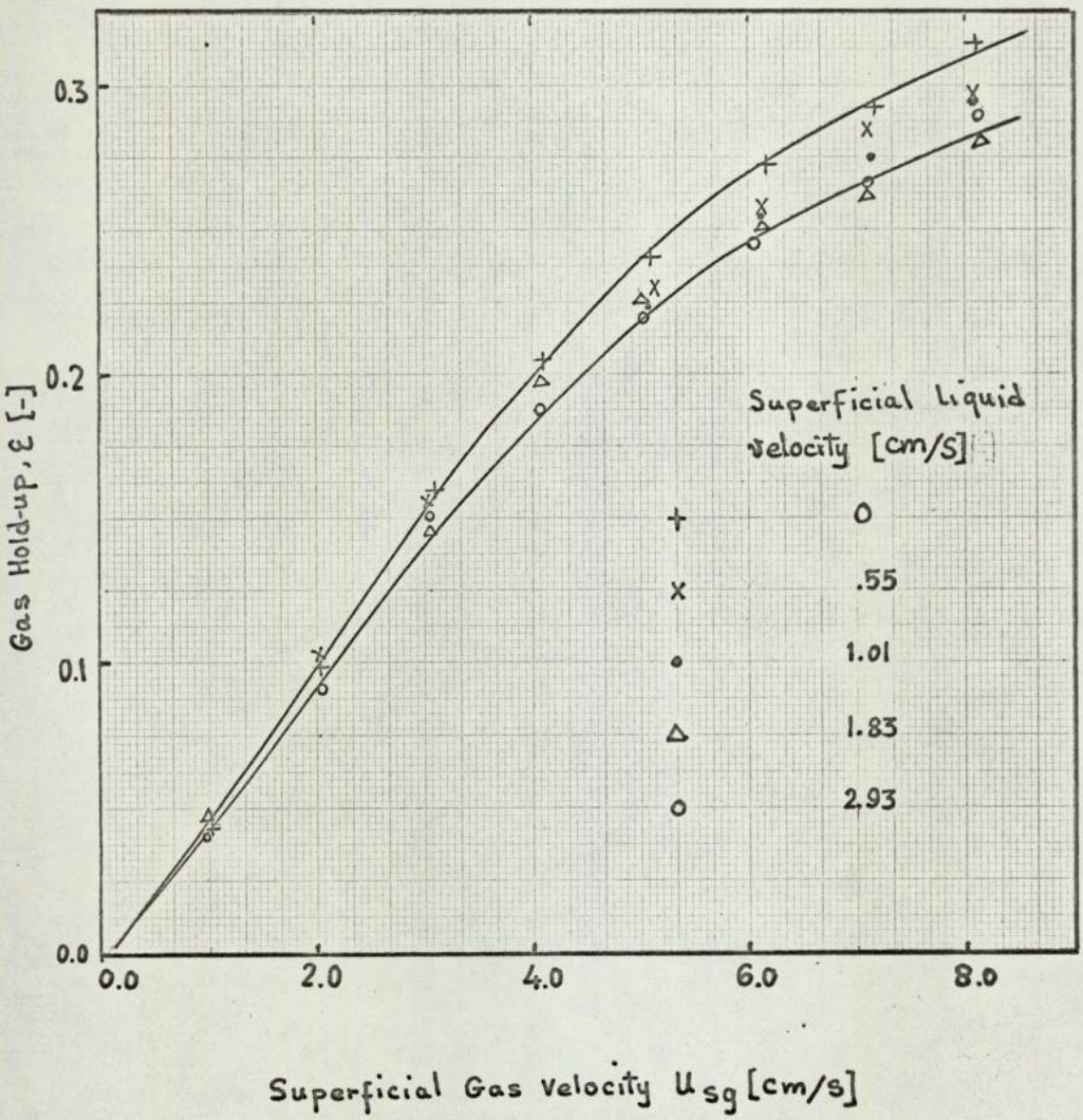

Fig 2.22 . Effect of Superfical Liquid and Gas Velocity on Gas Hold-up for 7.6 Cm. Diameter Column.

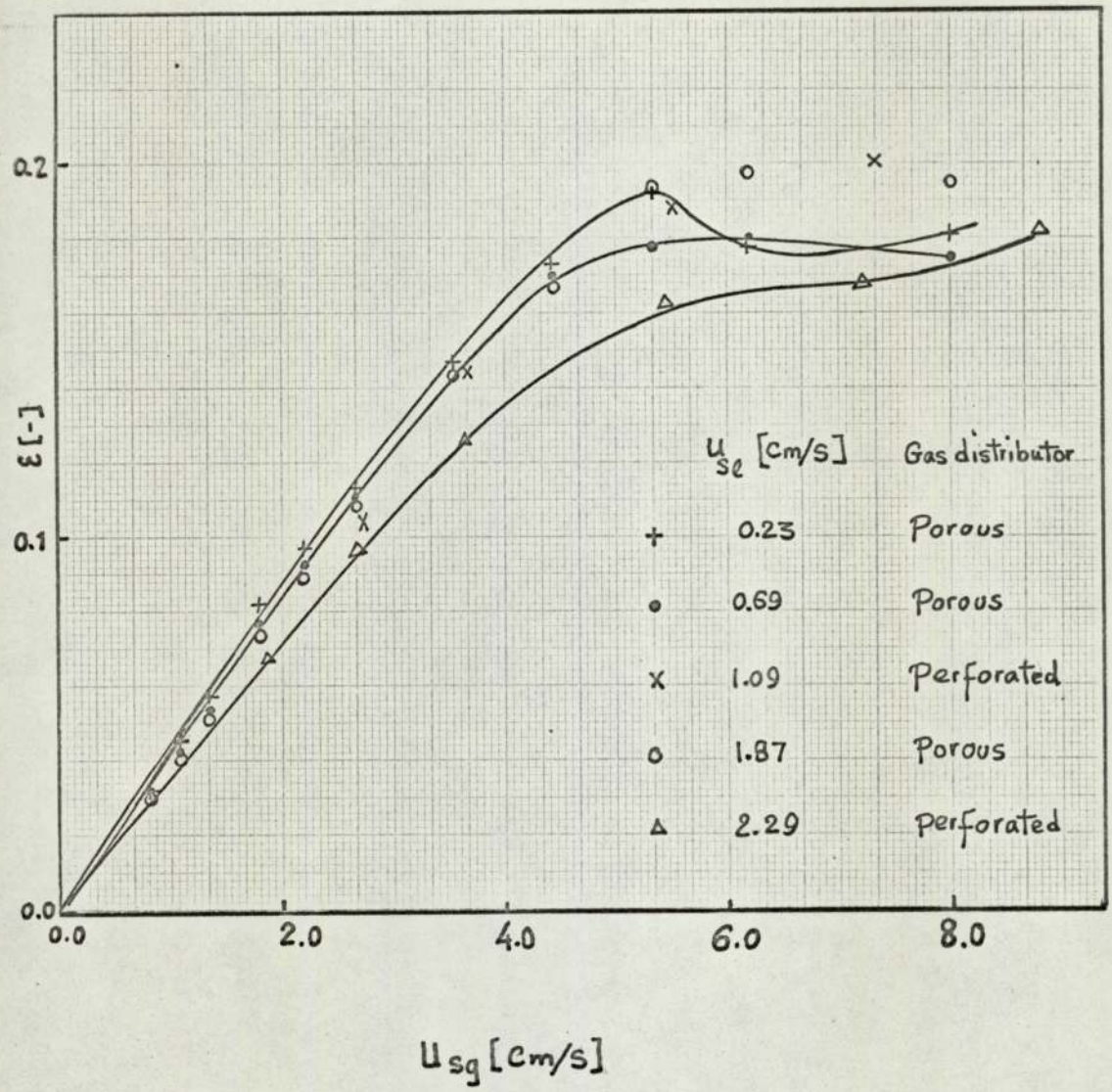

Fig 2.23. Effect of U_{sg} and U_{sl} on Gas Holdup for 15.2 Cm. Column.

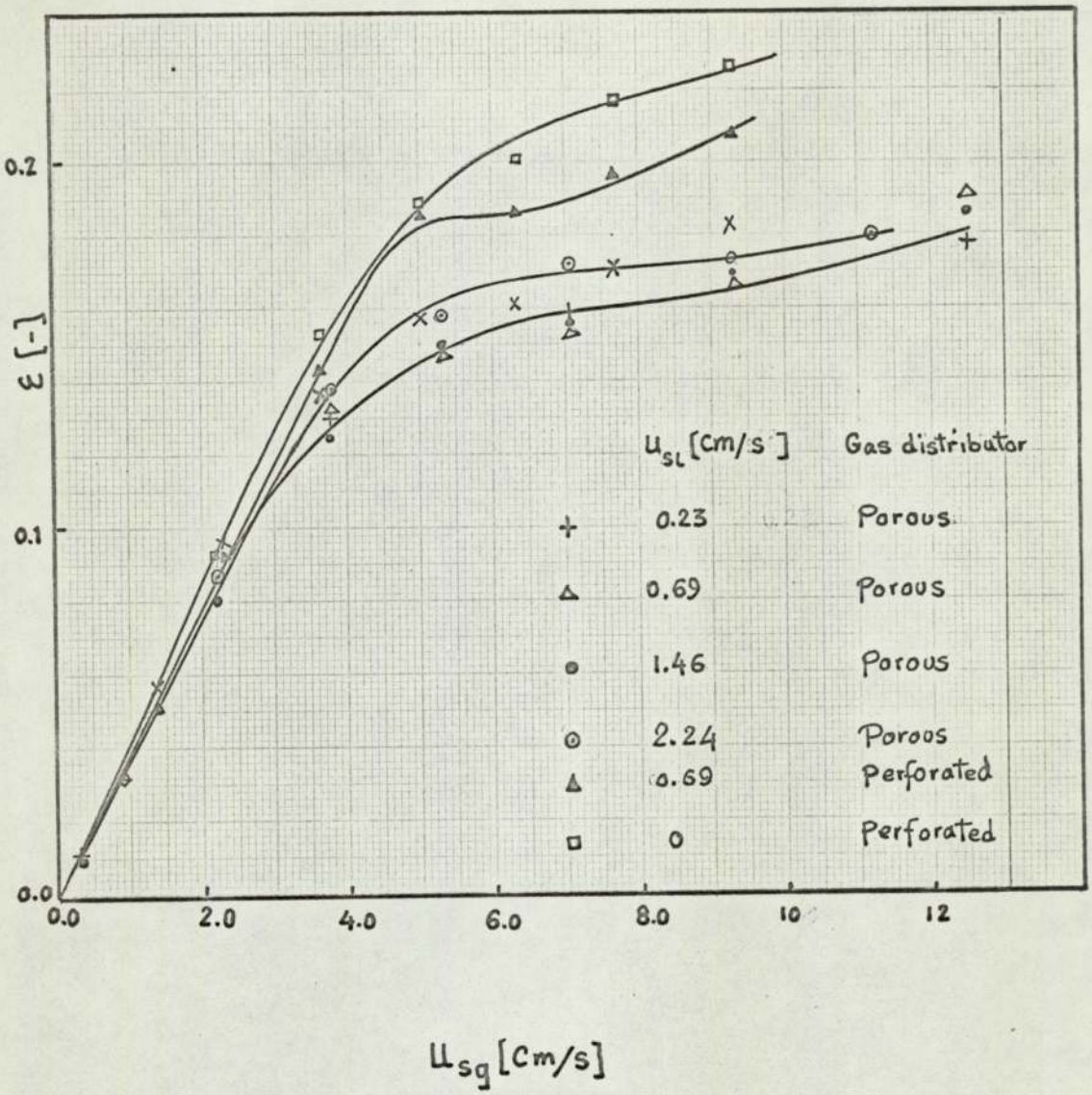

Fig 2.24. Effect of U_{sg} and U_{sl} on Gas Holdup for 30.5 cm Column.

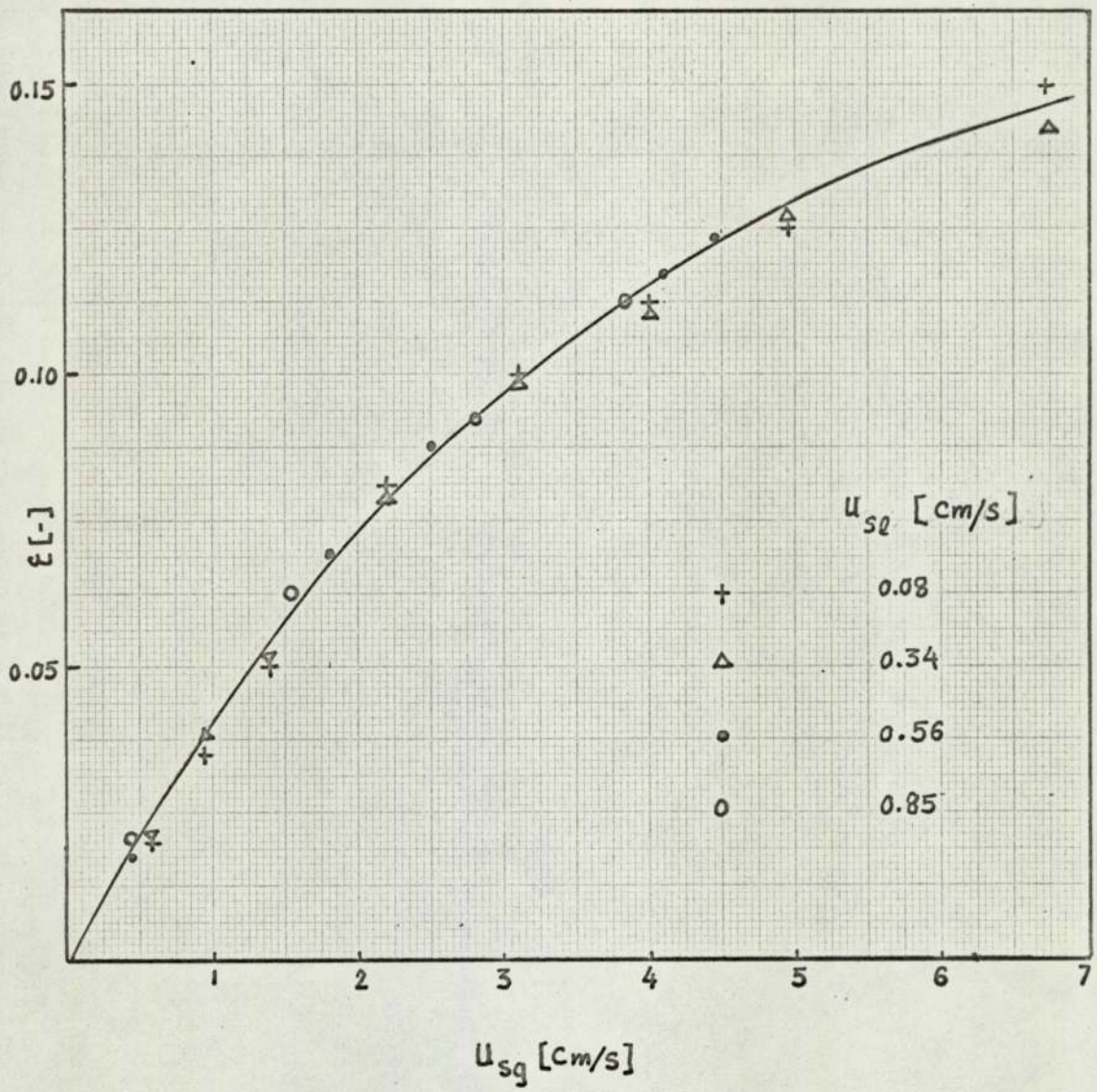

Fig 2.25. Effect of u_{sg} and u_{sl} on Gas Holdup for 61.0 cm Column.

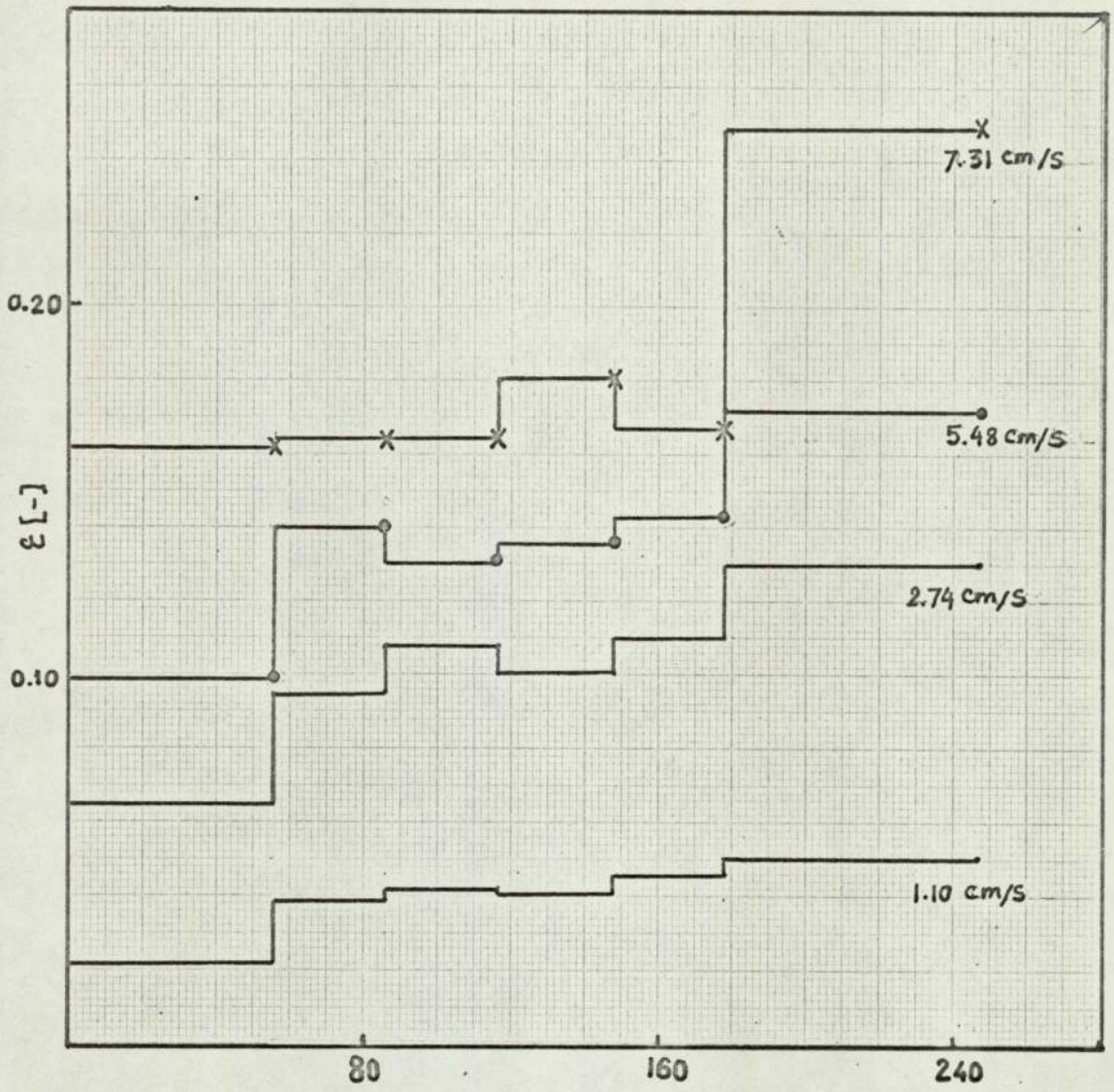

Fig 2.26. Average Gas Holdup Distribution for 15.2 Cm. Column.

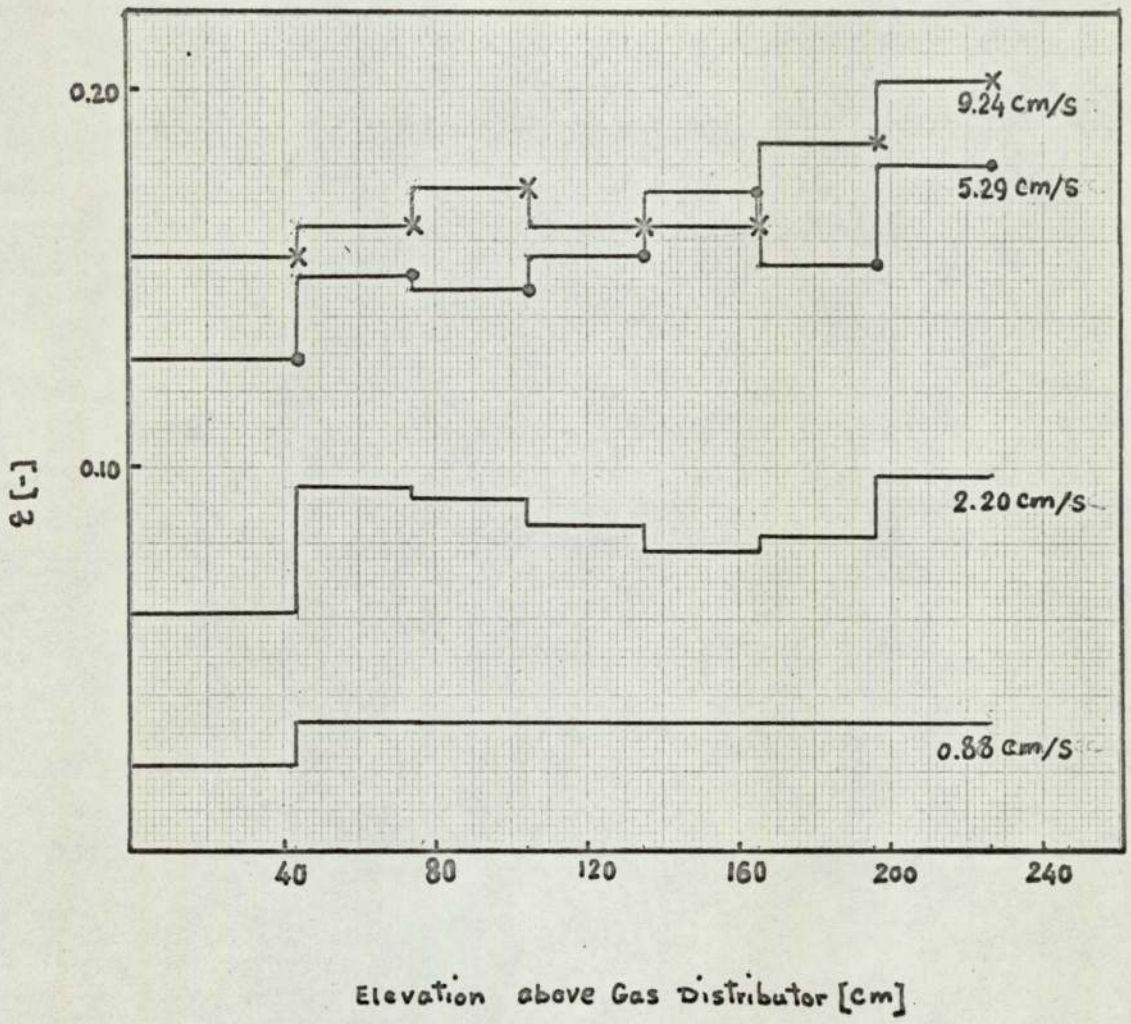

Fig 2.27. Average Gas Holdup Distribution for 30.5 Cm Column.

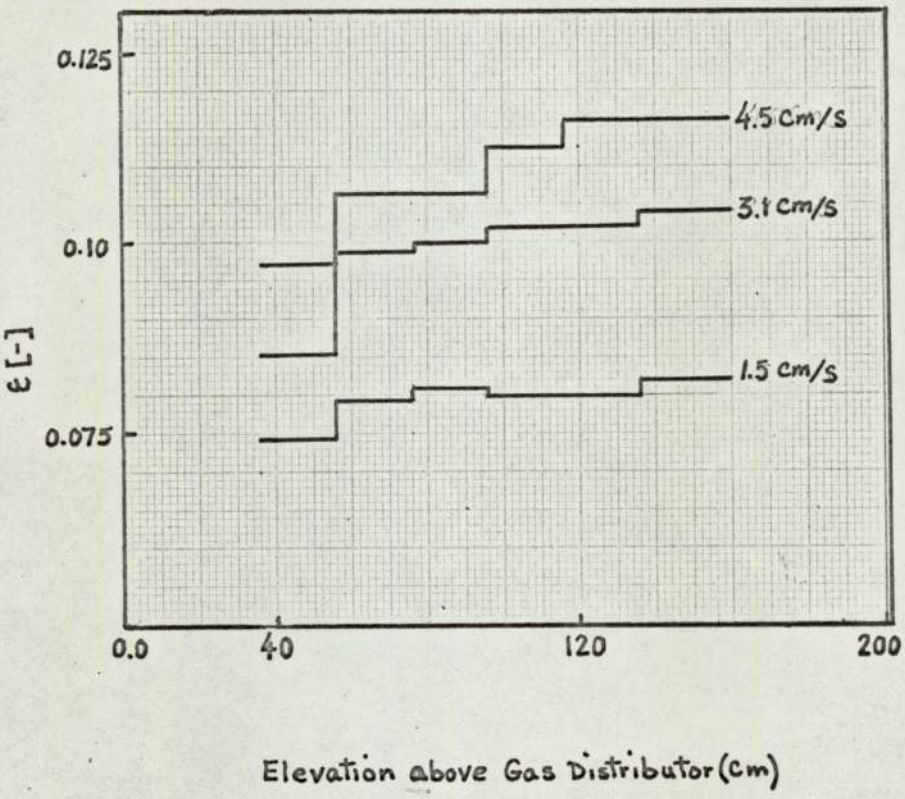

Fig 2.28. Averaged Gas Holdup Distribution for 61 Cm Column.

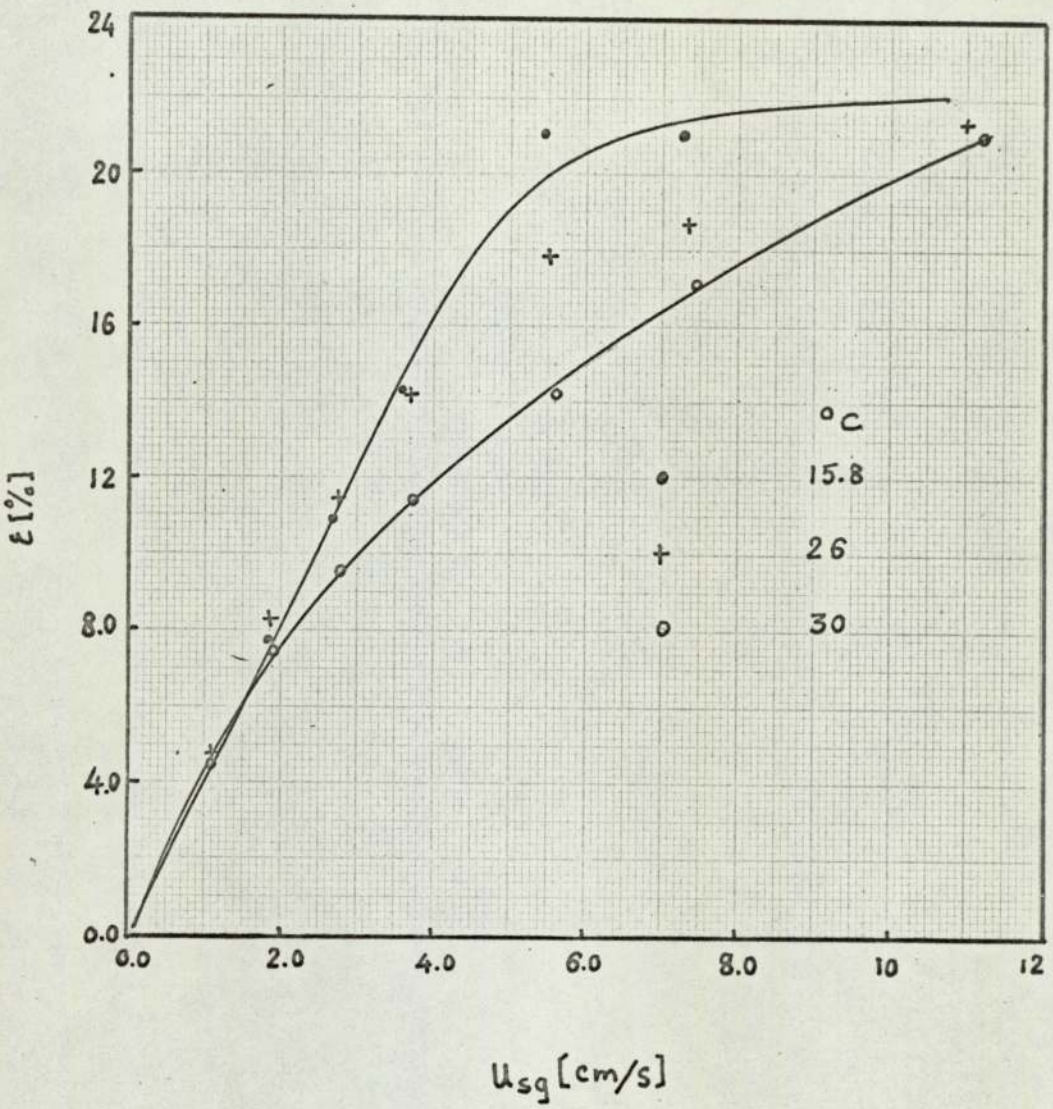

Fig 2.29. Effect of Water Temperature on Gas Holdup for $U_{sl} = 0$

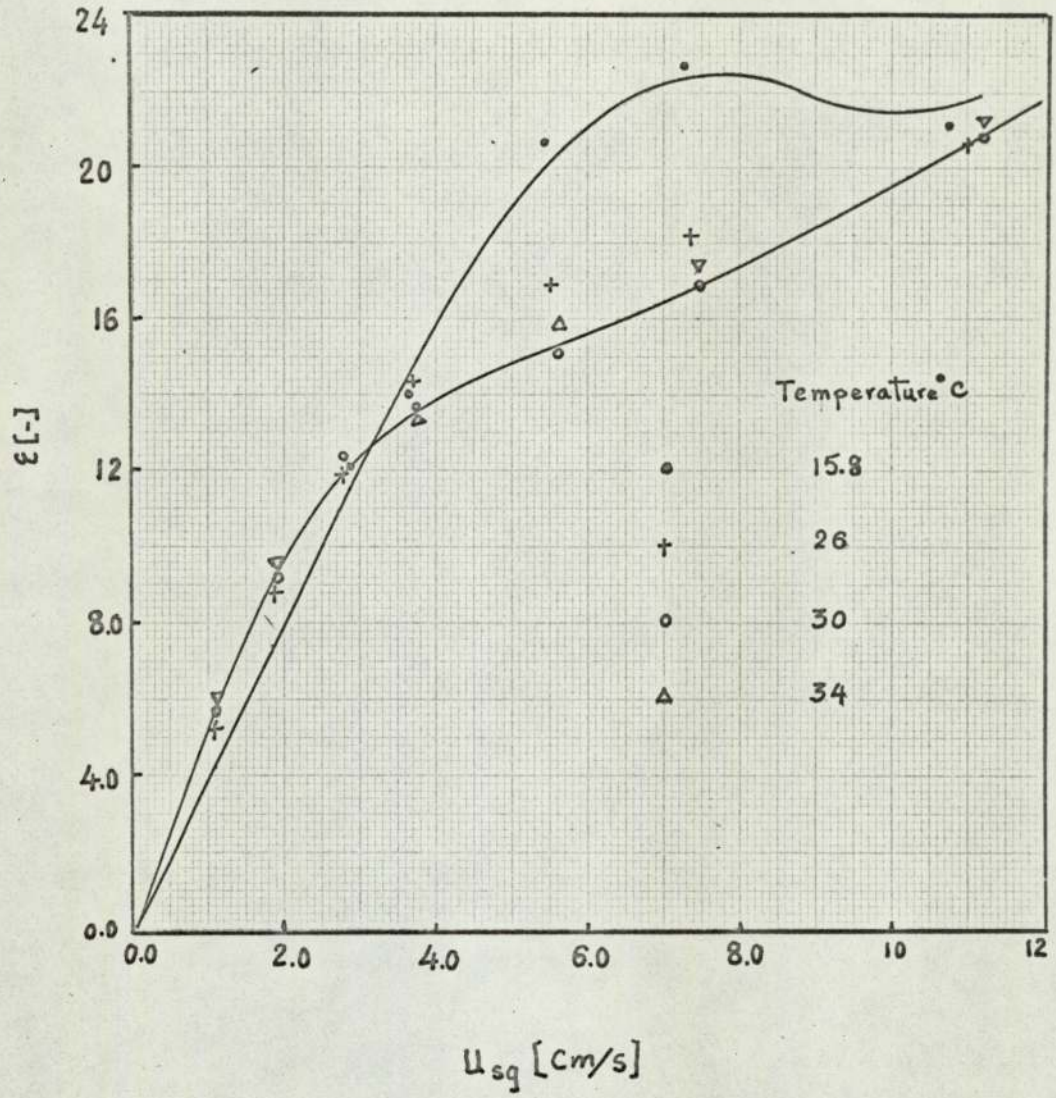

Fig 2.30. Effect of Water Temperature on Gas Holdup

for $U_{sl} = 1.87$ cm/s

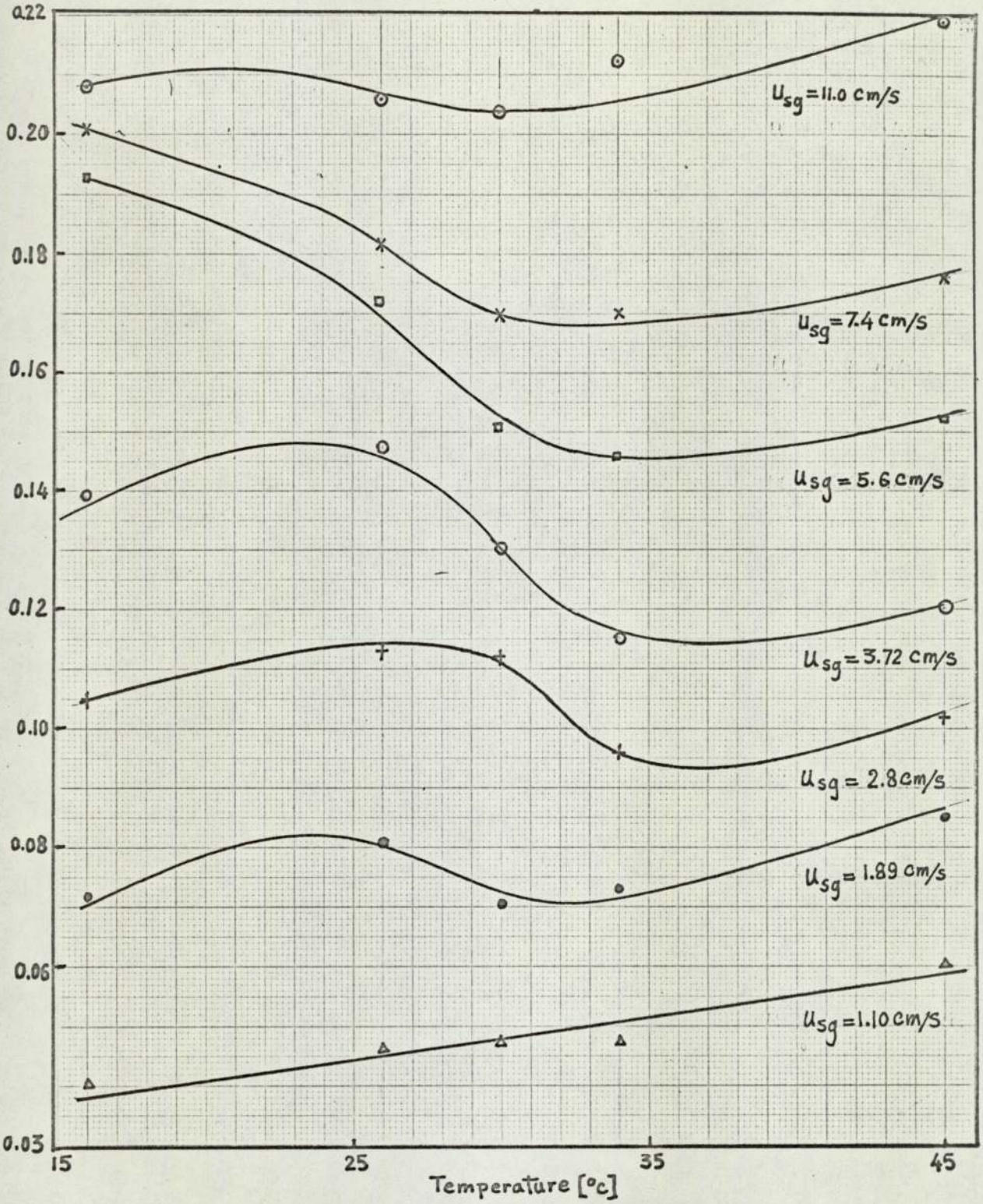

Fig 2.31. Effect of water Temperature on Gas Holdup for U_{sl}=0.23 cm/s.

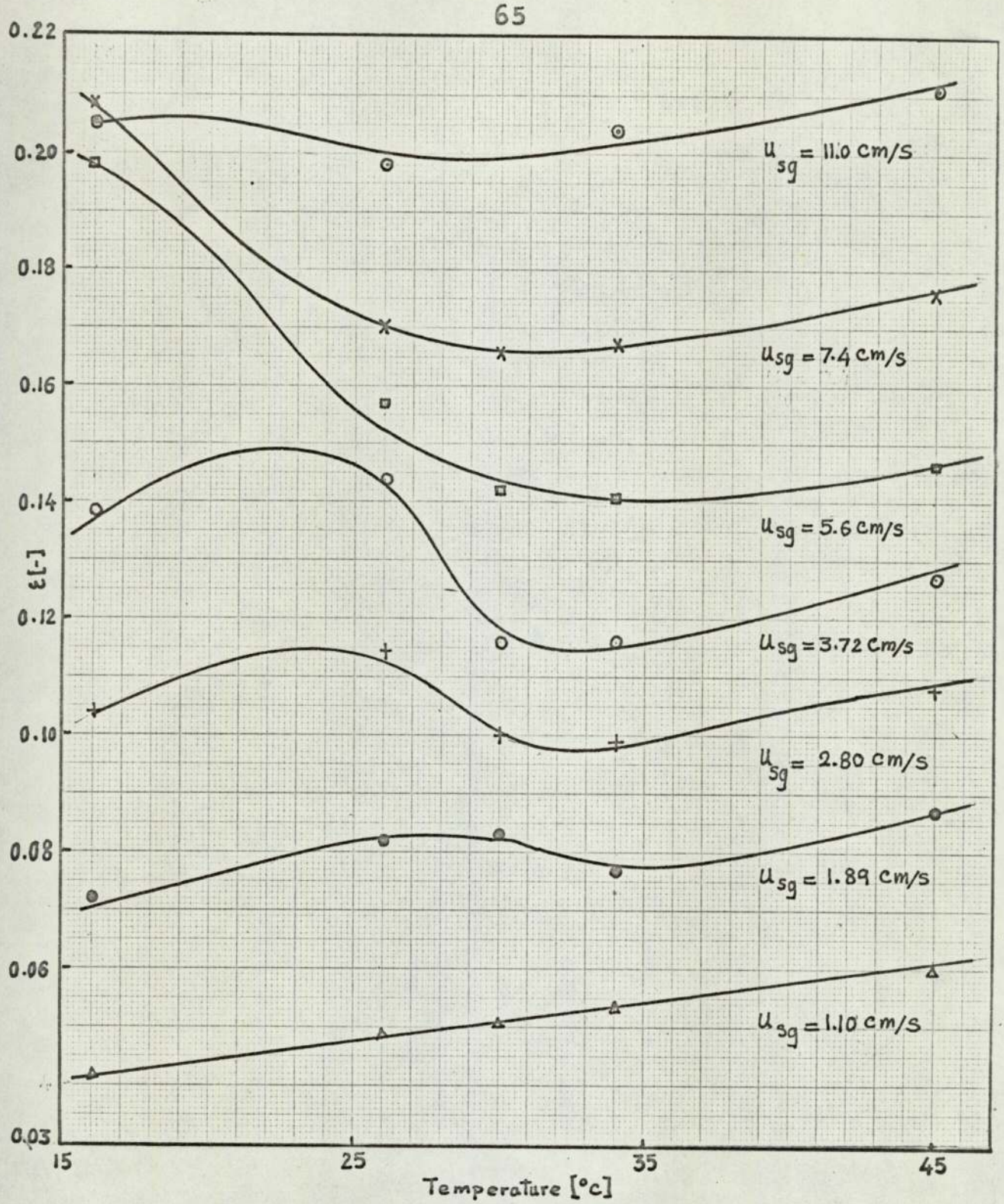

Fig 2.32. Effect of Water Temperature on Gas Holdup for u_{sl} = 0.91 Cm/s.

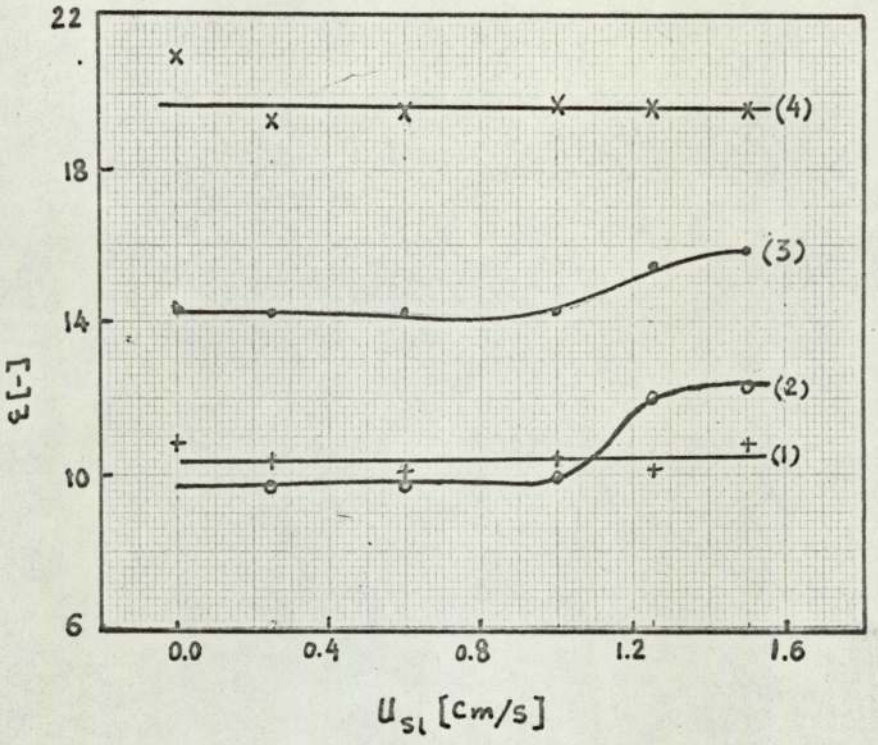

	U_{sg}	Temperature
(1)	2.71	16
(2)	2.80	33
(3)	5.59	33
(4)	5.43	16

Fig 2.33. Effect of Liquid Flow-Rate on Gas Holdup at Different Temperatures.

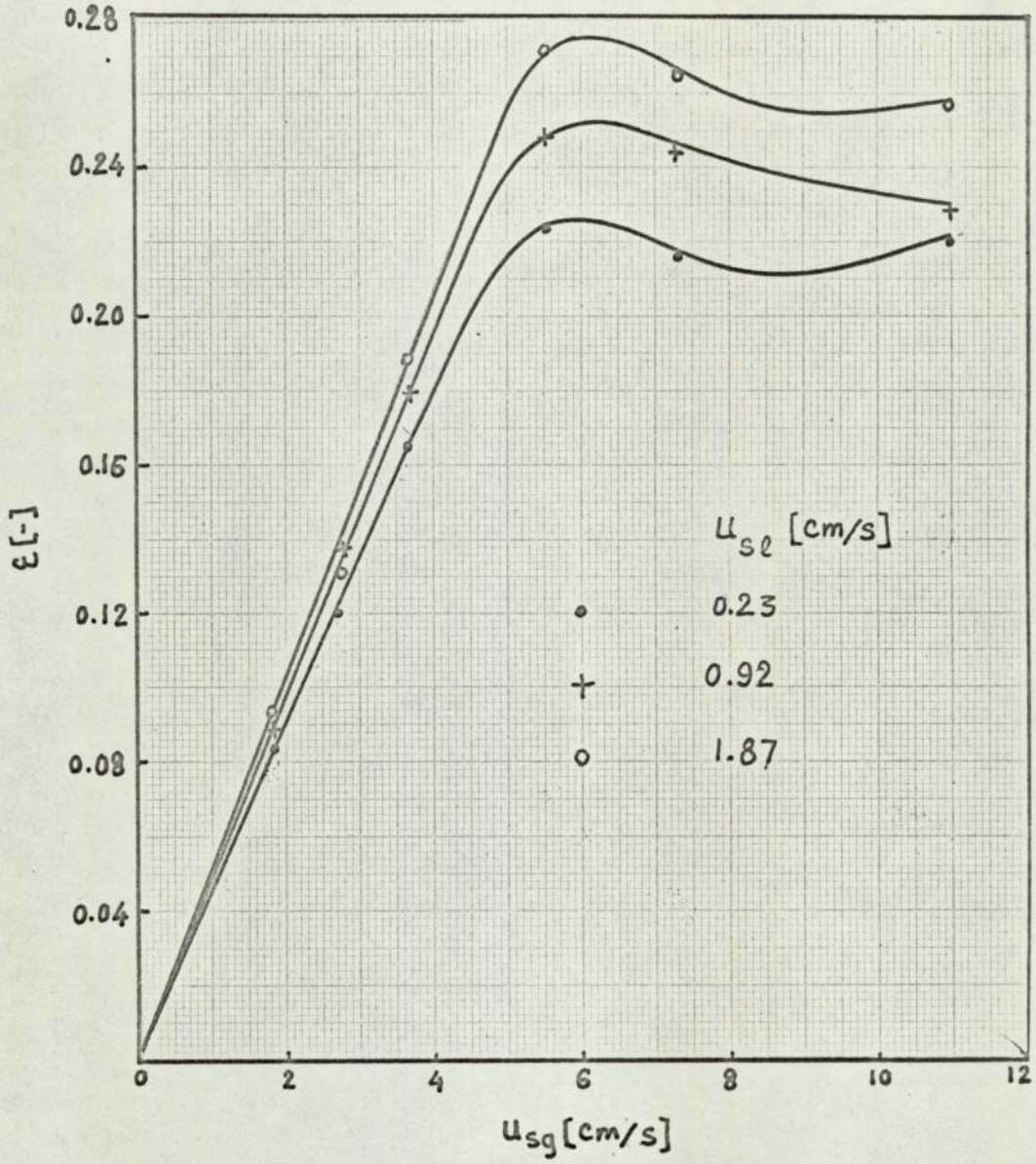

Fig 2.34. Effect of Electrolyte Solution (1% wt/wt KCl) on Gas Holdup.

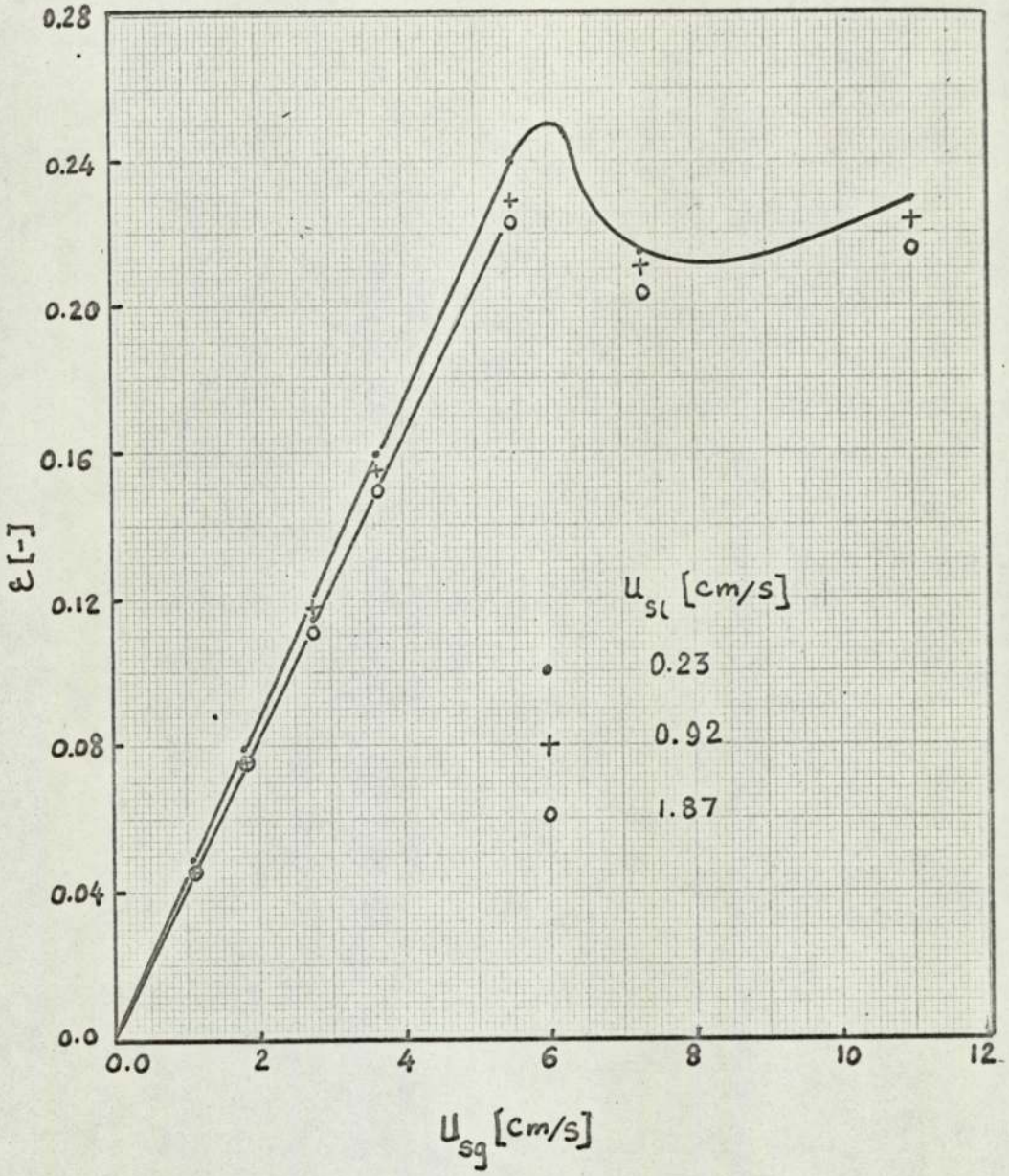

Fig 2.35. Effect of Electrolyte Solution (4% wt/wt Kcl) on Gas Holdup.

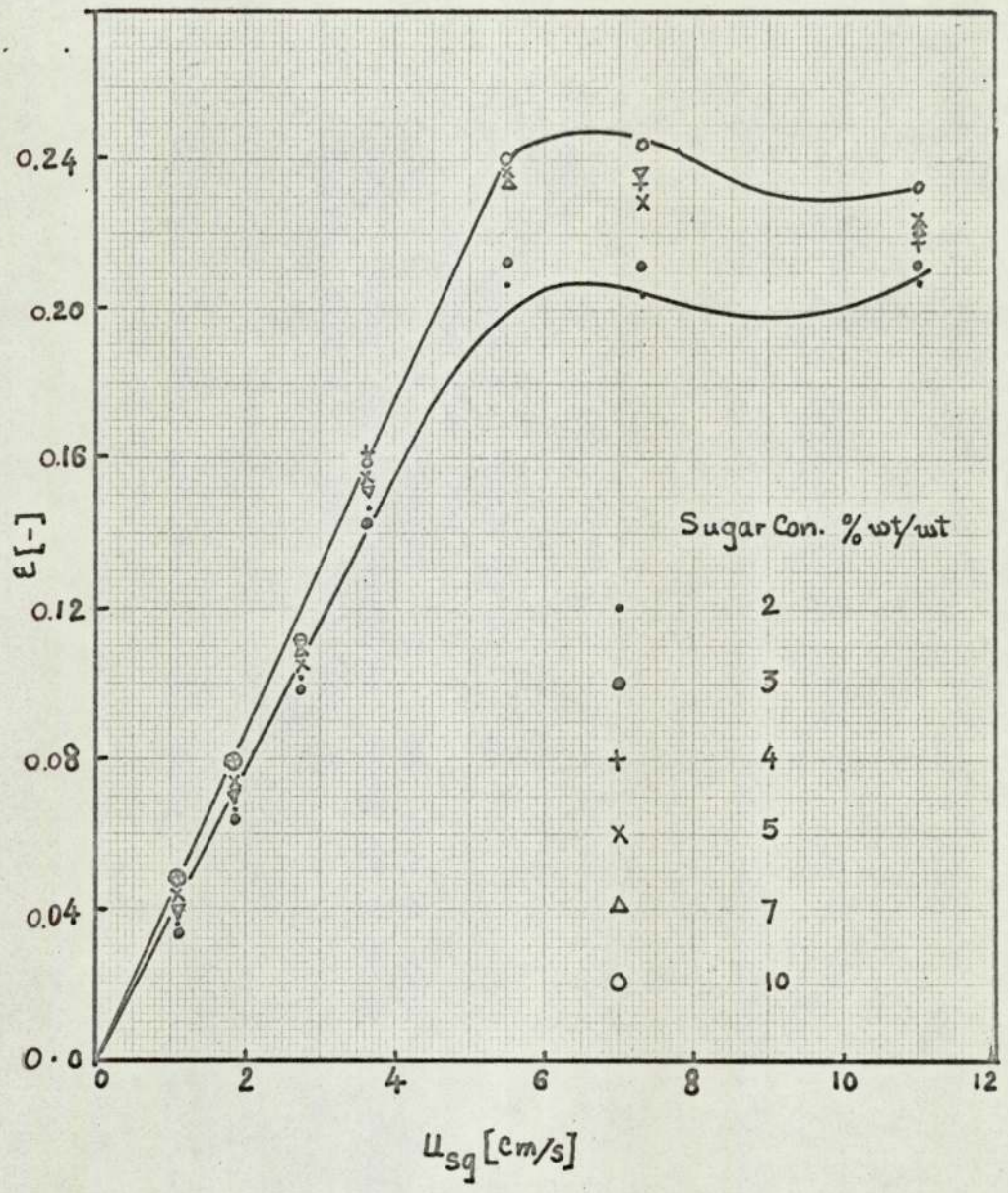

Fig 2.36. Effect of Different Concentrations of Suger Solutions on Gas Holdup.

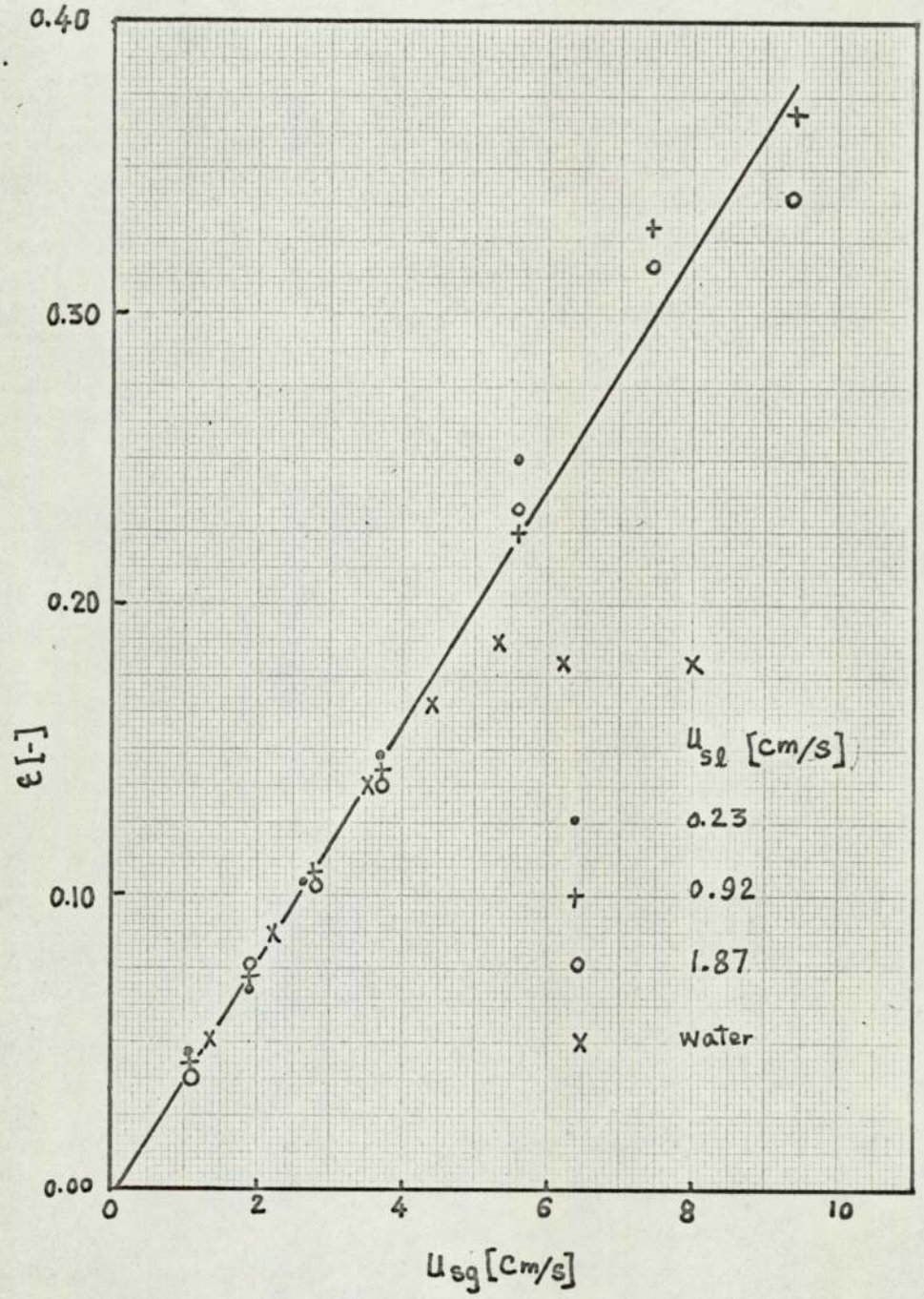

Fig 2.37. Effect of Diluted Malt Extract on Gas Holdup.

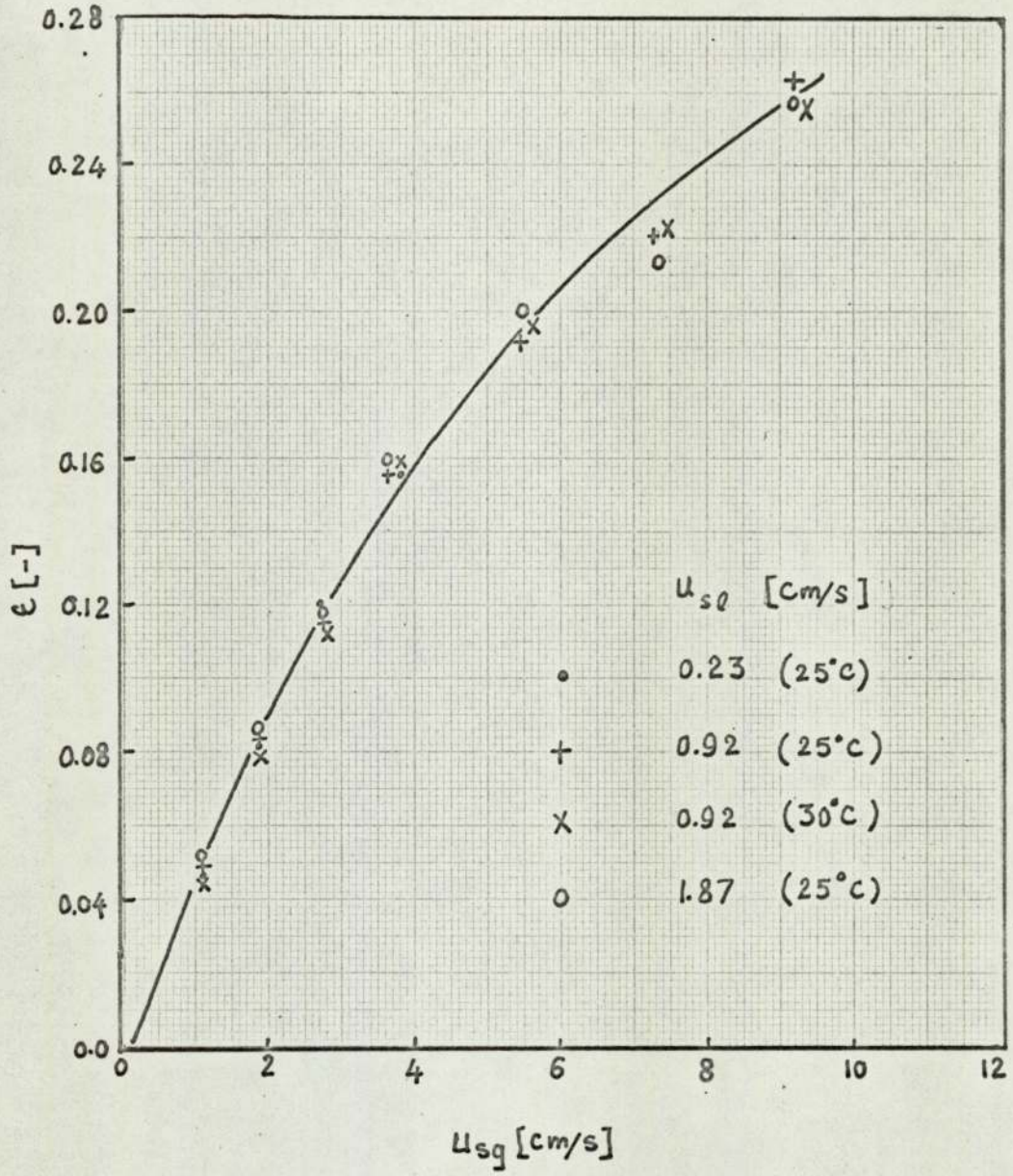

Fig 2.38. Effect of charging wort on Gas Holdup.

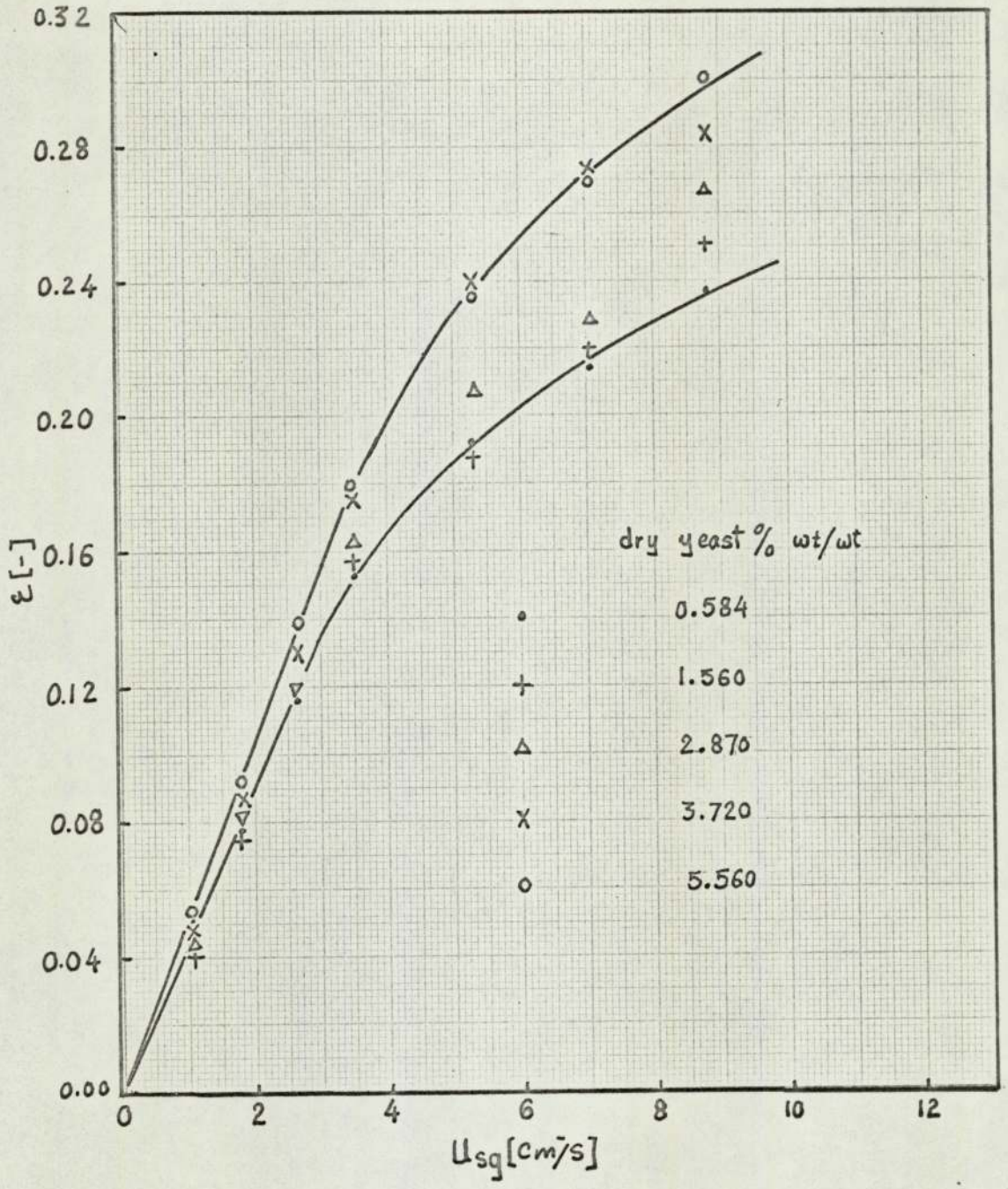

Fig 2.39. Effect of U_{sg} on ε For Different yeast Suspensions at $U_{s\ell} = 0.92$ cm/s.

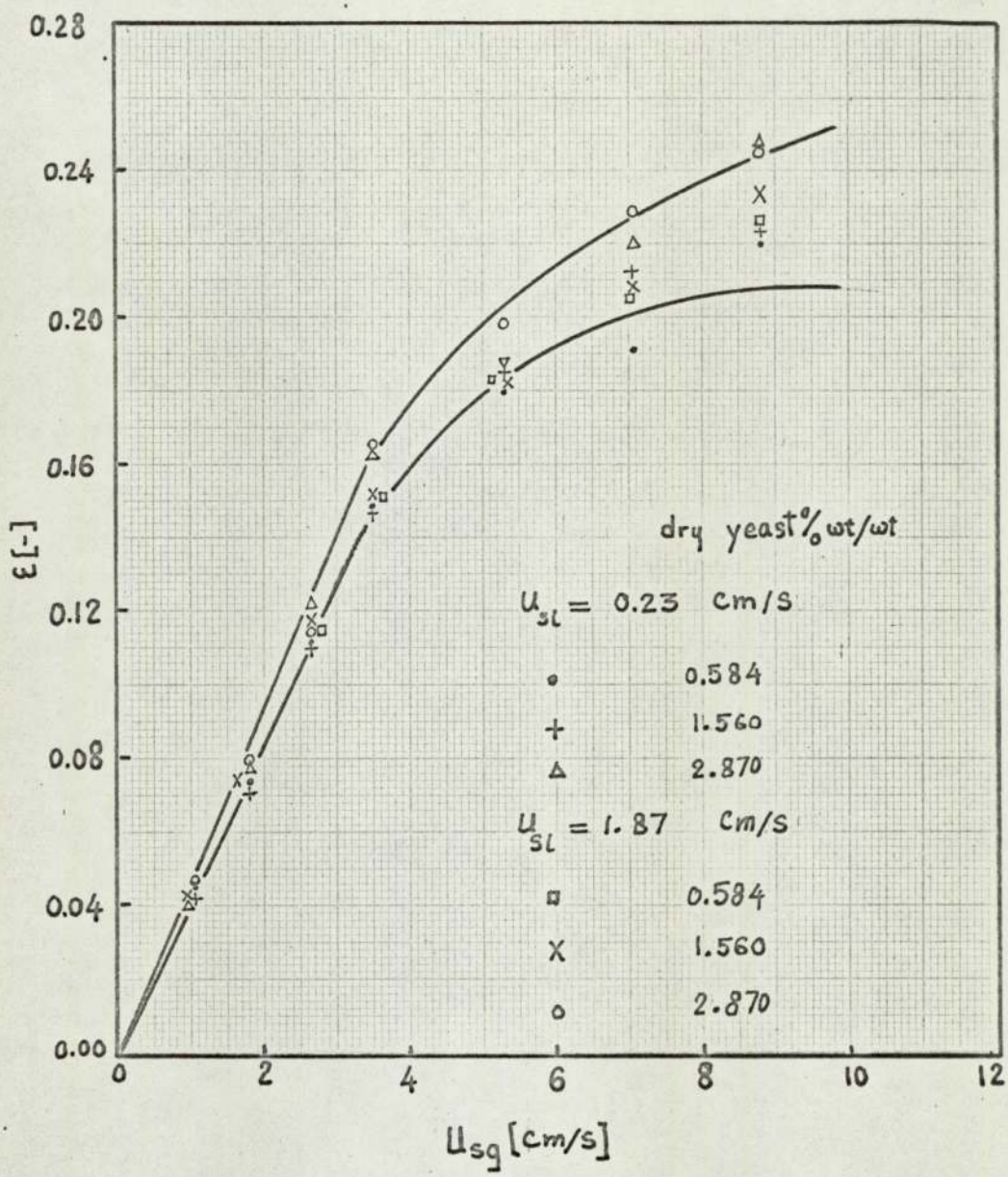

Fig 2.40. Effect of U_{sg} on ε for Different Concentrations of yeast Suspensions at Different Flow-Rates.

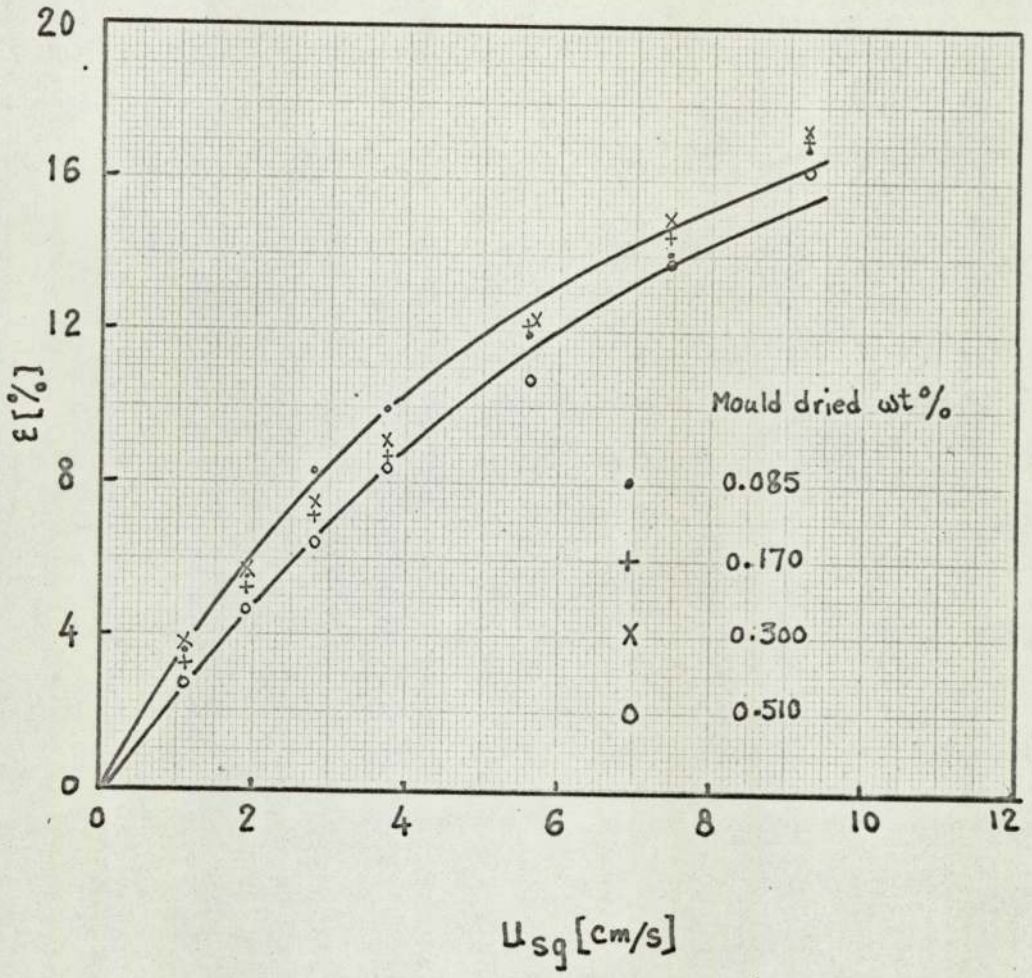

Fig 2.41. Effect of U_{sg} on ε for Mould Suspension.

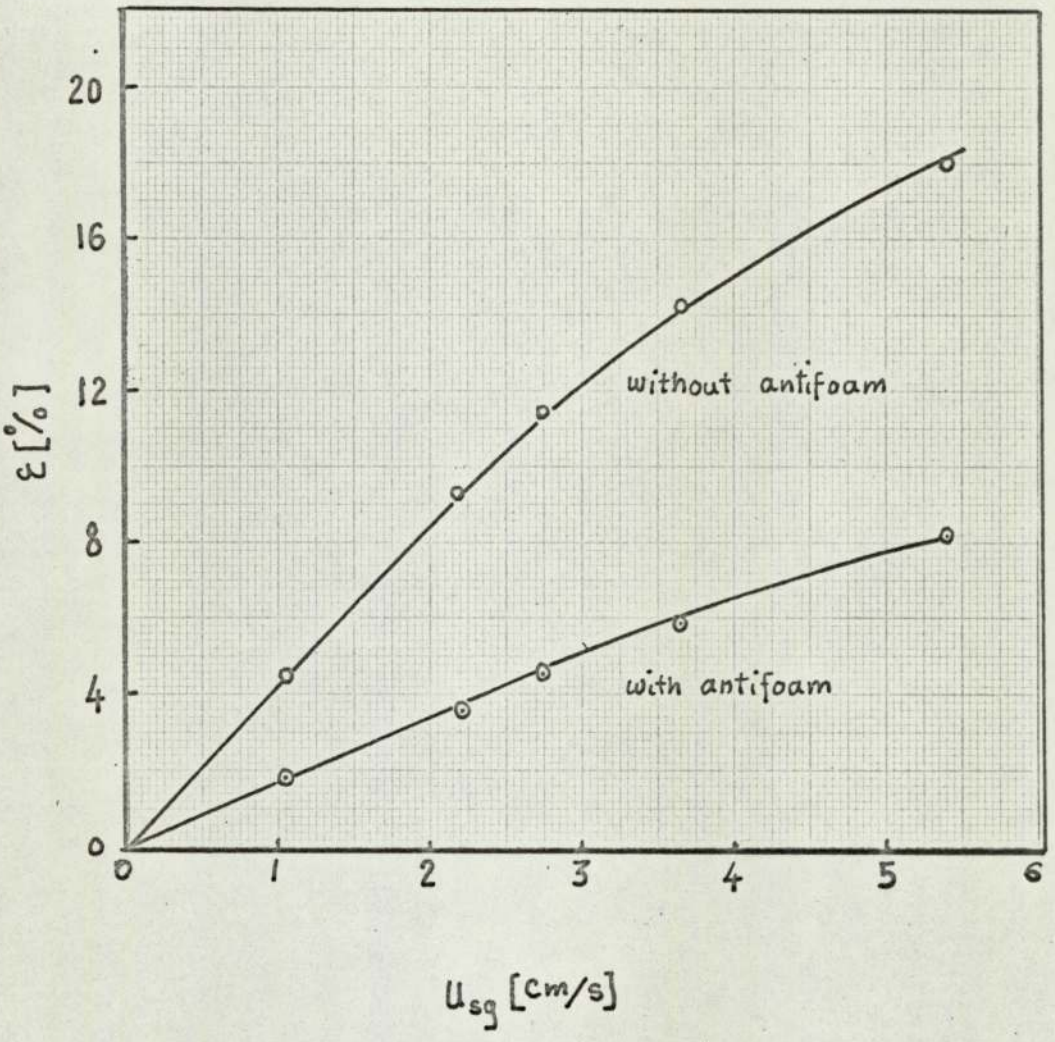

Fig 2.42. Effect of U_{sg} on ε with and without Antifoam.

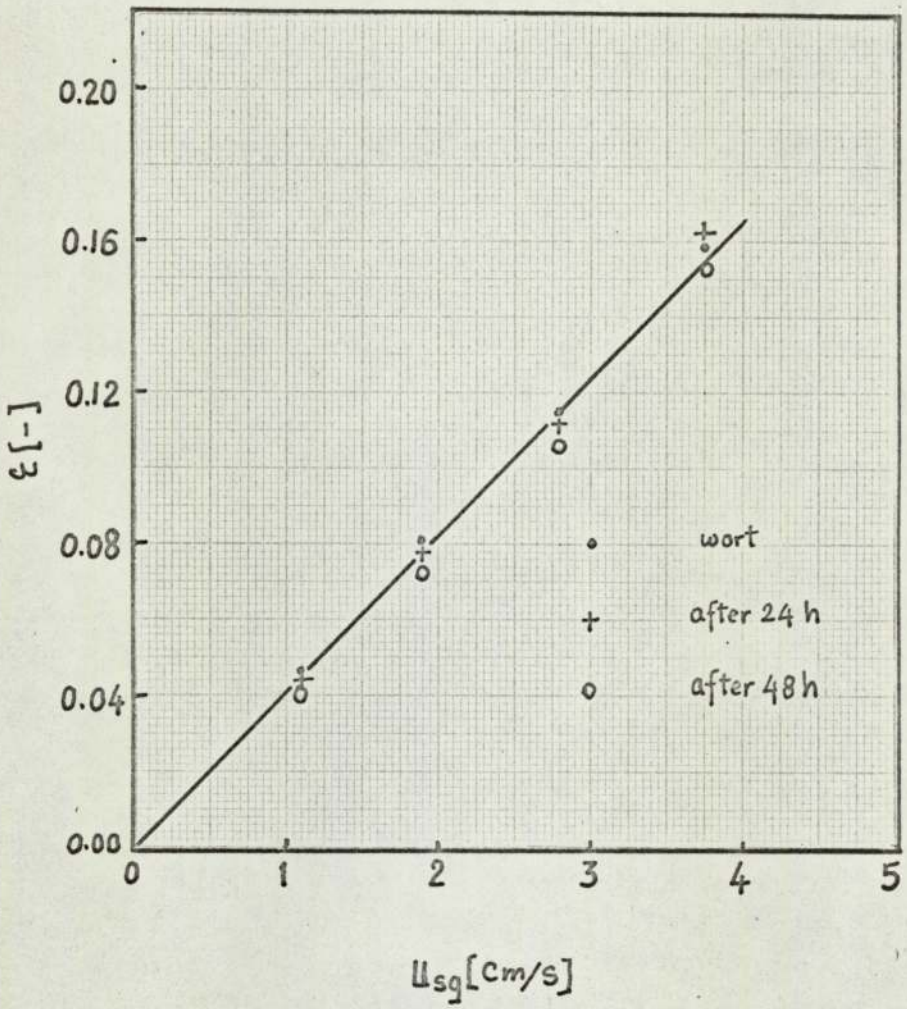

Fig 2.43. Effect of U_{sg} on ε at Different stages of vinegar production.

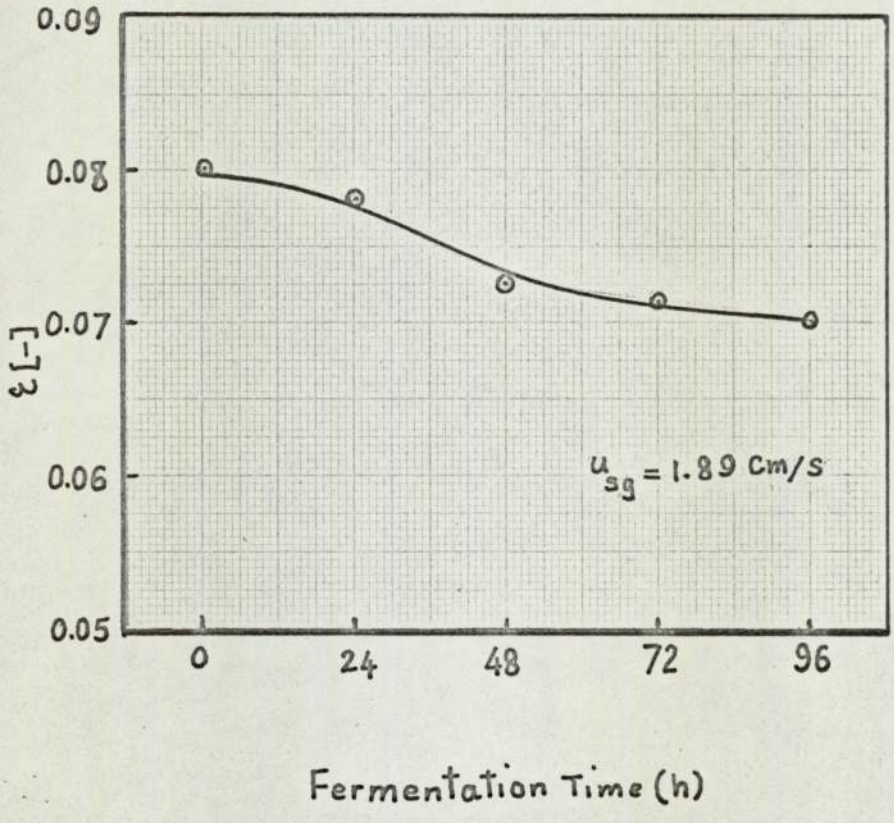

Fig 2.44 Variation of Gas Holdup with Time in production of Vinegar.

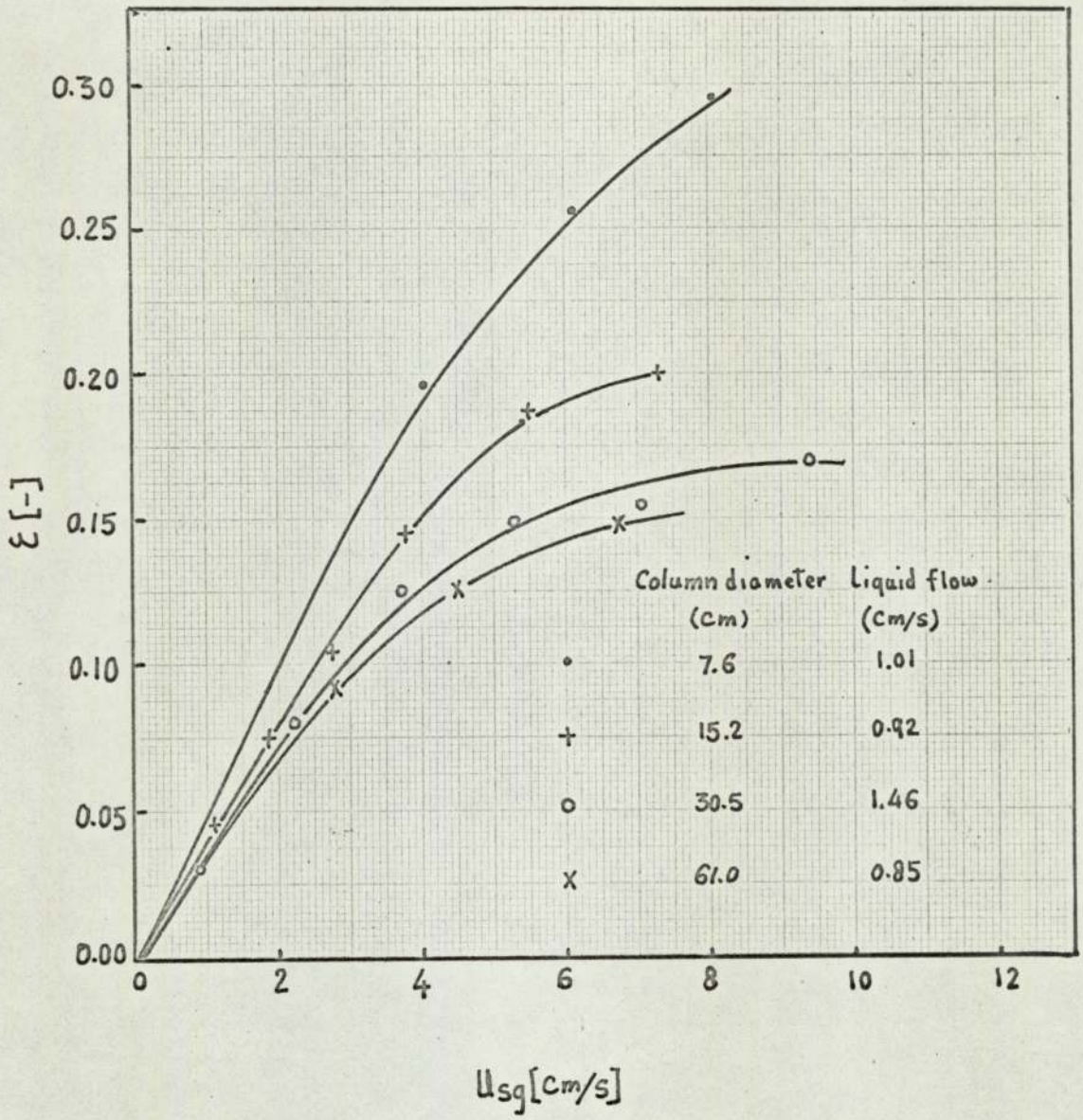

Fig 2.45. Effect of Column Diameter on Gas Holdup.

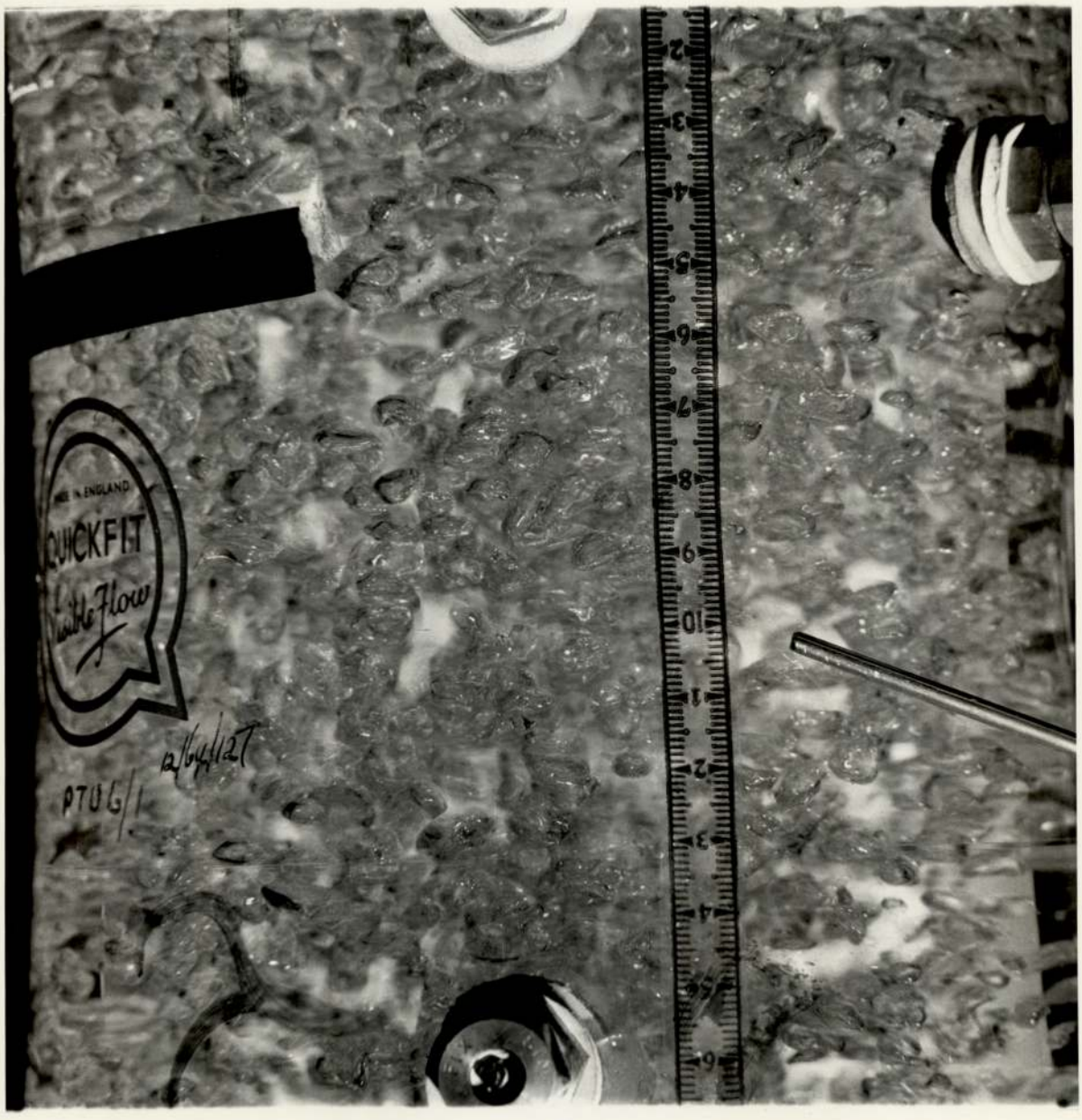

Fig 2.46. Air-Water without Antifoam (U_{sg} = 2.74 cm/s).

Fig 2.47. Air-Water with Antifoam (u_{sg} = 2.74 cm/s).

2.5. Discussion and Conclusions

2.5.1. Introductory Comments

The Complexity of System Behaviour

Experimental results in section 2.4. suggest that the superficial gas velocity is not the only important factor affecting the gas holdup. Superficial liquid velocity, column geometry and the physical properties of the liquid phase all affect gas holdup, although these effects are more pronounced in certain special cases. For instance, the effect of superficial liquid velocity on gas holdup is not significant for air-water systems at normal temperatures (see Figs.2.22, 2.23, 2.24, and 2.25) : however, its effect on holdup increases when the temperature of the system is raised above 30°C (see Fig.2.33). Again, a rise of temperature may not have such a marked influence on holdup when other physical properties of the system are changed (see Fig.2.38).

Relationship between Holdup and Gas Velocity

In general, the relationship between gas holdup and superficial gas velocity in the bubbly flow regime can be put in the form

$$\varepsilon = q \cdot u_{sg} \qquad (2.38)$$

where q, the "characteristic" of the system, can be dependent on column geometry, distributor design and the physical properties of the system.

Table 2.1 shows the values of q for different systems.

Turner (19) assumed $q = \frac{1}{u_\infty}$ since for air-water systems u_∞ appears to be reasonably constant for the range of superficial gas velocities and bubble size. Under conditions of zero liquid flow, suggestions for predicting q proposed by other workers can

System	q
7.6 cm diameter column	0.048
30.5 cm diameter column	0.034
61.0 cm diameter column	0.028
15.2 diameter column	
Air-water system	0.040
KCl solution	0.042
Malt extract	0.042
Charging wort	0.043
Yeast Suspension	0.043
Air-water with antifoam	0.018
Vinegar fermentation	0.041

Table 2.1. Average value of q defined by Equation 2.38 ($u_{sg} < 4$ cm/s)

be put in the form

$$q = \frac{1}{u_\infty (1-\varepsilon)^n} \qquad (2.39)$$

where n takes values from -1.0 to +2.0. In the bubbly flow regime, $0.15 > \varepsilon > 0$ and so changes in the term $(1-\varepsilon)^n$ are not very large. Because of the errors inherent in most methods of measuring holdup it is not possible to select a value for n with confidence. With the present state of knowledge about the hydro-dynamic behaviour of bubble columns, it is recommended that Turner's equation be used. This equation fits most of the author's experimental data for the smallest column up to relatively high gas velocities (8 cm/s). However, for air-water systems deviations from a straight-line

relationship become more pronounced as the column diameter is increased.

Liquid flow Patterns

Bubbles, when they rise, displace the liquid around them and can also carry a considerable amount of liquid in their wakes. When the net flow of liquid is zero, liquid must flow downwards to balance that carried upwards. The question therefore arises as to how and where the liquid travels downwards. As the bubbles follow paths of least resistance, there is a tendency for them to move away from the column walls: intuition therefore suggests that there will be a zone close to the wall relatively free of gas where it is easy for liquid to flow downwards. The area occupied by this zone compared with the total cross-section of the column could clearly have an important influence on the flow patterns of liquid and bubbles in the system. For air-water systems, at low superficial gas velocities, the average bubble diameter can be taken to be 5 mm. If it is also assumed that the 'bubble-free' zone extends for a distance of 10 mm from the wall, then the data shown in Table 2.2 are readily obtained.

Column diameter	Cross-section area (cm^2)	10 mm annular area (cm^2)	% (-)
7.6	45.58	20.87	45.8
15.2	182.3	44.7	24.5
30.5	729.3	92.6	12.7
61.0	2917	188	6.4

Table 2.2. Effect of Column Diameter on Relative Area occupied by "Bubble-Free" zone

Table 2.1 demonstrates the extent of the wall effects in smaller columns. Almost half of the total cross-section in the 7.6 cm diameter column could be affected by the wall effect, whereas this figure is only 6% in the 61.0 cm diameter column.

The volume of the wake or liquid transported upwards by each bubble is likely to vary with conditions in the column. In order to get an idea about the amount of liquid travelling downwards and its velocity, it will be assumed that (1) the wake volume is identical to that of the bubble, (2) $u_{sg} = 5$ cm/s and (3) $\varepsilon = 0.20$. Using these figures the holdup of the bubbles and wakes ε_{g+w} is 0.4. Consequently, the cross-sectioned area left for liquid to flow downwards is 0.6. If say half of this area were used for downwards flow, then the interstitial liquid velocity would be 15 cm/s. That such high velocities occur is supported by visual observations of the movement of bubbles and tracer-particles inside the column.

At low gas velocities, when the space between individual bubbles is relatively large, liquid downwards flow is small and does not greatly affect the movement of bubbles. At higher gas velocities the space between the bubbles reduced and at the same time the liquid circulation rates increase. This causes the bubbles to deviate from a vertical flow path.

Fig 2.48 . Effect of Liquid Downwards Flow on Bubble Movement.

Fig 2.48 shows bubble (a) being carried down by liquid and bubble (b) slipping sideways and rising at different points in the column.

In smaller columns it seems likely that most of the liquid flow downwards will take place near the walls with the bubbles concentrated over the central area (see Fig.2.49.)
In large columns, where the "free" area near the wall is not so great, "liquid streams" moving counter-currently to highly concentrated "bubble swarms" might be expected to appear over the whole of the column cross-section.
Fig 2.50 shows this arrangement of bubbles and liquid in a very simplified fashion.

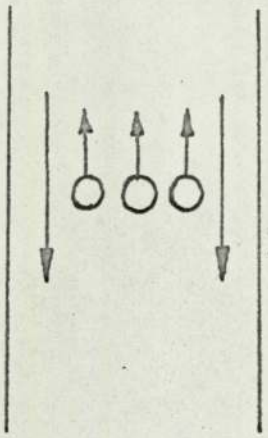

Fig 2.49 Downwards Liquid Streams in Small Bubble Columns.

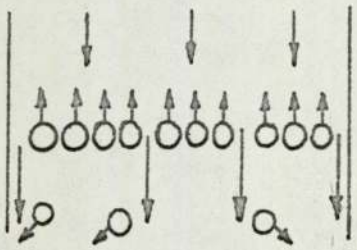

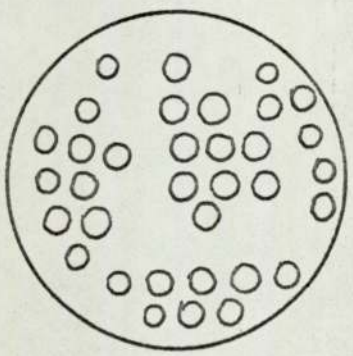

Fig 2.50 Downwards Liquid Streams in Large Bubble Columns.

The local swarms of bubbles will obviously create pressure differences over the column cross-section and so swirling of liquid streams and eddy formation will occur. Such movements of gas and liquid may help to explain the level fluctuations observed in the manometers during the course of gas holdup measurements. The modified form of gas-liquid flow patterns in large columns may also account for the reduction in gas holdup (at a fixed value of u_{sg}) with increase in column diameter.

2.5.2. Effect of Superficial Gas Velocity on Gas Holdup

In general, increasing superficial gas velocity increases the gas holdup to a greater or lesser extent, depending upon other factors. At very low values of u_{sg} the increase is almost linear with increasing gas velocity in most cases. The departure appears when bubbly flow is replaced by a less orderly turbulent-flow regime. In the case of air-water systems in medium size columns (15.2 - 30.5 cm), this happens at u_{sg} >4.0 cm/s Departure from bubbly flow causes a small reduction in ε in some cases followed by a gradual increase as the new regime develops (see Figs.2.23 and 2.24).

2.5.3. Effect of Superficial Liquid Velocity on Gas Holdup

Superficial liquid velocity has little effect on gas holdup for the range studied. In general increases in liquid-phase velocity cause a quicker wash-out of the gas-phase with a consequent reduction in gas holdup (see Fig.2.22).

Interactions between liquid flow and other variables complicate the picture. At higher values of u_{sl} (turbulent regime) the level of turbulence close to the gas and liquid distributors may lead to the formation of smaller bubbles and increased gas holdups.

Fig.2.33 shows the effect of superficial liquid velocity on gas

holdup for air-water systems at different temperatures. At 16°C there is almost no effect of liquid velocity on gas holdup, but at higher water temperatures the effect is more marked especially as the regime changes from laminar to turbulent.

2.54. Effect of Gas Distributor Design on Gas Holdup

Despite differences in the size of the holes in the various gas distributors, the bubbles produced usually reached a stable size within a few centimetres above the distributors. Any maldistribution also appeared to be evened out at a height equivalent to one or two column diameters.

Figs.2.26, 2.27 and 2.28 show that the gas holdup is somewhat lower near the base of the column: such differences get less significant as superficial gas velocity increases. It may be concluded that the dependence of gas holdup on gas distributor design is slight, provided gas distribution is uniform and the height to diameter ratio of the column is large.

2.5.5. Effect of Column Diameter on Gas Holdup

Fig.2.45 shows the effect of column diameter on gas holdup. In small columns the wall has an important effect on system behaviour (see p. 83). Downward liquid flow near the walls and bubble movements in the centre result in higher gas holdups. At a fixed value of u_{sg}, holdup gradually reduces as the diameter increases and liquid circulation spreads around the column.

2.5.6. Effect of Column Height on Gas Holdup

Figs.2.26 - 2.28 show the changes in gas holdup with height for the 15.2, 30.5 and 61.0 cm columns. Neglecting the two ends of the columns, the gas holdup varies very little from one section to another: this suggests that there are no significant changes in

bubble size and flow pattern with position up the columns. Behaviour at the extreme ends of the columns contrasts remarkably. At the bottom, lower gas hold-ups are observed due to jetting and mal-distribution. However, these effects gradually reduce as the superficial gas velocity increases and liquid circulation develops. At the top, holdup is above average due to reduction in hydrostatic pressure (and consequent expansion in bubble volume) and also to the formation of a layer of froth: these effects increase as the superficial gas velocity increases. In Figs.2.27 and 2.28 the increase in holdup at the top is not pronounced so much as in Fig.2.26. This is due to the fact that the very top sections of the 30.5 cm and 61.0 cm columns were not included in the measurements.

2.5.7. Effect of Liquid-phase Temperature on Gas Holdup

Figs.2.28 - 2.32 show the effect of liquid phase temperature on gas holdup for different superficial liquid velocities. Viscosity and surface tension measurements of water in the range of temperature studied are given in Table 2.3 below.

Temperature (^{o}C)	15	20	25	30	35	40	45
Surface Tension (dyn/cm)	73.8	72.6	71.5	70.5	69.7	69.1	68.3
Viscosity (C.P.)	1.15	1.01	0.891	0.754	0.725	0.658	0.601

Table 2.3. Values of Surface Tension and Viscosity of Birmingham Tap Water for Different Temperatures.

Figs.2.31 and 2.32 show that at low superficial gas velocities, i.e. U_{sg} = 1.0 - 1.5 cm/s (when the liquid downwards flow is small), a slight decrease in surface tension causes the formation of smaller bubbles (41) and a slight increase in gas holdup (42). As the

superficial gas velocity gradually increases, liquid circulation has an increasing effect. Increasing temperature reduces the viscosity significantly (see Table 2.2) and causes greater turbulence . Bubble coalescence is observed as temperature exceeds 25°C and this reduces the gas holdup. A number of very small, stable bubbles results from the vigorous collision and coalescence of the gas bubbles as the surface tension falls. With a further increase of temperature, the number of these bubbles increases and the gas holdup increases slightly.

In the turbulent flow regime, i.e. U_{sg} = 5.5 - 7.5 cm/s, a reduction in viscosity increases bubble mobility and interaction leading to a sharp reduction in gas holdup. As the volume of fine bubbles increases substantially, hold-up slowly rises. Further increases in superficial gas velocity up to 11 cm/s create such turbulence that increasing temperature does not affect coalescence rate to any significant extent. Nevertheless the number of fine bubbles increases and gas holdup tends to rise.

2.5.8. Effect of Electrolyte Solutions on Gas Holdup

Experimental results (see Figs.234 and 2.35) suggest a significant increase in gas holdup in KCl solutions compared with figures for air-water systems. The presence of electrolytes somehow inhibits the coalescence and very fine bubbles appear. These fine bubbles - so-called "ionic bubbles" - have very low rise velocities and so increase gas holdup. Higher concentrations of KCl lead to slightly lower gas holdups.

2.5.9. Effect of Fermentation Media on Gas Holdup

In air-water systems, bubble size and the limited degree of coalescence are the two main factors limiting gas holdup to

around 0.2. Up to superficial gas velocities of 4 - 5 cm/s there is little noticeable change in bubble-cloud behaviour with bubbles maintaining their size and independence. Increasing superficial gas velocity above this limit leads to a breakdown in the stability of bubble flow and coalescence occurs. The consequent formation of large bubbles, with their much higher rise velocity, halts the linear increase of gas holdup with superficial gas velocity (see air-water plot in Fig.2.37). This sudden decrease in the slope of the curve has also been reported by previous workers (see p. 23)

Any additive in the system which causes a reduction in bubble size or hinders the bubble coalescence or both can raise the gas holdup. Fermentation media, because of their surface active properties do just this. In the case of malt extract solution, which has very low surface tension, the break in the ε vs u_{sg} curve never occurred and gas holdup increased almost linearly with superficial gas velocity in the range studied.

The results with different concentrations of yeast (see Figs.2.39 and 2.40) show that the gas holdup increased as the yeast level was raised. This was expected as surface tension was reduced and the foaming ability of the system increased. For practical purposes one could say that at high yeast contributions the gas holdup increases by 20 - 30% compared with that in air-water systems.

Charging wort behaves in a similar way. Fig.2.38 shows a smooth increase of gas holdup with superficial gas velocity but the plot is not as linear as in the case of malt extract solution. This is because of the lower foaming ability of charging wort compared with malt.

The gas holdups measured with the mould A. niger were much

lower (see Fig.2.41). At first, the reason for this was not clear, but later it was learnt that anti-foam had been used during the course of the mould growth. This led to a study of the effect of anti-foam on gas holdup.

2.5.10. Effect of Antifoam on Gas Holdup

In general, antifoams are employed to break up stable surface foams and it is suggested that they function by rapidly spreading on the bubble surface, sweeping away surfactant, and thereby rupturing the bubbles. They appear to be most effective against thin-walled, well-drained foams.

Silicoplase 437 made by I.C.I.Ltd. was used as the antifoam agent, the same one as used by the Department of Biological Sciences during growth of the mould. This agent consists of a 30% silicone solution as methyl polisiloxane and it was diluted by the addition of two parts of water to one part of antifoam emulsion.

The behaviour of the bubble column was entirely changed by adding a small quantity of the emulsion. The departure from bubbly flow occurred at a much lower superficial gas velocity. A wide range of bubble sizes appeared with large bubbles carrying most of the air at very high rise velocities. Pictures on p.79 and p.80 give an indication of the state of the column before and after the addition of 0.5 cc of antifoam to the system; and Fig.2.42 shows the reduction of gas holdup compared with that for the air-water system. Increasing the amount of antifoam agent did not make a significant difference judged both by visual observation and by measurement of gas holdup.

2.5.11. Gas Holdup Variations in Vinegar Production

To avoid using antifoam agent the range of superficial gas velocities used was limited to an upper figure of 2 cm/s. However,

the graph obtained (see Fig.2.43) from the experimental data provides valuable information. For practical purposes it can be assumed that the gas holdup varies almost linearly with superficial gas velocity over the range explored. Fig.2.44 shows the slight reduction in holdup that occurred during the course of fermentation for a given superficial gas velocity. It is interesting to note that the Acetobacter concentration was high at the time of gas holdup reduction.

3. Mixing Studies

3.1 Literature Survey

3.1.1 Continuous Phase Mixing in Two-Phase Systems

Introduction

Studies of mixing in the liquid phase of bubble columns have been carried out by numerous investigators over the last twenty years. Although the extent of mixing has been measured by different techniques, consistent results have not been obtained. The flow patterns and liquid circulation which are caused by upward bubble movement have been paid little attention, although this area has been explored more extensively in the case of gas-solid systems and liquid-liquid systems. The analogy of bubble columns with such systems has not yet been developed.

Bubble Columns

Liquid circulation can occur in a bubble column with or without liquid flow. The work to create the circulation is supplied by expansion of the gas as it rises through the liquid. The circulation generally consists of an upward flow region where liquid relatively rich in entrained bubbles moves upwards and a compensating region where liquid poor in bubbles moves downwards.

In a review article Calderbank (45) mentioned the phenomenon of bubble-street formation in gas-liquid columns without mentioning the circulation and ascribed the phenomenon to the formation of bubble agglomerates or to bubble coalescence.

Towell et al (6) analysed high speed motion pictures taken during operation of a 40 cm diameter column. They observed strong turbulence, mixing, and overall circulation in the liquid-phase by rising gas bubbles, and found that the real rising velocity of the bubbles was strongly increased by the circulation. They suggested that large gas bubble columns behave like a perfectly mixed system. Although this is probably

true for systems in which the height to diameter ratio is not much greater than unity, it may not be true for long, thin vessels.

De Nevers (46) described experiments in an air-water column and found strong circulation of the water phase. He supposed that the circulation was caused by density differences between those parts which were rich and poor in the dispersed phase. Stable circulations could not be obtained when no baffles were present in the system: in this case a chaotic, moving bubble-street was observed. When vertical baffles were situated along the wall or a vertical concentric cylinder was mounted in the column, stable circulation occurred.

Reitema and Ottengraph (47) have also reveiwed circulation in gas-liquid systems and describe experiments in a glass column 22.5 cm in diameter and 122 cm high, with air and glycerol (viscosity 11 poise). Without the use of baffles the circulation was irregular; when vertical baffles were placed along the wall, a symmetrical bubble-street could be readily created. The velocity profile clearly showed a downwards velocity region where radius exceeded 5 cm. Fig 3.1 shows the kind of velocity profile they obtained. They concluded that the principle of minimum energy dissipation can be used to predict circulation in bubble columns, at least when the flow is purely laminar and inertia terms can be neglected.

Ohki and Inoue (75) concluded from the experimental studies of other researchers that the form of the velocity distribution is approximately parabolic. They also suggested that the superficial liquid velocity at the centre of the column u_{slc} is independent of column diameter and can be represented by the following equation for bubbly flow conditions:

$$u_{slc} = 12\, u_{sg}^{0.6}$$

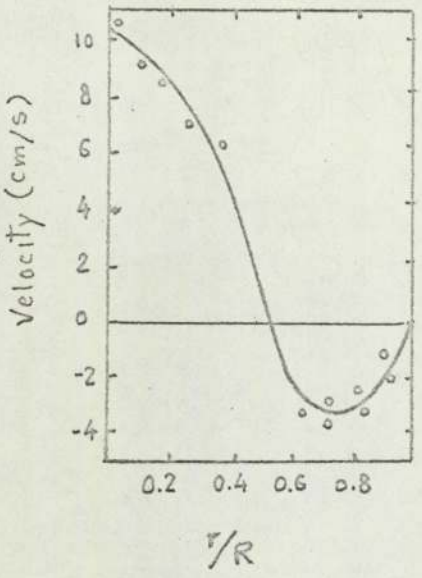

Fig 3.1 Velocity Profile Determined Experimentaly by Rietema and Ottengraf (47).

Their experimental data show that the superficial liquid velocity near the wall, U_{slw} is nearly equal to $-U_{slc}$

Freedman and Davidson (21) observed certain qualitative and quantitative similarities between a column in which internal circulation was induced and one in which a central draught-tube was used to order the flow pattern. They developed a theory for the draught-tube apparatus; and by using an analogy between columns with and without draught-tubes, they provided a method for calculating holdup in circulating systems. This could be extended to describe the mixing and other characteristics of bubble columns. However, they have ignored the mixing attributed to the translation of the continuous phase in the wakes of the bubbles.

Liquid-Liquid and Gas-Solid Systems

Bed circulation has been observed in two-phase systems other than gas-liquid. Donders et alia (48) have carried out experiments in spray-columns used for fat-splitting, and conclude that they exhibit a strong circulation pattern caused by the presence of a droplet-free layer near

the wall of the columns and a homogeneous core of turbulent dispersion. Based on this assumption, Wijffels and Rietema (49) derived a model to predict the circulatory flow profile and the effective axial-mixing coefficient in the continuous phase. Translation of material by transport in the wake of the droplets as well as by circulatory flow has been taken into account. They found that the predominant cause of axial mixing in small columns is translation by wakes and in large columns it is translation by circulatory flow.

Similar phenomena for solid-liquid systems are described by Handley et alia (50). They determined particle paths in a uniformly fluidized bed. Uniform fluidization was produced with a distributor which gave a flat fluid-velocity profile in its immediate vicinity. It was then found that bulk solid circulation could be induced by blanking off the centre of the distributor. This led to a circulation upwards at the wall and downwards at the centre, while blanking off an annular area at the walls produced a circulation upwards at the centre and downwards at the wall. They determined the variation of the average length moved by a particle between deflections and found that the ratio of the vertical and horizontal turbulent particle velocity components was approximately constant at 2.5.

In gas-solid fluidized systems such phenomena have been mentioned by several authors. Whitehead and Young (51) found that for beds exceeding 2ft in diameter, the bubbles have a tendency to rise either centrally or along certain other 'tracks'. This tendency becomes more marked the coarser the gas distributor. Once the bubbles start rising in this preferential way the condition of a uniformly bubbling fluidized bed may no longer exist and 'defluidized' regions can occur with a consequent decrease in the efficiency of gas-solid contacting.

Mixing Mechanisms

Now that the existence of circulation patterns has been clearly demonstrated in different two-phase systems, further consideration will be given to mixing mechanisms.

De Nevers (45) has assumed the mechanism to be very similar to the mechanism of natural convection but with much larger driving forces.

Crabtree and Bridgewater (52) in their report examined theoretically and experimentally the liquid motion induced by a chain of bubbles in a viscous liquid. They were able to account for their experimental results by supposing the gas to be equivalent to a line of force acting vertically upwards along the axis of the column.

Rowe (53) has suggested that consideration of the displacement of fluid by a solid sphere moving upwards can help in understanding mixing phenomena in two-phase systems. Fig 3.2, which has been taken from his article, shows the kind of loop which an element of fluid follows and which leads to an overall displacement, Δx. The heavy line in Fig 3.2 is a path-line on which are shown the positions of an element of fluid at times corresponding to the different sphere positions. This mechanism and the model of Crabtree and Bridgewater provide one explanation of the vertical displacement of fluid by bubble motion. But bubbles, drops and solid particles moving in a continuous medium carry with them wakes of the continuous medium. These wakes can have a crucial effect on the shape, stability and interaction of the bubbles or drops and also an important role in the mechanisms of momentum, heat and mass transfer.

Letan and Kehat (54-56) and Yeheskel and Kehat (57-58), during their studies of spray columns, developed a wake model to account for continuous phase circulation. They based their model on the following

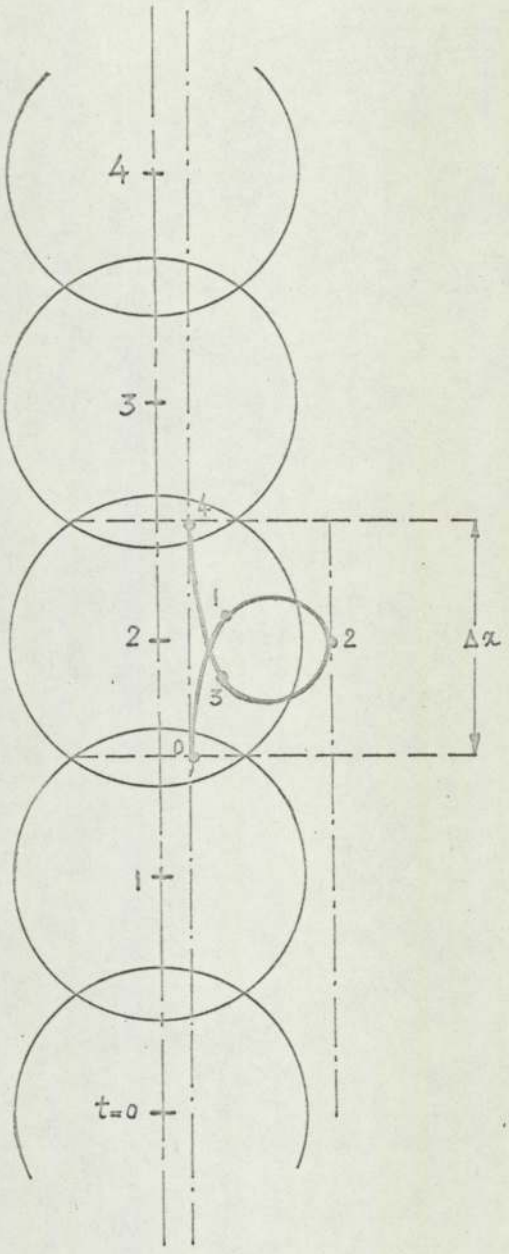

Fig 3.2. A steady state stream-line and the corresponding Fluid path-Line for Flow around a sphere.

sequence of events:

a) Wake growth, immediately following droplet detachment:

b) Wake shedding and replenishing by continuous phase flow through the boundary layers of the dispersed phase;

c) Wake detachment and droplet coalescence.

Yeheskel and Kehat (58) in their most recent article measured the ratio of the wake to drop size and the rate of wake shedding in a liquid-liquid fluidized bed. They found the ratio of wake to drop volume was 0.2 to 2.4, and the rate of wake shedding, as time required for shedding the volume of the wake, was 0.7 to 2.4s, depending on drop holdup and continuous phase velocity.

Grace (59) in his review of fluidized-bed reactors refers to periodic wake-shedding and suggests a simple way of estimating the downward flow of the continuous phase. This is to compensate for the upwards flow in bubble wakes.

$$u_d = - \frac{f_w \varepsilon u_{bs}}{1-\varepsilon-f_w \varepsilon} \qquad (3.2)$$

The different mechanisms mentioned for continuous phase circulation could be applicable to every two-phase system, although in some cases one particular mechanism might dominate the others. For a particular system, all possible causes should be taken into account, and then the final model made as simple as possible, bearing in mind the fluid dynamics. This may be easier said than done as is illustrated by Fig.3.3. This shows the complex motions of fluid and particles around and within a single bubble rising through a fluidized bed. This figure is taken from an article by Toei (60) describing his approach to the modelling of fluidized beds.

Rowe (61) in a recent review looks at an arbitrary two-phase system. Fig 3.4 summarises some of the more frequently used approaches

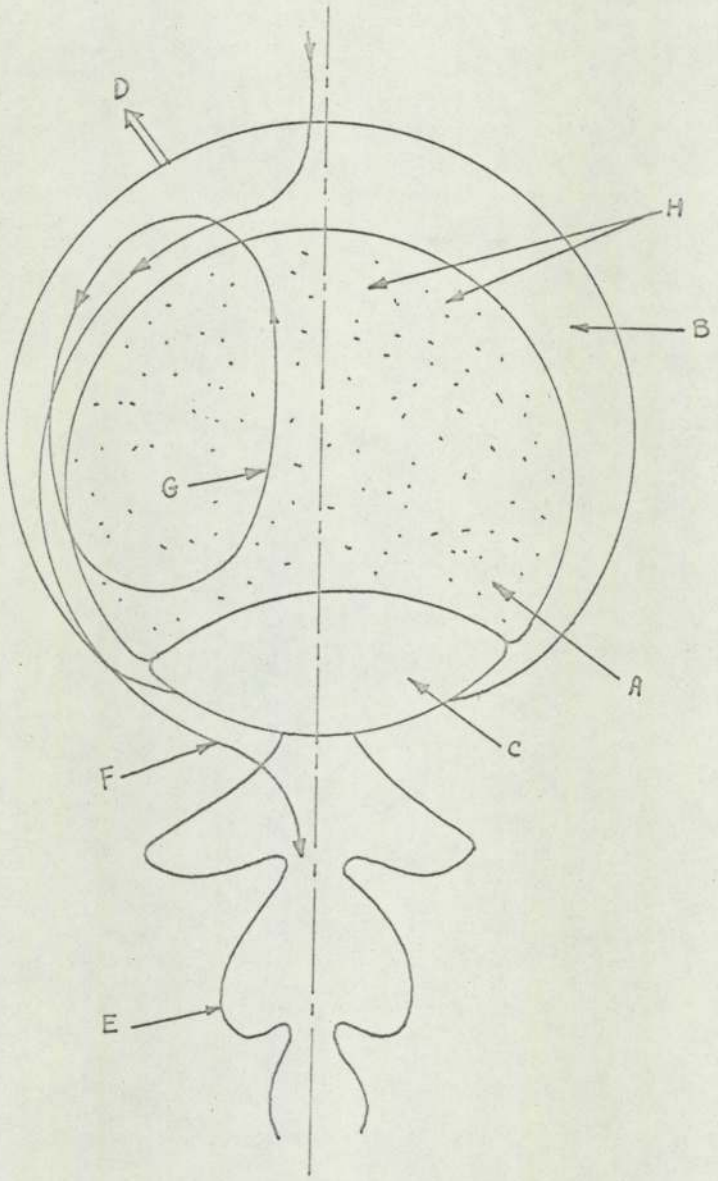

Fig 3.3. *Physical Behaviors of Fluid and Particles around and in a Single Bubble :*
A. Bubble ; B. Cloud ; C. Wake ; D. Diffusion of Gas ; E. Shedding out of Cloud Gas ; F. Flow of Particles through Cloud ; G. Circulating Gas ; and H. Dispersed Particles in the Bubble.

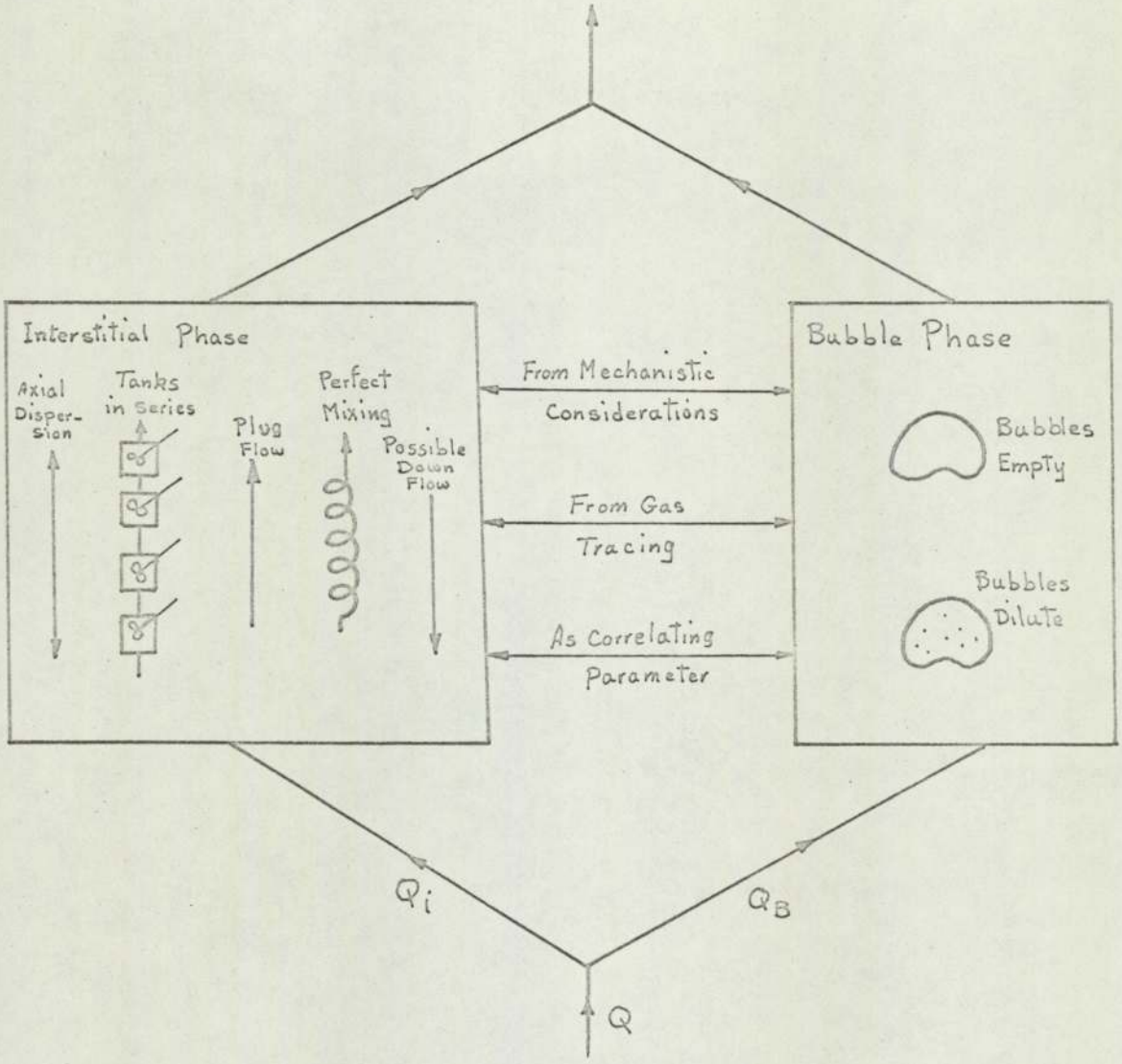

Fig 3.4. Rowe's Arbitrary Two-phase Flow Model.

used in modelling two-phase systems. For gas-liquid systems a number of authors have carried out extensive work to develop different techniques to measure, qualitatively and quantitatively, the extent of mixing and flow circulation. Different models have been suggested and the experimental results have been treated in order to establish the validity and accuracy of the models. But perhaps a sentence from a very recent article by Hills [62] best describes the present knowledge about bubble columns: "We are still a long way from being able to predict either theoretically or empirically the gas holdup and liquid circulation".

3.1.2 Mixing Models and Axial Dispersion in Bubble Columns

Several models are used to characterize mixing effects and non-ideal flow patterns in process vessels. Among these dispersion models are, perhaps, the most popular. These can be presented by diffusion-type equations in which dispersion coefficients replace ordinary molecular diffusivities. Such coefficients can be determined by means of suitable tracer injection experiments.

Levenspiel and Bischoff [63] reviewing the patterns of flow in chemical process vessels gave the following differential equation for the general dispersion model including chemical reaction and source terms:

$$\frac{\partial C}{\partial t} + u \nabla C = \nabla \cdot (D \cdot \nabla C) + S + r_c \qquad (3.3)$$

Because of the difficulties of specifying velocity profiles and limitations in experimental methods, the above equation is often simplified by assuming that:

a) bulk flow occurs in the axial direction only with radial symmetry;

b) dispersion co-efficients are independent of position;

c) fluid flows at the mean velocity (plug flow);

d) there is no variation in properties in the radial direction (axial dispersed plug flow).

Then equation (3.3) can be written:

$$\frac{\partial c}{\partial t} + u\frac{\partial c}{\partial x} = D_l \frac{\partial^2 c}{\partial x^2} + S + r_c \qquad (3.4)$$

Equation (3.4) is the model used by many researchers when studying mixing in bubble columns and evaluating dispersion coefficients.

The usual method of finding the dispersion coefficient is to inject a suitable tracer at a point or plane in the system and monitor the changes in tracer concentration at one or more points: the dispersion coefficient may then be found from an analysis of the concentration data. In such stimulus-response experiments chemical reactions do not occur and so $r_c = 0$ in Eqn. 3.4.

When the injection point for the tracer and the measuring points are sufficiently far apart and when there is no flow of liquid through the column Eqn (3.4) reduces to:

$$\frac{\partial c}{\partial t} = D_l \frac{\partial^2 c}{\partial x^2} \qquad (3.5)$$

Ohki and Inoue[75] assumed the following boundary conditions :

$$\frac{\partial c}{\partial x} = 0 \quad \text{at} \quad x = 0 \quad \text{and} \quad x = l_n \quad ;$$

and the initial condition that

$$C(x, 0) = C_0' \quad \text{for} \quad 0 \leq x \leq \lambda$$

$$C(x, 0) = 0 \quad \text{for} \quad x \geq \lambda$$

where λ is the height filled with tracer. They obtained the following

solution for the set of equations:

$$\frac{C}{C_E^*} = 1 + 2 \sum_{n=1}^{\infty} \left[\left(\cos \frac{n\pi}{\ell_n} x \right) \cdot \exp\left(-n^2 \frac{\pi^2}{\ell_n^2} D_\ell t \right) \right] \qquad (3.6)$$

Kunugita et alia [27] assumed that their bubble column was infinitely long and proposed the following boundary conditions:

1) $F(x,0) = 0 \quad , \quad -\infty < x < +\infty$

2) $-2 D_\ell \frac{\partial F}{\partial x} = \delta(t) \quad , \quad x = 0$

3) $\lim_{x \to -\infty} F(x,t) = 0 \quad \text{and} \quad \lim_{x \to +\infty} F(x,t) = 0 \quad , t \geq 0$

Their solution for equation (3.5) was:

$$F(x,t) = \frac{1}{2\sqrt{\pi D_\ell}} \exp\left(-\frac{x^2}{4 D_\ell t} \right) \qquad (3.7)$$

Eq. (3.7) can be put in the form of the normal distribution function by substituting $\sigma^2/2t$ for D_ℓ.

For steady-state conditions equation (3.4) reduces to:

$$u \frac{\partial c}{\partial \ell} = -D_\ell \frac{\partial^2 c}{\partial \ell^2} \quad , \qquad (3.8)$$

where ℓ is measured downwards from the top of the bubble column. Integration of this equation with the boundary conditions:

$$c = c'_o \quad \text{at} \quad \ell = 0 \quad \text{and} \quad c = 0 \quad \text{at} \quad \ell = +\infty$$

leads to:

$$\ln \frac{c}{c'_o} = -\frac{u_{s\ell}^{**}}{D_\ell} \ell \qquad (3.9)$$

If $\frac{u_{s\ell}}{D_\ell}$ is constant, a plot of $\ln(c/c'_o)$ vs. ℓ gives a straight line of slope $-u_{s\ell}/D_\ell$.

** $u_{s\ell} = \frac{u_{s\ell}}{1-\varepsilon}$

* C_E Equilibrium concentration of the tracer.

3.1.3 Experimental Techniques, Computational Methods and Data

Unsteady State Methods

Three methods are commonly used to find the effective axial dispersion coefficient, all involving unsteady injection of a tracer either in the form of a pulse or delta function, a step function, or a periodic function such as a sine wave. The tracer concentration is then measured downstream from the injection point. The modification of this input signal by the system can then be related to the dispersion coefficient which characterized the intensity of axial mixing in the system. Pulse methods are often preferable from the point of view of simplicity of experimental equipment and ease of mathematical analysis.

If a pulse of tracer is injected into a flowing stream, this discontinuously spreads out as it moves with the fluid past a downstream measurement point. For a fixed distance between the injection point and measurement point, the amount of spreading depends on the intensity of dispersion in the system and can therefore be used to characterize quantitatively the dispersion phenomenon. Levenspiel and Smith [64] first showed that the mean and variance of the tracer curve can be used to compute the dispersion coefficient.

The first moment of the concentration distribution about the origin and the second moment about the measuring point are computed from the following relationships [65] :

$$\mu = \frac{u_t}{l_m} \int_0^\infty c\, t\, dt \Big/ \int_0^\infty c\, dt \cong \frac{u_t}{l_m} \sum_1^N c\, t\, \Delta t \Big/ \sum_1^N c\, \Delta t \qquad (3.10)$$

$$\sigma^2 = \left(\frac{u_t}{l_m}\right)^2 \left[\int_0^\infty c\, t^2 dt \Big/ \int_0^\infty c\, dt\right] - \mu^2$$

$$\cong \left(\frac{u_t}{l_m}\right)^2 \left[\sum_1^N c\, t^2 \Delta t \Big/ \sum_1^N c\, \Delta t\right] - \mu^2 \qquad (3.11)$$

For an experimental section of infinite length beyond the second of two response points in the flow direction the following relationships are valid:

$$\mu_2 - \mu_1 = \tau \qquad (3.12)$$

$$\sigma_2^2 - \sigma_1^2 = 2\tau^2 / N_{Pe} \qquad (3.13)$$

Subscripts 1 and 2 refer to the first and the second measuring points; N_{Pe} is the Peclet Number defined by the expression:

$$N_{Pe} = \frac{u_t \ell_m}{D_\ell} \quad ; \qquad (3.14)$$

and τ is the mean residence time defined by

$$\tau = \frac{\ell_m}{u_t} \quad , \qquad (3.15)$$

where u_t is the true flow velocity, ℓ_m the distance between measuring points and D_ℓ the coefficient of axial dispersion. When the response at two points is monitored the input signal need not be a perfect pulse.

Bischoff and Levenspiel [66] have computed the error introduced by use of equations (3.12) and (3.13) for a system consisting of a finite experimental section followed by an exit section of infinite length.

Use of the imperfect pulse method is complicated by the problem of tailing. Mixon et alia [67] pointed out that the tails of concentration distributions contribute heavily to the moments computed by equations (3.10) and (3.11), and small unavoidable errors in the experimental measurements may be reflected as very considerable errors in the moments. They suggested that, in order to overcome the problem of tailing and reduce the computational error, the experimentally determined tracer concentration should be multiplied by a weighting function exp. (-st)

(where S is an arbitrary, selected constant), and the moments computed for the weighted distribution. By using several values of s the validity of the axially dispersed plug-flow model can be assessed by comparison of the resulting values of residence time and Peclet Number. Østergaard and Michelsen [68 - 72] have extended and used this method for determination of the effective diffusivities of the fluid phases in a gas-liquid fluidised system using the axially dispersed plug flow model for both phases.

The transfer function , F(s), for a system fitting the axially dispersed plug flow model is:

$$F(s) = \bar{c}_2(s)/\bar{c}_1(s) = \exp\left\{N_{Pe}\left[1-(1+4s\tau/N_{Pe})^{1/2}\right]/2\right\} \quad (3.16)$$

By differentiation of equation (3.16) with respect to S and finding the values of $\mu_{1,s}$ and $\mu_{2,s}$ one obtains:

$$\Delta\mu_s = -\frac{F'(s)}{F(s)} = \left[\frac{\bar{c}_2'(s)}{\bar{c}_2(s)} - \frac{\bar{c}_1'(s)}{\bar{c}_1(s)}\right] = \frac{\tau}{(1+\frac{4s\tau}{N_{Pe}})^{1/2}} \quad (3.17)$$

which can be rearranged to give

$$\left(\frac{1}{\Delta\mu_s}\right)^2 = 1/\tau^2 + 4s\cdot\frac{1}{\tau N_{Pe}} \quad (3.18)$$

A plot of $\Delta\mu^{-2}$ vs. S gives a straight line of slope and intercept $1/\tau^2$. Eq.(3.12) is a special case of equation (3.18) with $s = 0$. The range of s-values recommended by Østergaard and Michelsen is from $0.5/\tau$ to $2/\tau$. The advantage of this method of calculation is that the increasing weighting functions t and t^2 are replaced by the decreasing weighting functions e^{-st} and te^{-st}.

Boyadzhiev and Atanasova[73] have suggested that the error involved in equations (3.10) and (3.11) due to approximation in summation

can be avoided by using an analogue computer either on-line or off-line. For off-line computations it is necessary to record response data on magnetic tape.

Towell and Ackerman [74] used the position of the steep front of the response curves to estimate the axial diffusity. Since the superficial liquid velocity is very small compared with the rate at which the tracer front moves, the front of the response curve will be almost the same as that obtained with no flow of liquid through the column and equation 3.5 can be used.

Unsteady state methods, despite the disadvantages mentioned, have been used by a number of investigators and some of their results are briefly reviewed below. Siemes and Weiss [76] were the first to use the method to study mixing in a bubble column. They used a column 4.2 cm in diameter filled with water to a height of 140 cm: air was introduced through a porous plate distributor. The dispersion coefficient was found to increase from about 2 cm^2/s at a superficial gas velocity of 1 cm/s to 30 - 70 cm^2/s at a velocity of 7 cm/s. They also found that the dispersion coefficient varied with bubble size, and thus, because of coalescence, with distance from the gas distributor.

Tadaki and Maeda [72] examined the axial mixing characteristics of a 50 mm column with downflowing liquid. Oxygen and water were the fluid media, the gas being distributed through a perforated plate. They reported that the dispersion coefficient was independent of column height (in contrast to the findings of Siemes and Weiss), as well as of liquid flow-rate. There was a rapid increase in mixing with gas flow rate in a manner similar to

that observed by Siemes and Weiss and the numerical values of the coefficients were of the same order of magnitude. Tadaki and Maeda also noticed some variation of diffusion coefficient with gas orifice diameter and column diameter.

Bischoff and Phillips (30) studied cocurrent flow of air-water systems in a column 2.54 cm. in diameter. The column length was varied and different gas distributors consisting of orifice plates with either one hole (6.4 mm i.d.) or 16 equally spaced holes (1.6 mm i.d.) were used. They found that mixing characteristics in short tubes were different from those in long ones. Plate design appeared to have little effect on axial dispersion: this was also true of liquid flow-rate despite the fact that high superficial liquid velocities (up to 30 cm/s) were employed.

Ohki and Inoue (75) carried out their work in 4.0, 8.0 and 16.0 cm diameter columns with different perforated plates as gas distributors. Air and water were used as the fluid phases. Since there was no flow of water through the columns they used Eq. (3.5)to calculate the dispersion coefficient. They also presented two theoretical models for correlating their experimental data. The first model was applied to results in the bubbly-flow regime, while the second was used with data obtained for coalesced bubble-slug flow conditions.

Kato and Nishiwaki (33) recently published the results of their mixing studies in three bubble columns with inside diameters equal to 6.6, 12.2 and 21.4 cm and with respective heights of 201, 200 and 405 cm. They used perforated plates for distribution of air into water. Superficial gas and liquid velocities were varied from 0-30 and 0 - 1.5 cm/s respectively. They found

that the longitudinal dispersion coefficient increased with increasing U_{sg} and increasing column diameter (e.g. 50 cm^2/s for the 6.6 cm column at U_{sg} = 1 cm/s and 600 cm^2/s for the 21.4 cm column at 1.8 cm/s). There was almost no effect of liquid velocity and little effect of gas distributor design.

Steady State Methods

The principle of the method is very simple. A steady stream of tracer is usually injected at the top of the column. The tracer travels downwards due to the liquid circulation patterns (see Section 2.5) and eventually the system reaches a steady state — the concentration over the length of the column remaining unchanged. Samples can then be taken at different points over the length of the column and analysed for tracer, alternatively in-line detectors can be used. Dispersion coefficients are then evaluated using equation(3.9).

Less criticism has been levelled at this method. The main difficulty is, perhaps,the attainment of the steady-state condition. However, provided this condition can be met and assuming that the dispersed plug-flow model holds,very little error is involved. The method has been used to evaluate the flow-patterns in bubble columns by a number of investigators, and some of their work is briefly reviewed below.

Argo and Cova[28] investigated axial mixing in water-nitrogen and water-ammonia synthesis gas systems in both co-current and counter-current flow situations. The columns used were 4.7, 10.2 and 44.8 cm in diameter and were fitted with sintered and stainless steel discs as gas distributors. Superficial gas velocities were varied over the range 0.41 to 20.27 cm/s and

superficial liquid velocities ranged from 0.38 to 1.62 cm/s. They found that the dispersion coefficient increased steadily with an increase in gas superficial velocity until slugging occurred: at this point there was a marked increase in D_ℓ (as much as ten times) but thereafter only a slight increase with gas flow-rate was observed. They also found that the presence of baffles reduced the dispersion coefficient for a fixed gas flow-rate and by moving the baffles an even greater decrease was observed. The dispersion coefficient was found to increase rapidly with column diameter, while liquid velocity had no noticeable effect.

Aoyama et alia[36] used the same technique to measure the coefficients of thermal and mass dispersion for 5.0, 10.0 and 20.0 cm columns. They found that the mechanism of thermal dispersion in bubble columns is also governed by liquid mixing. Tests were made with air distributed by various porous or perforated plates in liquids such as deionised water, tap water, 61.5% volume glycerine-water solution and 0.1 wt % Tween 20 solution in solution. They correlated the dispersion coefficient with experimental conditions in the bubbly flow and slug-flow regimes but it was not possible to do this for the transition region.

Reith et alia[5] measured the liquid-phase axial dispersion coefficient using air and water in bubble columns of 5.08, 14.0 and 29.0 cm diameter. The water had a superficial velocity of approximately 1.0 cm/s and the air was introduced through a perforated plate (with approximately one hole of 0.2 cm diameter/cm^2) at superficial velocities up to 45 cm/s. Axial dispersion in the 14 and 29 cm columns was characterised by a nearly constant Peclet number (based on column diameter) for superficial gas velocities between

10 - 45 cm/s. It was also observed that the axial dispersion coefficient was affected by the addition of ions to the water and had a lower value in columns of smaller diameter.

Eissa et alia [78-79] have studied mixing during co-current and counter-current flow of air and water. The column diameter used throughout their work was 5.0 cm. They introduced the tracer in the middle of the column and measured the concentration profile both downstream as well as upstream. The results were plotted in the form of the intensity of dispersion, $D_e / u_t d$, against superficial gas velocity and it was found that in the laminar, transition and turbulent flow regimes, a different pattern of flow existed. It was also observed that the dispersion number decreased with increasing liquid flow-rate.

Towell and Ackerman[74] have carried out an extensive investigation of axial mixing of liquid and gas in large bubble columns. The columns used were 40.6 cm and 106.7 cm in diameter with aspect ratios of about 5. Air and water were used as the experimental fluids. Two-fluid distributors with 0.64 cm holes were used for most of the experiments. Both steady state back mixing tests and unsteady-state pulse tracer tests were used and it was found that the two methods gave comparable results. Distributor design only had a small effect on the value of the liquid axial mixing coefficient. The addition of a draft tube increased mixing, whilst discs and doughnut cross baffles decreased it. Column diameter was found to have a very large effect on the value of the mixing coefficient, as did superficial gas velocity in the range 0 - 1.5 cm/s. They concluded that normally the degree of backmixing in large columns is so great that for the

column lengths studied complete mixing is closely approached.

Some Japanese investigators, Kunugita et alia[27] argued that by adding salt solutions as tracers the behaviour of the column is changed. Instead they have followed the motion of a solid particle with a camera to measure the degree of liquid mixing. Their experiments were carried out in a column 5.0 cm in diameter equipped with a porous gas distributor. From the observed flow pattern, the axial dispersion coefficient was calculated by a statistical method, and the results showed that gas holdup and dispersion coefficient were controlled by bubble expansion.

3.1.4. Correlation Methods for Liquid Phase Dispersion Coefficients in Bubble Columns

Reith et alia[5] showed that the longitudinal mixing could be characterised by a nearly constant Peclet number for relatively high gas flow-rates (10 - 45 cm/s):

$$N_{Pe} = \frac{U_{sg} d_c}{D_\ell} = 3.0 \pm 0.3 \qquad (3.18)$$

Ohki and Inoue[75] applied a velocity-distribution model for the bubbly flow regime and so-called "expansion" model for the coalesced bubble-slug flow regime. They proposed the following equations:

$$D_\ell = 0.3\, d_c^2\, U_{sg}^{1.2} + 170\, d_o \qquad \text{for bubbly flow} \qquad (3.19)$$

and

$$D_\ell = 14\, d_c / (1-\varepsilon)^2 \qquad \text{for coalesced bubble-slug flow} \qquad (3.20)$$

They found the dispersion coefficients calculated from these equations were in good agreement with their experimental data.

Aoyama et alia[36] measured the dispersion coefficient for a 5.0 cm column, and then proposed the following equation to account for the effect of column diameter on dispersion coefficient:

$$D_\ell = (D_\ell)_5 \cdot \left(\frac{d_c}{5.0}\right)^{1.5} \qquad (3.21)$$

This is applicable when the relative velocity of bubbles in a liquid is greater than 25 cm/s (i.e. coalesced bubble-slug flow).

Kato and Nishiwaki[33] showed that using columns greater than 12 cm in diameter and gas distributors having holes greater than 0.2 cm in diameter, the Peclet Number could be related to the Froude Number. This relation is given by Equation 3.22.

$$\frac{U_{sg} d_c}{D_\ell} = 13\left(U_{sg}/\sqrt{g d_c}\right)\left\{1 + 6.5\left(U_{sg}/\sqrt{g d_c}\right)^{0.8}\right\} \qquad (3.22)$$

Towell and Ackerman[74] proposed an empirical relationship for correlating back mixing data for large bubble columns. In this, the dispersion coefficient is plotted against $d_c^{1.5} \cdot U_{sg}^{.5}$ They found that

$$D_\ell = K\, d_c^{1.5} \cdot U_{sg}^{0.5} \quad , \qquad (3.23)$$

where K is a constant (K = 73.5 for ft. and hr. units). Deckwer et alia[80] using this relation found the following three equations represented their data at a significance level of 15 per cent.

In the lower region of the column:

$$D_\ell = (1.2 \pm 0.12)\, d_c^{1.5} \cdot U_{sg}^{0.5} \quad [cm^2/s]\,; \qquad (3.24)$$

in the upper region:

$$D_\ell = (2.4 \pm 0.18)\, d_c^{1.5} \cdot U_{sg}^{0.5} \quad [cm^2/s], \quad (3.25)$$

and if no splitting into different back-mixing zones occurs:

$$D_\ell = (2 \pm 0.15)\, d_c^{1.5} \cdot U_{sg}^{0.5} \quad [cm^2/s] \quad (3.26)$$

These authors noticed that over a certain range of gas throughput the mixing in the liquid phase was not uniform but was of different intensity over two distinct zones. This occurred up to a gas velocity of about 6 cm/s, which corresponds to the transition from bubbly flow to coalesced bubble flow.

3.1.5. Radial Mixing

Reith at alia[5] investigated the extent of radial mixing by introducing a steady tracer stream at a point source along the axis of a column operating co-currently, and then measuring the concentration downstream of the injection point at several radial positions. They found that the radial concentration gradient had completely disappeared within a few centimetres of the injection point.

Eissa et alia[78] measured the concentration profile of tracer at different levels above and below the tracer injection point in their narrow column (5 cm in diameter). The profiles downstream of the injection point became flattened within a distance of 3.0 cm. Upstream the profiles tended to retain their peculiar shape with the highest concentration near the wall, lower concentrations in the central core and a very small peak at the centre. They concluded that radial mixing effects play a secondary role to that of axial mixing effects.

3.2. Experimental Programme

3.2.1. Axial Mixing Studies

The mixing studies could have been performed by either steady-state or unsteady-state tracer techniques (for details see Section 3.1). Preliminary studies of mixing were carried out, using both techniques and dyes as tracers. Details of these tests are given in Section 3.4. Mixing patterns revealed by either a "one-shot" or continuous injection of dye tracer at the bottom or top of a column were carefully and frequently watched. Tracer introduced at the top of a column spreads downwards in a matter of seconds, even at low gas velocities and if the flow of tracer is made continuous, a stable concentration profile is observed over the length of the column. This extensive backmixing and deviation from plug flow means that tracer introduced as a pulse takes a long time to clear from the column: for example, tracer is still present even after a period of 15 minutes. Consequently response curves obtained using unsteady-state tracer techniques show an appreciable tail, and as previously mentioned this creates difficulties when evaluating the dispersion co-efficient. For this reason and because of the advantage of analysing samples off-line, the steady-state tracer method was selected.

The operating conditions used in the experimental programme were similar to those used in the gas hold-up work. The literature survey (see Section 3.1) revealed a need for more detailed results particularly in the bubbly flow regime and at different liquid flow-rates. The effect of column diameter on mixing is now known to be important, but when the project was started comprehensive

data was not available. The experimental programme is summarised below:

Column Diameter (cm)	Range of u_{sl} (cm/s)	Range of u_{sg} (cm/s)
15.2	0.5 - 2.5	0.5 - 11.0
30.5	0.5 - 2.0	0.5 - 8.5
61.0	0.2 - 1.0	0.5 - 4.5

3.22 Radial Mixing Studies

Although it has been reported that radial mixing plays a secondary role compared to axial mixing (see Section 3.1) it was decided to explore the extent of radial mixing in the case of the larger columns. The existence of radial concentration profiles can provide valuable information about liquid circulation patterns within the columns.

Column Diameter (cm)	Range of u_{sl} (cm/s)	Range of u_{sg} (cm/s)
15.2	1.0 - 5.5	1.0 - 2.5
30.5	1.25	2.0
61.0	0.2 - 1.0	0.5 - 4.0

Preliminary experiments showed that provided the bulk concentration of KCl $\leq$ 0.2 % wt/wt the hydro-dynamic behaviour of the system was the same as for air-water.

3.3. Experimental Equipment

Mixing studies were carried out in the three columns used for the gas holdup experiments: the diameters of the columns were 15.2 cm, 30.5 cm and 61.0 cm in diameter. Construction of these columns as well as their common storage tanks, liquid phase pumping and metering systems and air supply and metering systems are mentioned in Section 2.3. The tracer system, sampling points and system for analysing the samples are described below.

3.3.1. Tracer System

A schematic lay-out of the tracer system is given in Fig.3.5. The tracer reservoir (1) was a 100 litre plastic container with a tap (2) and removable lid which could be screwed and sealed. The tracer, a 20% KCl solution, was fed to a 10 litre constant-head aspirator (5) by means of a peristaltic pump (type MHRE/200, Watson and Marlow) (3) and the flow was measured by a 7 K metric Rotameter. The aspirator was situated in a position from which the tracer could flow through a 7K metric Rotameter into all columns under a constant head. The tracer flow could be altered by stop-cock (6). The overflow was returned to the tracer reservoir.

Tracer distributors for the 15.2 cm and 30.5 cm columns were made of glass tubes 6 mm in diameter with a dead-end. A 2-mm diameter hole was made on the side very close to the end. The tube was inserted into the column with this hole positioned on the top side of the tube and in the centre of the column. Due to the different aspect ratio of the 61.0 cm column the tracer distributor design was modified. The tracer was delivered through a 0.64 cm i.d. stainless steel tube into a hollow drum (7.5 cm in diameter and 1.0 cm in width) with 10 equally spaced 0.07 cm diameter holes drilled in the

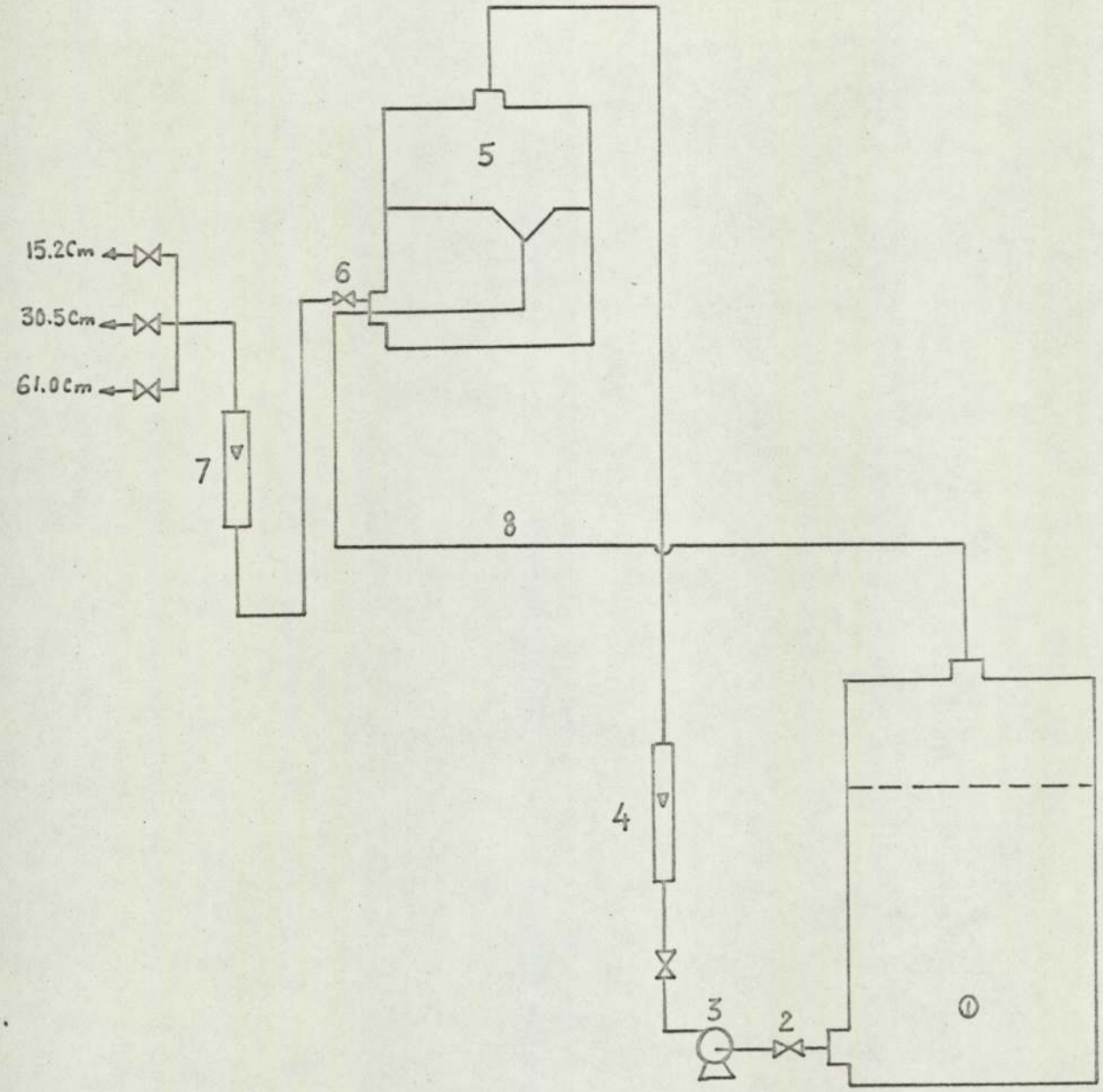

Fig 3.5. Schematic Flow Diagram of KCl Tracer Feed System

For the 15.2 cm, 30.5 cm and 61.0 cm Columns.

side.. This design ensured an even distribution of tracer over the cross-section of the column.

3.3.2. Sampling Points

Sampling positions for the 15.2, 30.5 and 61.0 cm columns are shown in Figs.3.6, 3.7 and 3.8 (also see Figs.2.12, 2.15 and 2.19). For the 15.2 and 30.5 cm columns, 1.3 cm holes were drilled along the length of the columns and these were supplied with suitable fittings and rubber washers so that 3.2 mm o.d. stainless steel tube could easily be inserted into the columns at any desired radial position. For the case of the 61.0 cm column the stainless steel tubes were welded at fixed positions to the body of the column. For measurements in a radial direction a number of holes were drilled at a height of 90 cm above the distributor plate, and tubes of different lengths were inserted into the column and welded. Fig.3.8(b) shows the pattern of these tubes inside the column: they were positioned at a distance of 0, 5.1, 10.2, 15 2, 20.3, 25.4 and 30.5 cm from the wall. The stainless steel tubes were connected to a group of stop-cocks all at the same level.

3.3.3. Tracer Analysis System

This consisted simply of a constant temperature bath (E.270 Standard Thermostate Bath, Townson & Mercer Ltd., Croydon, England) and a conductivity meter (LKB 5300B Conductolyzer, LKB-Produkter AB, Stockholm, Sweden) (see Fig.3.9) to measure the conductivity of the samples taken from the columns and held at constant temperature in the bath.

Scale 1:20 Unit: cm.

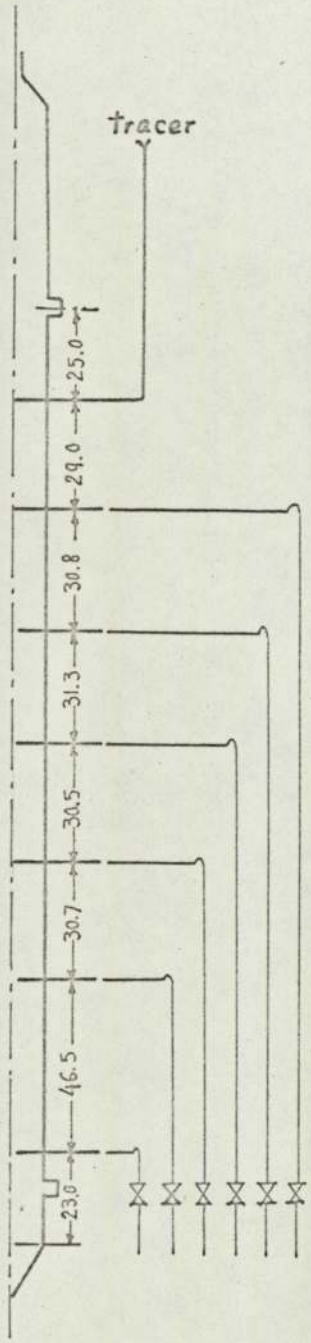

Fig 3.6. Sampling Arrangement for 15.2 cm Column.

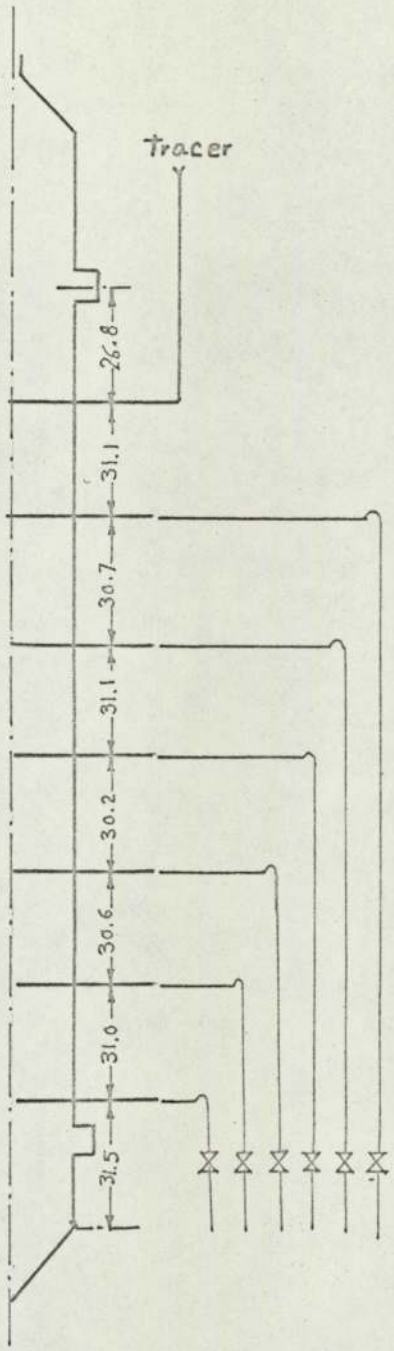

Fig 3.7. Sampling Arrangement for 30.5 cm Column.

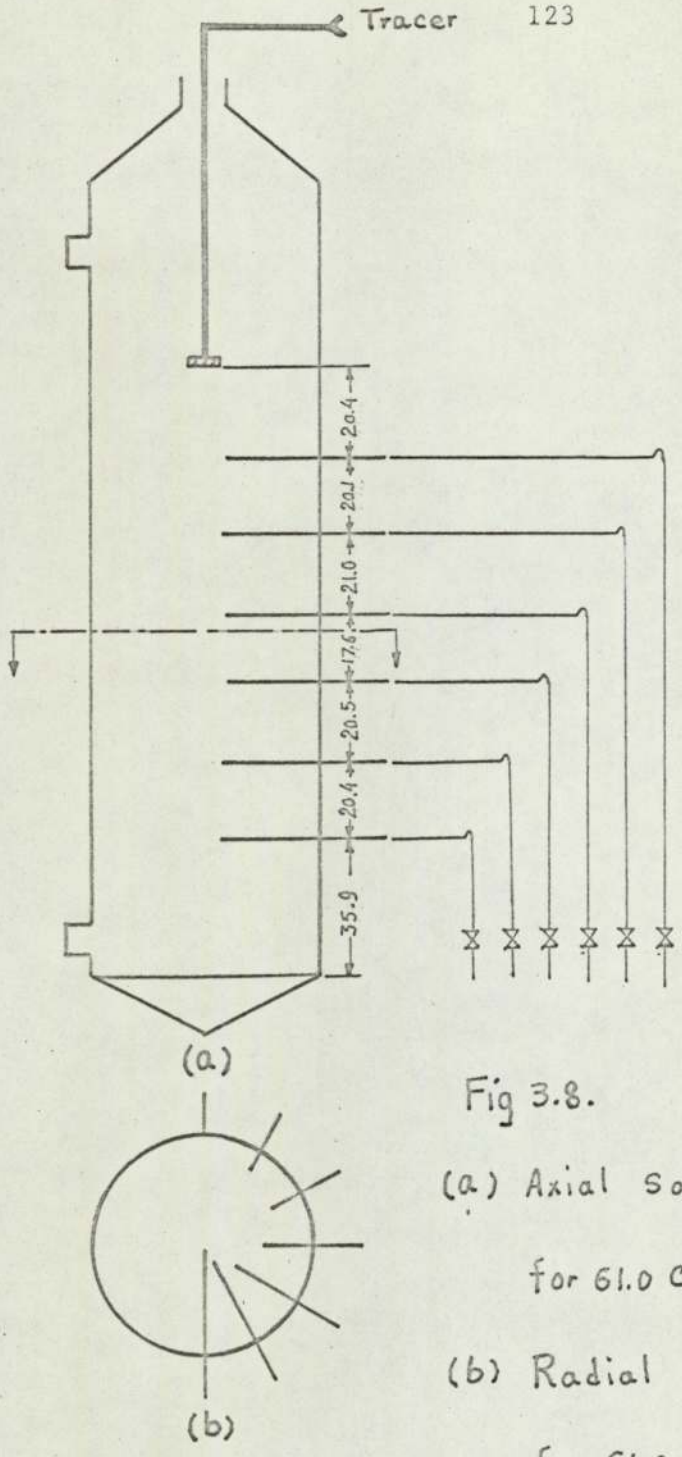

Fig 3.8.

(a) Axial Sampling Arrangement for 61.0 Cm Column.

(b) Radial Sampling Arrangement for 61.0 cm Column.

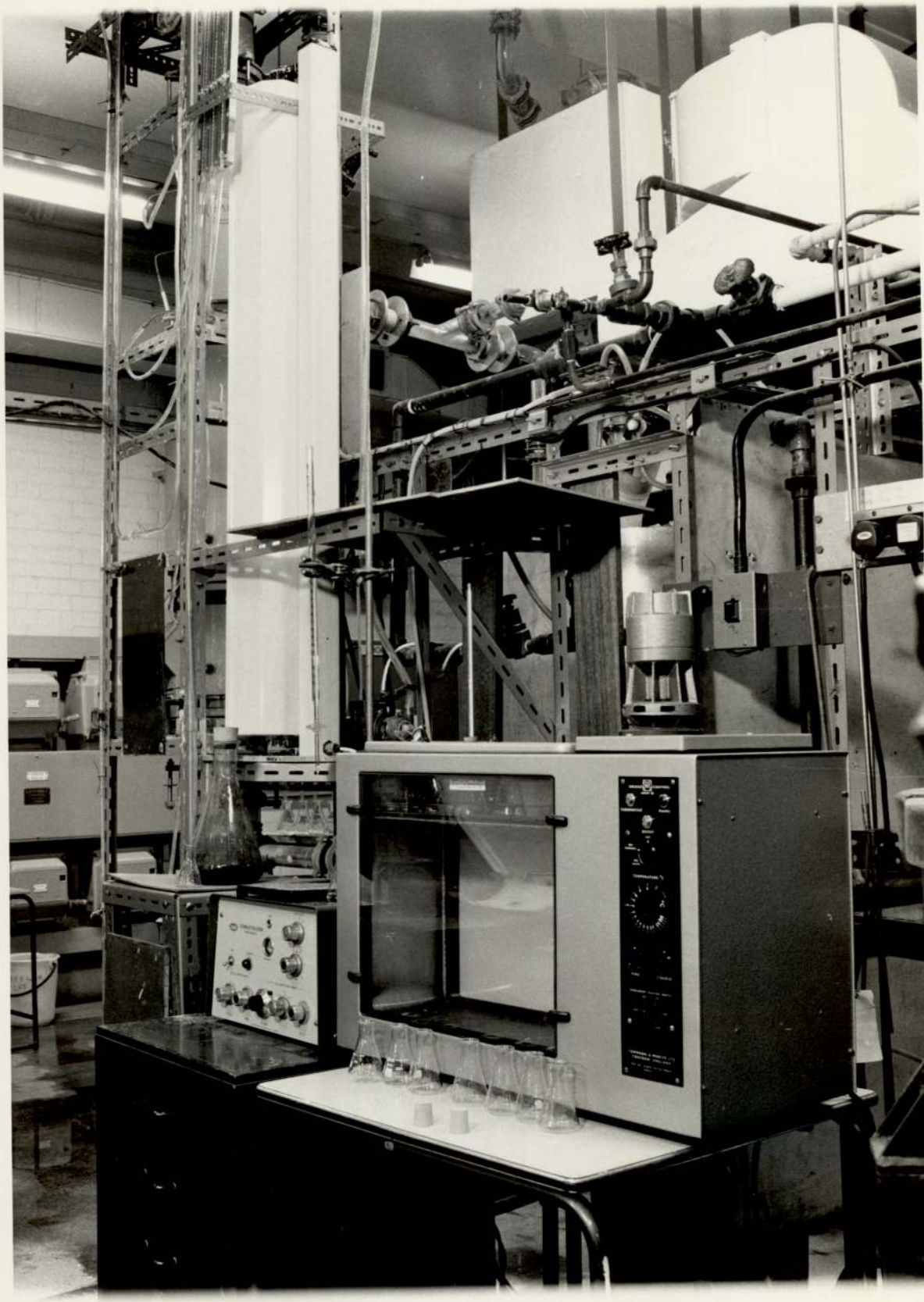

Fig 3.9. General View of the Measuring Units.

3.4. Experimental Procedure and Results

3.4.1. Comments on the Method of Measurement

Air and tap water were used throughout the mixing studies as the gas and liquid phases. A 20% KCl solution prepared by dissolving KCl (G.P.R., Hopkin and Williams, Essex, England) in tap water was used as the tracer solution.

For each experiment, after setting the appropriate gas and liquid flow rates, tracer was introduced at the top of the column. Samples were taken from the bottom of the column at regular time intervals to assess whether or not the steady-state condition had been reached, and then samples were taken simultaneously in 50 ml conical flasks. The average time required for sampling was one minute. Samples were then analysed for conductivity at constant temperature (25°C).*

The experimental plan for each column was carried out in a completely random fashion, and each experiment was repeated at least twice.

Accuracy and Reproducibility

Air and water flow-rates could be kept reasonably constant with, at most, fluctuations of ±1%. Tracer flow-rate, due to very careful design of the system, was extremely constant over long time periods, and certainly for periods in excess of that required to reach steady-state (within 30 - 45 mins).

The thermostat bath was highly sensitive and reliable, and samples in conical flasks were allowed to reach 25°C before measurements of conductivity were made. The reproducibility of the conductolizer was checked, and the results of this test showed that

* At no time did the KCl concentration in the system exceed 0.2% (See also page 118).

the measurements for 10 identical samples were in good agreement (<0.2% difference).

Results for repeat experiments were also in good agreement with each other: in most cases the discrepancy was less then ±3% .

3.4.2. Comments on the Method of Calculating the Dispersion Coefficients

Conductivity measurements were averaged and normalised with respect to the conductivity of liquid flowing out of the column. The natural logarithm of these data was plotted versus the distance from the liquid outlet. A least squares method was used to find the slope, and then the dispersion coefficient was readily calculated (see Section 3.1 Equation 3.9).

The superficial gas velocity was modified to take account of the pressure change over the height of the column, and the average superficial gas velocity, U_{sg}, was defined as the value of superficial gas velocity at the middle of the column. Fig. 1 of Appendix B gives the corresponding value of U_{sg} for u_{sg} .

3.4.3. Qualitative Studies: 15.2 cm Diameter Column

In order to get an idea about the extent of mixing, dye tracer ($KMnO_4$ solution) was injected either from the top or bottom of the column and the dispersion of dye was carefully observed. Backmixing was so rapid that, even at low superficial gas velocities (about 1.0 cm/s), some tracer had travelled from the top to the bottom of the column within 10 to 15 seconds. When a pulse of tracer was injected at the bottom of the column, the time for

a. tracer to reach the top of the column,

b. the peak to reach the top of the column,

c. tracer to clear the base,

and d. tracer to clear the top of the column,

were estimated: figures are given in Table 3.1.

The results in Table 3.1. indicate that in the case of two-phase flow, although the time required for the tracer to reach to the top of the column is short (average 15 s), the time for tracer to clear the column is considerable. These observations illustrate the extent of the tail found in response to one-shot tracer injections, and the need for a long recording time in such tests. Further comments about this stimulus-response method are given in Section 3.5.

3.4.4. Axial Mixing Studies

15.2 cm Diameter Column

Table 3.2. gives the flow conditions used for all the experiments carried out in the 15.2 cm column and data in Table 3.3. illustrate the change in tracer concentration from start-up to steady-state.

Fig.3.10 shows the relationships between normalised tracer concentration and distance from the liquid outlet. All the data used in this graph are given in Table 1 of Appendix B.

Fig.3.11 shows the effect of average superficial gas velocity on the dispersion coefficient for different liquid flow-rates. Data required for Fig.3.11 are given in Table 2 of Appendix B.

30.5 cm Diameter Column

Table 3.4 gives the flow conditions used for all the experiments carried out in the 30.5 cm column. Fig.3.13 shows concentration-distance curves plotted on semi-log paper as for Fig.3.10. Data are given in Table 4 of Appendix B.

Table 3.1. Visual Tracer Observations : 15.2 cm Column

Gas hold-up ε (-)	Water Flow u_{se} (cm/s)	Tracer Reaches Top of Column (min)	Peak Reaches Top of Column (min)	Tracer Clears Base (min)	Tracer Clears Top of Column (min)
0.0	0.5	4.4	5.5	4.2	12.0
0.0	1.0	2.3	2.8	2.6	6.0
0.0	2.6	0.80	1.2	1.0	2.2
0.05	0.5	0.28	-	13.5	14
0.05	1.0	0.32	-	8.5	8.8
0.05	2.6	0.25	0.5	2.5	3.0
0.10	0.5	0.30	-	15.5	-
0.10	1.0	0.23	0.8	8.5	-
0.10	2.6	0.22	0.5	3.0	3.5
0.20	0.5	0.23	0.7	15.5	16.0
0.20	1.0	0.18	0.6	9.0	9.0
0.20	2.6	0.18	0.5	2.5	3.0

Average Residence Times - Zero Gas Holdup

Water flow cm/s	Residence Time (min)
0.5	7.3
1.0	3.7
2.6	1.4

Table 3.2. Experimental Conditions for Axial Mixing Studies
(15.2 cm Diameter Column)

Experiment Number	u_{sl} (cm/s)	u_{sg} (cm/s)	Average ε (-)	Experiment Number	u_{sl} (cm/s)	u_{sg} (cm/s)	Average ε (-)
A1	.46	1.10	.038	C5	1.37	7.31	.184
A2	.46	2.74	.097	C6	1.37	9.13	.184
A3	.46	4.11	.154	C7	1.37	11.9	.198
A4	.46	5.48	.182				
A5	.46	7.31	.184	D1	1.83	1.10	.041
A6	.46	9.13	.187	D2	1.83	2.74	.096
A7	.46	11.9	.202	D3	1.83	4.11	.143
B1	.91	1.10	.038	D4	1.83	5.48	.174
B2	.91	2.74	.095	D5	1.83	7.31	.178
B3	91	4.11	.143	D6	1.83	9.13	.185
B4	.91	5.48	-	D7	1.83	11.9	-
B5	.91	7.31	.180	E1	2.28	1.10	.039
B6	.91	9.13	.183	E2	2.28	2.74	.095
B7	.91	11.9	.202	E3	2.28	4.11	.134
C1	1.37	1.10	.039	E4	2.28	5.48	.171
C2	1.37	2.74	.092	E5	2.28	7.31	.179
C3	1.37	4.11	.142	E6	2.28	9.13	.180
C4	1.37	5.48	.176	E7	2.28	11.9	.200

Table 3.3. Change in Point Tracer Concentration from Start-up

Water Flow: 0.46 cm/s

Air Flow : 4.11 cm/s

Starting Time: 0 min

Time (min)	Conductalizer Reading
5	726
11	508
15	470
20	444
29	436
36	232
43	228
55	232

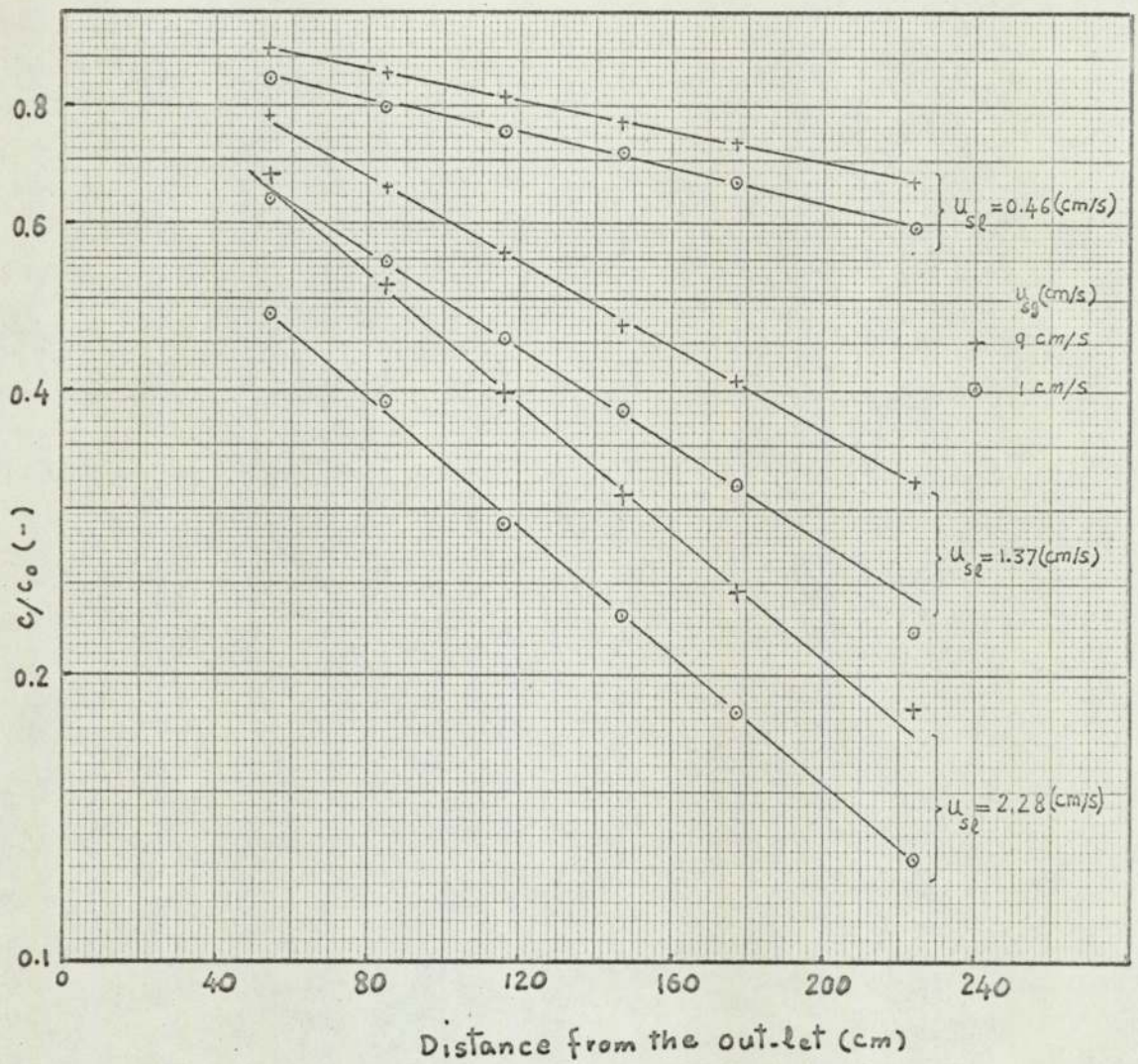

Fig 3.10 . Tracer Concentration Profiles over the Length of the 15.2 cm Column.

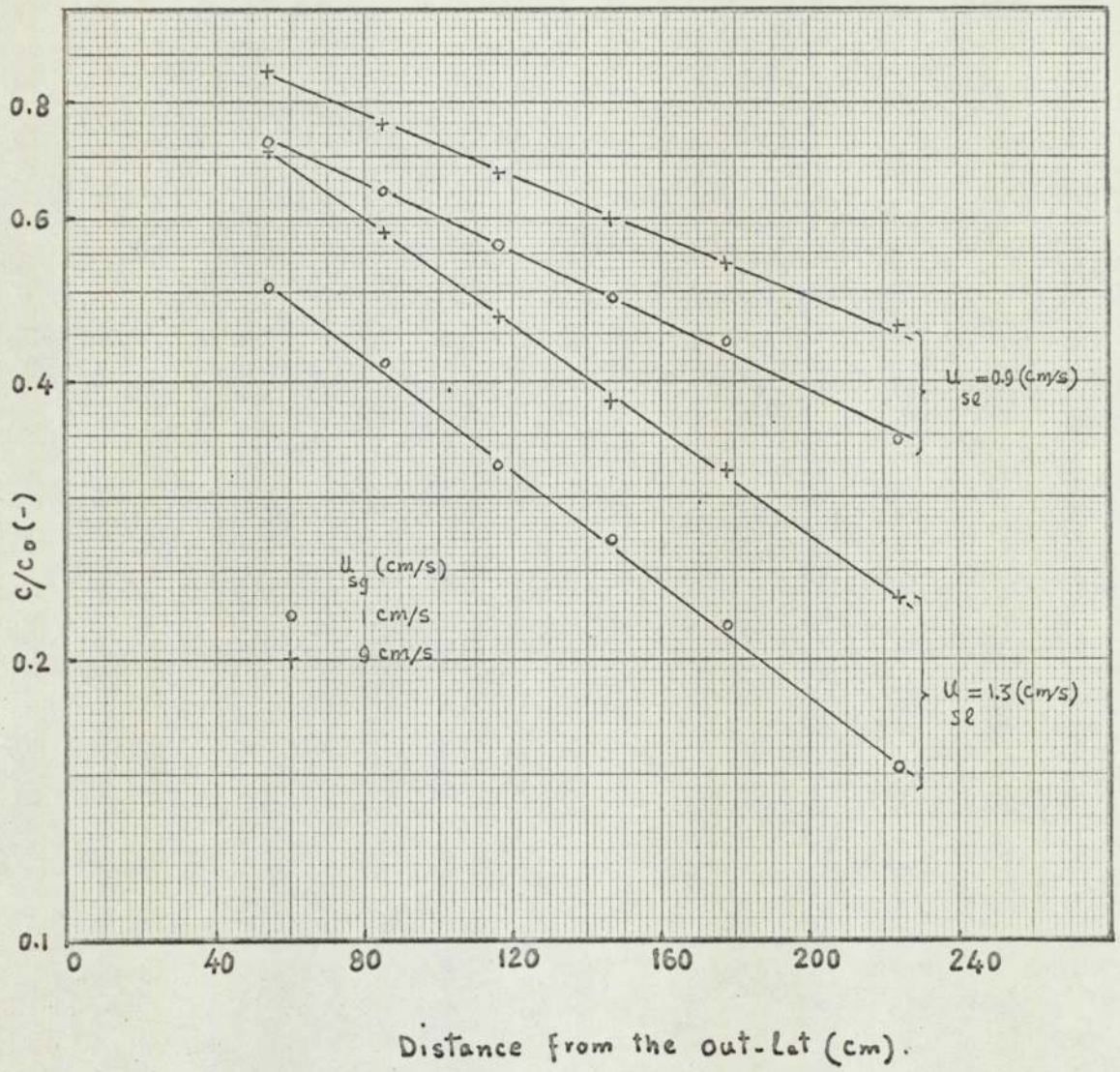

Fig 3.10 a. Tracer Concentration Profiles over the Length of the 15.2 cm Column.

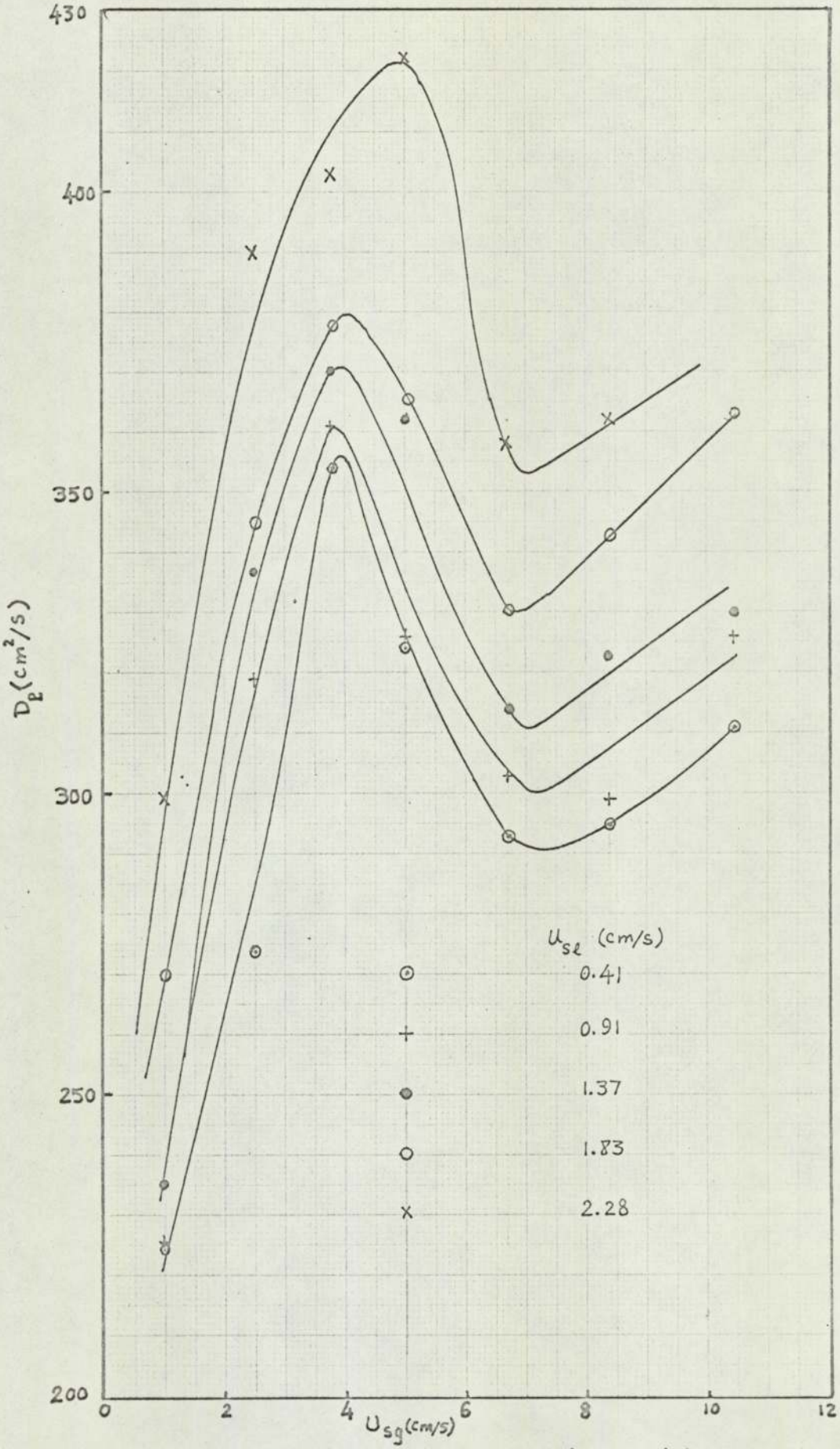

Fig 3.11. Effect of Gas and Liquid Superficial Velocity on Dispersion Coefficient.(15.2 cm Column)

Table 3.4. Experimental Conditions for Axial Mixing Studies
(30.5 cm Diameter Column)

Experiment Number	u_{sl} (cm/s)	u_{sg} (cm/s)	ε (-)	Experiment Number	u_{sl} (cm/s)	u_{sg} (cm/s)	ε (-)
F1	0.51	0.46	0.015	G4	1.25	4.65	0.151
F2	0.51	1.99	.084	G5	1.25	6.65	0.161
F3	0.51	3.32	.140	G6	1.25	8.64	0.164
F4	0.51	4.65	0.157	H1	2.03	.46	0.013
F5	0.51	6.65	0.161	H2	2.03	1.99	0.073
F6	0.51	8.64	0.167	H3	2.03	3.32	0.124
G1	1.25	0.46	0.014	H4	2.03	4.65	0.148
G2	1.25	1.99	0.077	H5	2.03	6.65	0.167
G3	1.25	3.32	0.128	H6	2.03	8.64	0.170

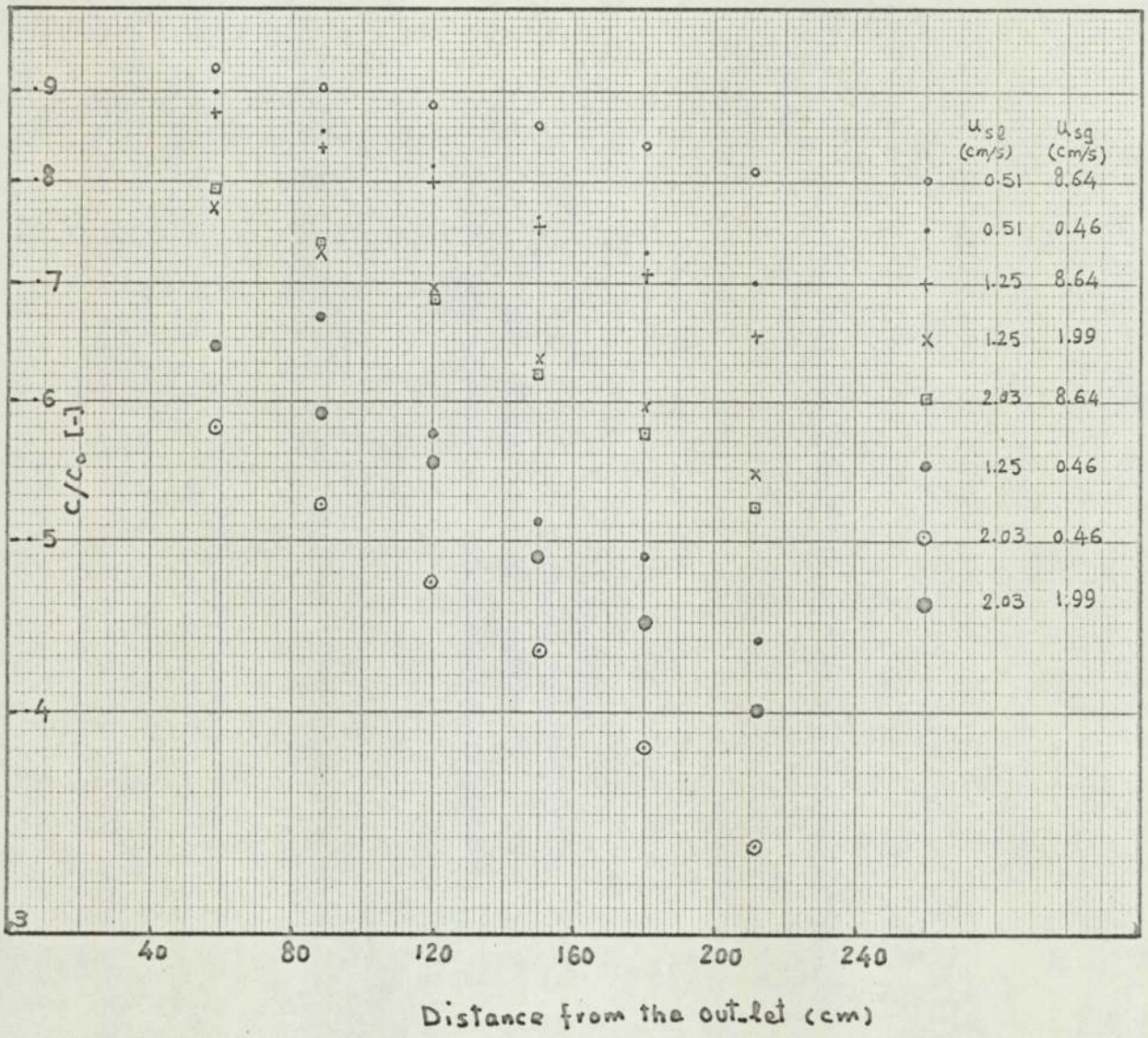

Fig 3.13. Tracer Concentration profiles over the Length of the 30.5 cm Column.

The effect of average superficial gas velocity on dispersion coefficient for different liquid flow-rates is shown in Fig.3.14 and the data used in the plots are given in Table 3 of Appendix B.

61.0 cm Diameter Column

The experimental conditions are given in Table 3.5. Fig.3.15 shows tracer concentration profiles over the length of column (100 cm) used in the study of axial mixing. Detailed data are given in Table 5 of Appendix B.

Table 3.6. gives the dispersion coefficients for different superficial gas and liquid velocities.

3.4.5. Radial Mixing Studies

15.2 cm Diameter Column

Figs.3.16 and 3.17 show the way in which the tracer concentration varied radially at four different heights of the column. The effect of superficial gas velocity is illustrated in Fig.3.16, whereas the effect of superficial liquid velocity has been shown in Fig.3.17.

Most of these experiments were repeated a number of times and it is the averaged values that are given in Table 6 of Appendix B.

30.5 and 61.0 cm Diameter Columns

Similar results were obtained in the case of the 30.5 cm column. Fig.3.18 shows the radial tracer concentration profiles at five different longitudinal positions for u_{sg} = 2.0 cm/s and u_{sl} = 1.25 cm/s. The experimental data are given in Table 7 of Appendix B.

The effects of gas and liquid superficial velocity on radial mixing for the 61.0 cm column are shown in Fig.19. Experimental results used in Fig.19 are summarised in Table 8 of Appendix B.

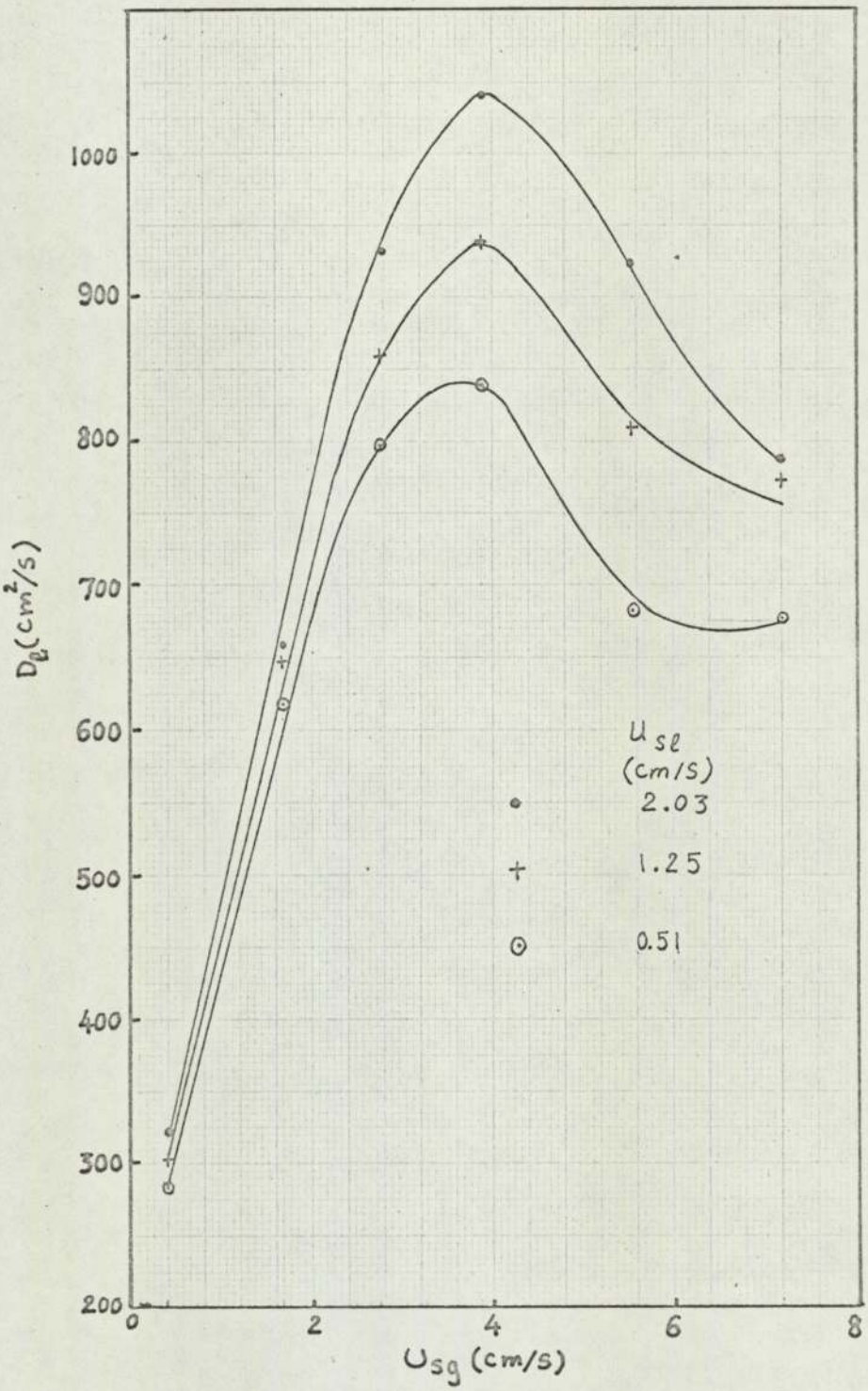

Fig 3.14. Effect of Gas and Liquid Superficial Velocities on Dispersion Coefficient (30.5 cm Column).

Table 3.5. Experimental Conditions for Axial Mixing Studies

(61.0 cm Diameter Column)

Experiment No.	u_{sl} (cm/s)	u_{sg} (cm/s)	Average ε (-)
J1	0.25	2.01	.073
J2	0.25	3.42	.102
J3	0.25	4.52	.123
K1	0.51	.050	.021
K2	0.51	2.01	.073
K3	0.51	2.26	.080
K4	0.51	4.0	.115
L1	0.82	0.5	.021
L2	0.82	3.42	.103

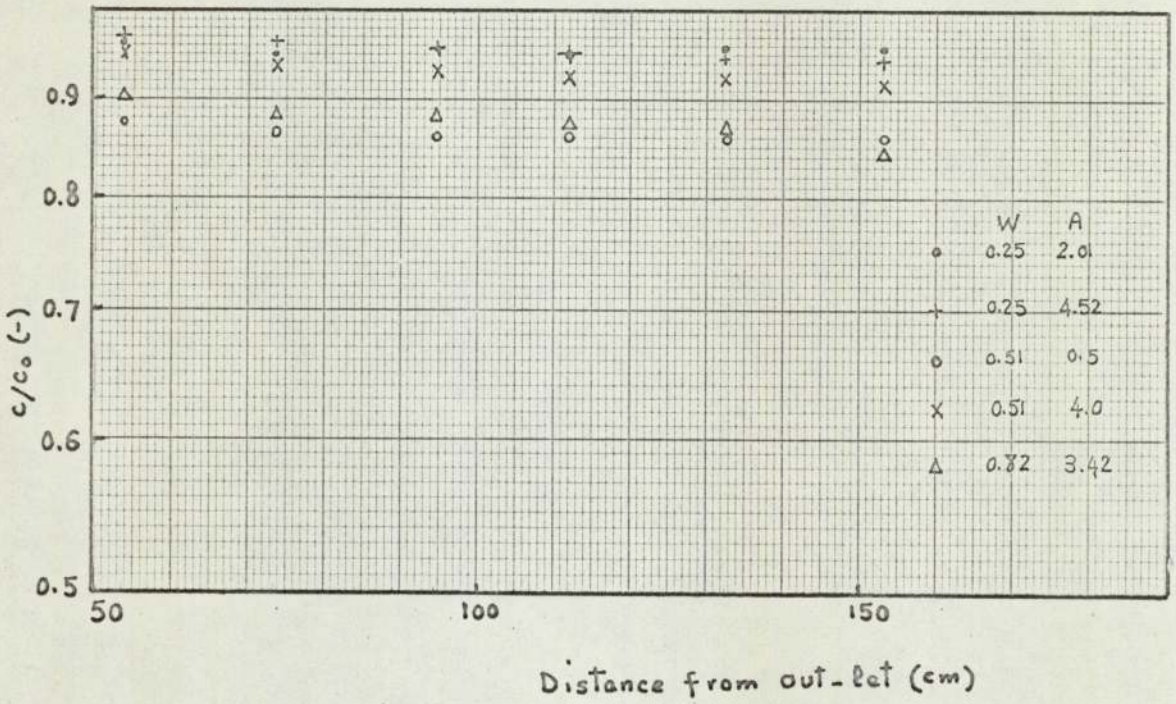

Fig 3.15. Tracer Concentration Profiles over the Length of the 61.0 cm Column.

Table 3.6. Dispersion Coefficients for Different Gas and Liquid Superficial Velocities.

(61.0 cm Diameter Column)

Liquid Flow: 0.25 cm/s

u_{sg} (cm/s)	2.01	3.42	4.52
D_ℓ (cm^2/s)	7397	4706	2328

Liquid Flow: 0.51 cm/s

u_{sg} (cm/s)	0.5	2.01	2.26	4.0
D_ℓ (cm^2/s)	8152	2976	3351	3157

Liquid Flow: 0.82 cm/s

u_{sg} (cm/s)	0.5	3.42
D_ℓ (cm/s)	3154	3280

	Height above Gas Distributor	U_{sg} (cm/s)	U_{sl} (cm/s)
○	70.2	5.30	1.0
●	70.2	2.74	1.0
◐	70.2	1.10	1.0
+	100.9	5.30	1.0
×	100.9	2.74	1.0
⧖	100.9	1.10	1.0
△	131.4	5.30	1.0
▲	131.4	2.74	1.0
▲	131.4	1.10	1.0
□	162.7	5.30	1.0
■	162.7	2.74	1.0
◧	162.7	1.10	1.0

Key to the Fig 3.16.

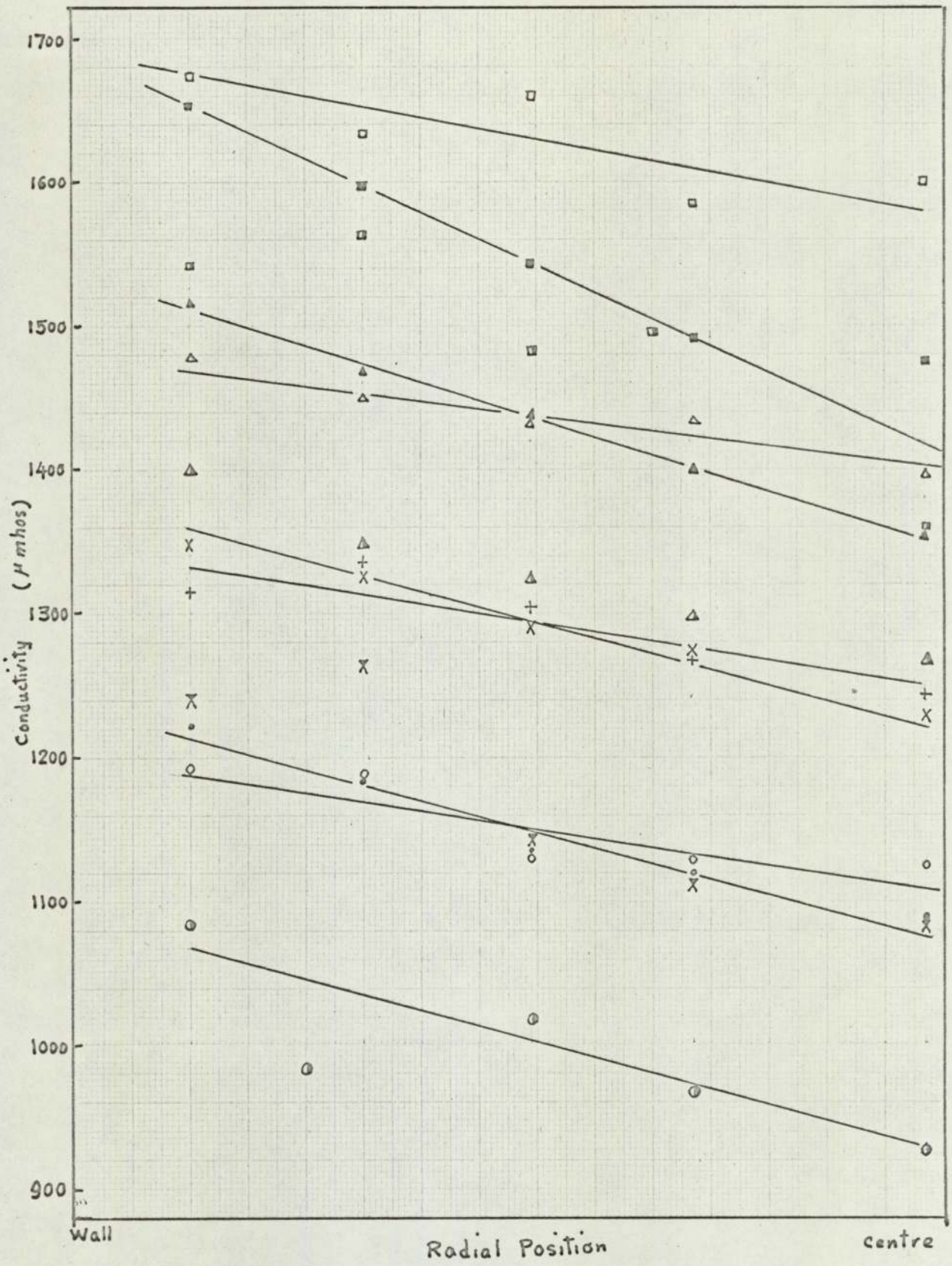

Fig 3.16. Radial Tracer Concentration Profiles at Various Heights of 15.2 cm Column: Effect of U_{sg} on Radial Mixing.

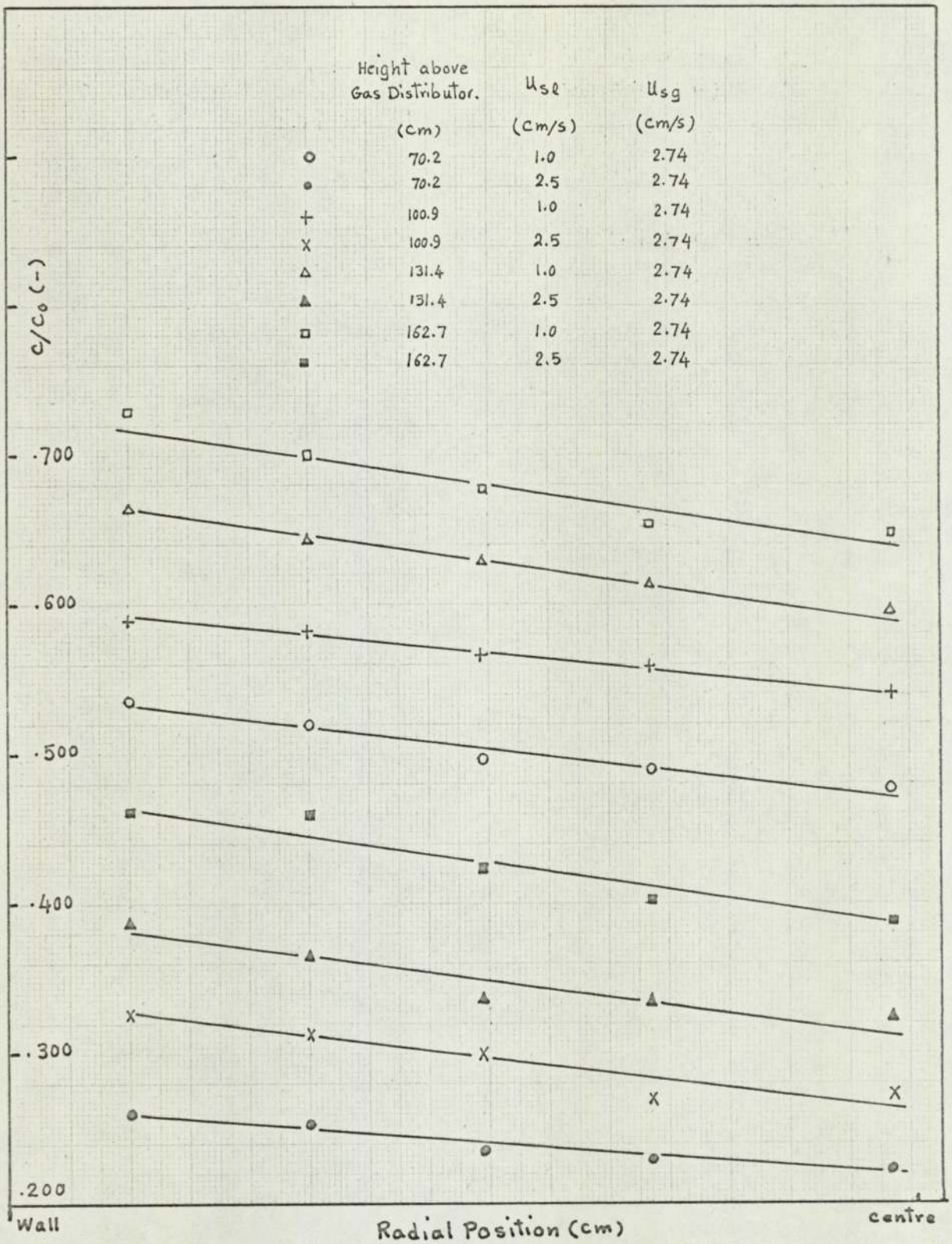

Fig 3.17. Radial Tracer Concentration Profiles at Various Heights of the 15.2 cm Column: Effect of U_{sl} on Radial Mixing.

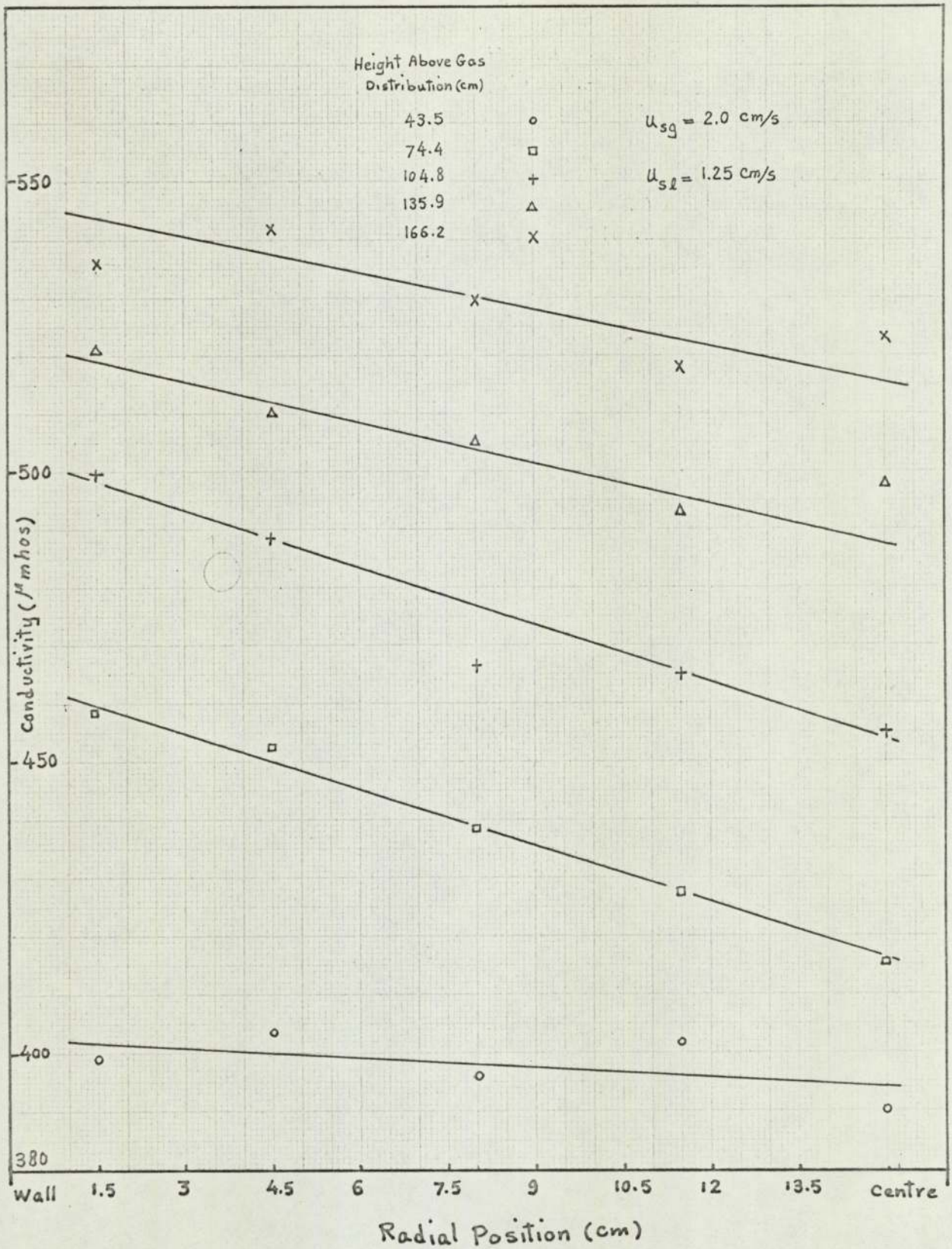

Fig 3.18. Radial Tracer Concentration Profiles at Various Heights of the 30.5cm Column.

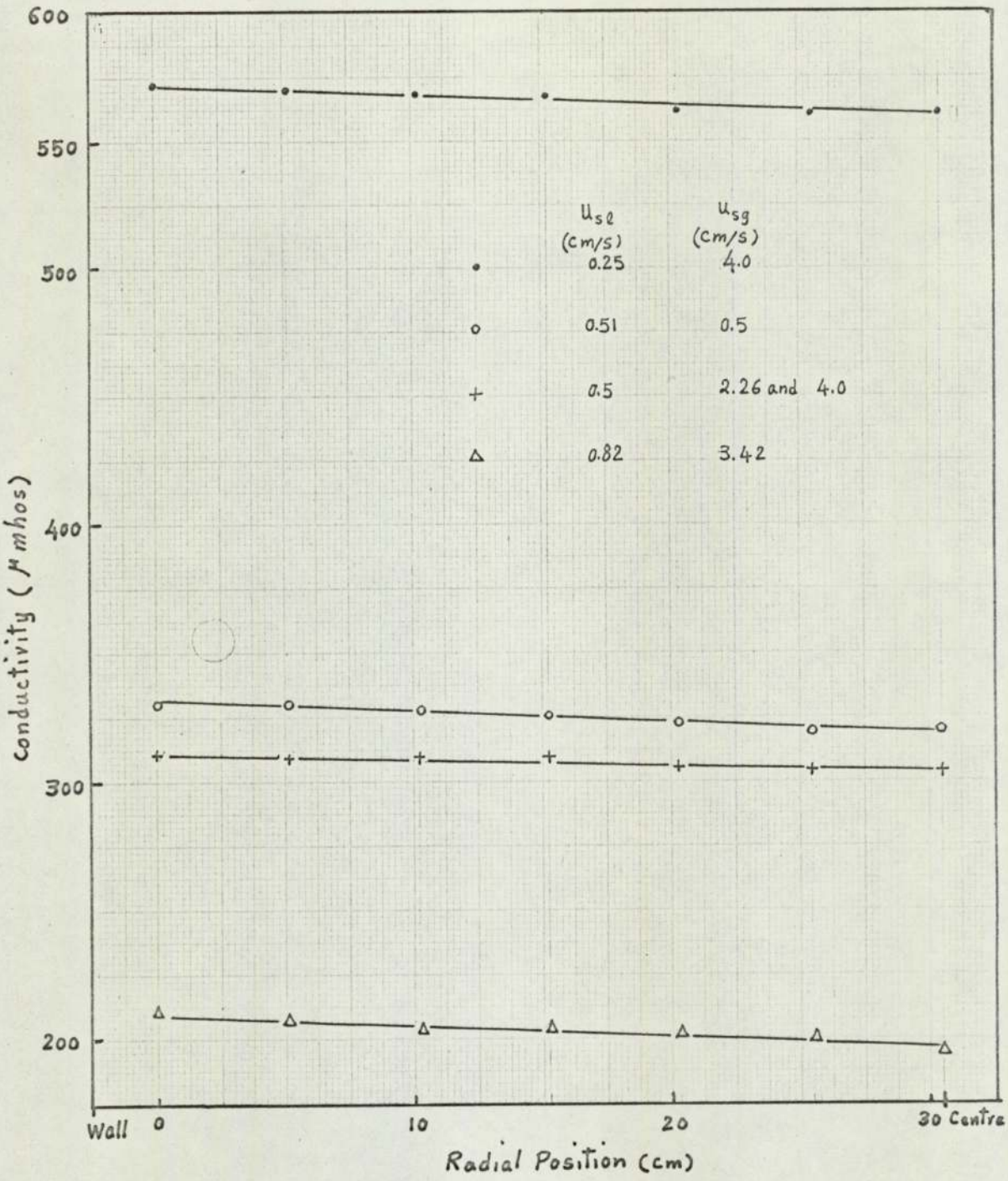

Fig 3.19. Radial concentration Profiles for 61.0 cm column.
(Effect of U_{sg} and U_{sl} on Radial Mixing)

3.5 Discussion and Conclusions

3.5.1. Introductory Comments

Liquid circulation, which has a dominating effect on continuous-phase mixing in bubble columns, is caused by a combination of the following phenomena:

a. density differences due to non homogeneity of the dispersed phase within the continuous phase;

b. downwards liquid flow compensating for the liquid translated by the bubble wakes;

c. liquid displacement due to bubble rise.

More detailed discussion of these mixing mechanisms is given in Section 3.1.

The contribution made by each of these probably varies with the operating conditions. In addition, there is some evidence that column geometry may affect the direction and location of "liquid circulation streams".

3.5.2. Discussion of Experimental Results

Axial Mixing

Effect of Superficial Gas Velocity

It can be said that the gas phase is the main cause of liquid-phase mixing in bubble columns. Figs.3.11 and 3.14 show how the dispersion coefficient reaches a maximum when u_{sg} is only about 4 cm/s. This corresponds to the bubbly flow regime, in which bubble flow is orderly and there is no coalescence. For $u_{sg} >$ 4 cm/s the axial mixing coefficient falls: (at such gas flow rates bubble coalescence takes place and in some cases a reduction in holdup is also observed) this may be due to a reduction in the volume of liquid transported with the gas phase. The dispersion

coefficient again increases with u_{sg} as the coalesced bubble-slug flow regime develops (u_{sg} >6 - 7 cm/s). Results obtained from experiments in both the 15.2 cm and 30.5 cm columns fit this pattern.

It is worth mentioning at this point that D_ℓ values for the 15.2 cm column all lie within the range 220 to 420 cm^2/s with an average of about 330 cm^2/s: in the case of the 30.5 cm column the corresponding figures are 400 to 1050 cm^2/s with an average of about 750 cm^2/s. Although these ranges are limited, the accuracy of the experimental method (see Section 3.4) and consistency of the results gives confidence in the shape of the plots in Fig.3.11 and 3.14.

The results from the experiments with the 61.0 cm column did not follow the same pattern. The value of the dispersion coefficient was high ($D_\ell \approx$ 3000 cm^2/s) and the effect of superficial gas velocity was relatively small. The reason for this marked increase in D_ℓ with column diameter is discussed later.

Effect of Superficial liquid Velocity ($u_{s\ell}$)

Experimental results show that superficial liquid velocity has a significant effect on dispersion. For the 15.2 cm column an increase in $u_{s\ell}$ from 0.46 to 2.28 cm/s increases D_ℓ from 355 to 420 cm^2/s (a 20% rise). The same is true in the case of the 30.5 cm column. Bearing in mind that in the absence of liquid flow interstitial liquid velocities, both upwards or downwards, are very high ($\sim$ 25 cm/s)[62], one would not expect such a big change in D_ℓ over the range of $u_{s\ell}$ explored. Finding an explanation for this is not made easier by the fact that for this range of $u_{s\ell}$ the gas holdup variation was almost negligibly

small (see Section 2).

The author did observe a slight reduction in bubble size with increasing u_{sl} when using perforated plate gas distributors. Although this change in bubble size might not have affected gas hold-up (since u_{∞} is constant for bubbles 4 - 8 mm in diameter) it might have had some effect on liquid circulation and hence mixing. Unfortunately data are not yet available on the effect of superficial liquid velocity on liquid circulation patterns.

Effect of Column Diameter on Mixing

By increasing the column diameter from 15.2 cm to 30.5 cm the dispersion coefficient increased by a factor of 2 when measured over the same height (see Figs.3.11 and 3.14). With the 61.0 cm column, having an aspect ratio of almost 2, very high dispersion coefficients (3500 cm^2/s) were obtained. Tracer concentration profiles for this case (see Fig.3.15) are almost flat.

The fact that the axial mixing coefficients are so dependent on diameter suggests that the mixing results from gross circulation patterns which are of the order of column diameter in scale.

Radial Mixing

Radial mixing had been given very little attention by previous workers (see Section 3.1). It has usually been assumed that radial mixing is sufficient to maintain a uniform tracer concentration over the column cross-section. Figs.3.16, 3.17, 3.18 and 3.19 show that radial concentration profiles exist. The extent of these, however, depends on operating conditions. The tracer concentration difference radially is almost of the same order of magnitude as the concentration difference over a length of 1 diameter in the axial direction ($\sim$ 10%).

The effect of superficial gas velocity on radial mixing is illustrated in Fig.3.16: it will be seen that on increasing U_{sg} the profiles flatten. In other words the radial mixing increases considerably on increasing superficial gas velocity. The pattern is consistent over the length of the column (excluding the two ends).

Superficial liquid velocity does not appear to have any significant effect on radial mixing. In Fig.3.17 in can be clearly seen that although the tracer concentration has been reduced on increasing U_{sl} the slope of the plots remains unchanged over the height of the column.

3.5.3. Data Treatment and Modeling

Downie's Mixing Data (see Section 1)

Downie used an unsteady state tracer method to evaluate dispersion coefficients for the 15.2 and 30.5 cm. columns. This involved "one-shot" tracer injection and measurement of changes in tracer concentration very near to the liquid distributor and about 30 cm below the outlet. The dispersion coefficient was then calculated by analysing the first and second moments of the concentration distribution curves. His data for the 15.2 cm column are summarised in Table 3.7.

A review of his experimental results revealed that the datum line for the concentration-time curves had not been correctly chosen in all cases. Recirculation of water contaminated with tracer also led to difficulties when re-analysing results from some of the experiments. In addition, the marked tailing of some curves made accurate analysis very difficult. After correcting for some of these errors, the dispersion coefficients were recalculated and are

Table 3.7. Results obtained from Downie's Experimental Data[7] from the 15.2 cm column

u_{sl} (cm/s)	ε (-)	* D_l (cm/s) Downie's original data	Data corrected for experimental error	Method of Computation modified to include Weighting Function
0.5	0	1.2	0.9	0.9
0.5	0.025	3.12	15.9	18.4
0.5	.05	2.18	12.7	11.3
0.5	0.075	1.99	10.2	10.2
0.5	0.10	1.90	12.3	20.1
0.5	.20	2.44	23.3	25.7
1.0	0	4.3	3.0	3.0
1.0	0.05	7.87	33.4	46.6
1.0	0.10	13.8	27.7	42.1
1.0	0.20	17.0	41.0	61.5
2.6	0	12.3	4.3	3.9
2.6	0.025	189.5	104.2	118.8
2.6	0.05	180.2	77.9	105.4
2.6	0.075	-	128.9	164.4
2.6	0.10	45.7	52.4	71.5

* D_l is calculated from Peclet Number using equation:

$$N_{Pe} = \frac{u_{sl} \cdot L}{D}$$

included in Table 3.7.

In an attempt to minimise errors arising from tailing, the method of calculation was modified by introducing the weighting function e^{-st} (see Section 3.1). A computer programme for this has been written by Fidgett[81] and the dispersion coefficients calculated in this fashion are also listed in Table 3.7.

The only firm conclusion to be drawn from Downie's results is that mixing is increased as U_{sl} is raised. The effect of U_{sg} on dispersion is not very marked. What is more important, the numerical values obtained for D_l are considerably lower at low values of U_{sg} than those obtained by the author. The probable reason for this is that Downie did not record the response curves with sufficient accuracy and for a long enough time period. Downie's data at the higher liquid flow-rate are considered to be more reliable : D_l values from these are closer to those obtained by the author.

The two methods of evaluating D_l from Downie's data lead to similar results. Figures obtained using the weighting-factor method are consistently higher, however.

Model Based on a Series of Perfectly Mixed Zone with Back Flow – The Back-mixing Model

The author has given considerable thought to the possibility of modelling mixing in the liquid phase. It will be clear from Figs. 3.11 and 3.14 that the effect of U_{sg} on mixing is complex. Evidence of radial mixing and recently published results showing that velocity and hold-up profiles can vary over column diameter add to the problems of setting up a model.

However, as an alternative to the axially dispersed plug-flow

model consideration has been given to what will be called "The Back-mix Model". This model is based on a series of perfectly mixed zones with back-flow between zones: the idea for this originally arose from visual observations of mixing in the larger bubble columns.

Fig. 3.21 is a sketch of the model. A mass balance on tracer leaving and entering the n^{th} tank leads to :

$$\frac{V_n}{A} \cdot \frac{dC_n}{dt} = p\,C_{n-1} - (p+q)C_n + q\,C_{n+1} \qquad (3.27)$$

At steady-state:

$$p\,C_{n-1} - (p+q)C_n + q\,C_{n+1} = 0 \qquad (3.28)$$

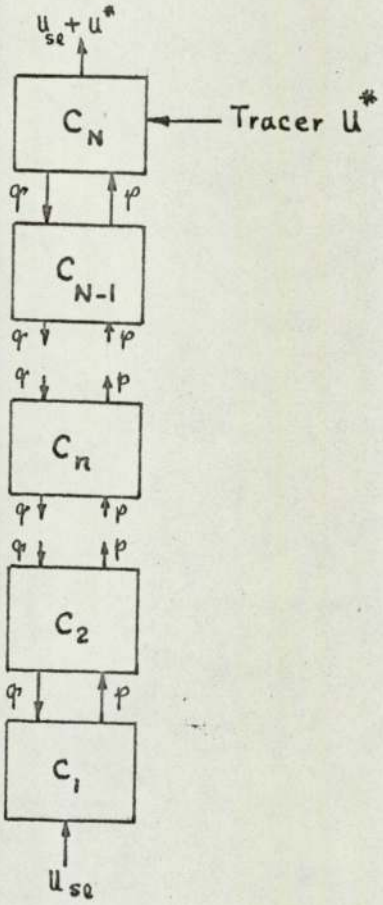

Fig.3.21. Series of Stirred Zones with Back-Mixing

Defining the back-mixing coefficient, f, as equal to $\frac{q}{p}$ then for the first tank:

$$c_1 = f c_2 \qquad (3.29)$$

and for the n^{th} tank: $c_1 = f^{n-1} c_n$

(3.30)

The equivalent steady-state solution for the axially dispersed plug flow model is:

$$\frac{c}{c_o} = \exp\left(\frac{-U_{tl} x}{D_l}\right) \qquad (3.9)$$

(details are given in Section 3.1). This can now be related to the back-mixing model by reference to Fig.3.22

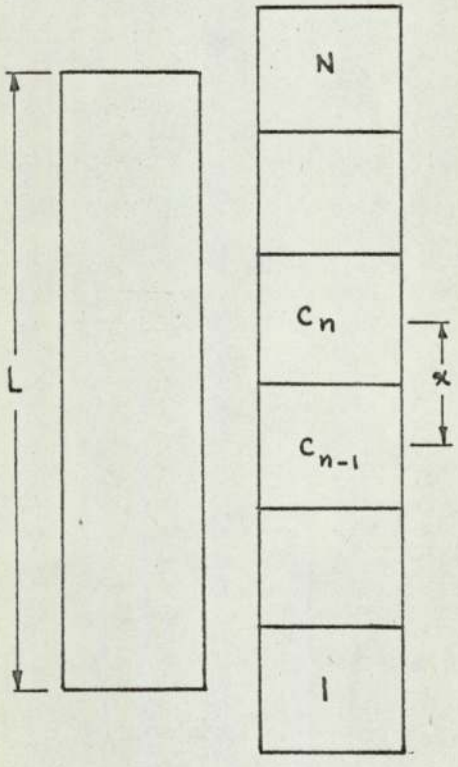

Fig.3.22. Configuration of Back-mix Model with Column Height

By equating: $$\alpha = \frac{L}{N-1} \qquad (3.31)$$

and $$\frac{C_{n-1}}{C_n} = f \qquad (3.32)$$

then $$f = \exp\left(\frac{-u_{t\ell}}{D_\ell} \cdot \frac{L}{N-1}\right) \qquad (3.33)$$

Now it is possible that the back-mix flow, q, might be related to u_{sg} by a relationship of the type:

$$q = \omega u_{sg} \qquad (3.34)$$

where ω is a constant. In this simple form of equation ωu_{sg} is considered to be equivalent to the amount of the liquid translated by bubble motion. If it is also assumed that the number of stages is defined by

$$N = \frac{L}{d_c} \qquad (3.35)$$

then, by using equations (3.33),(3.34),(3.35) and $f = \frac{q}{q + u_{s\ell}}$

$$\frac{\omega u_{sg}}{\omega u_{sg} + u_{s\ell}} = \exp\left(\frac{-u_{t\ell}}{D_\ell} \cdot \frac{L d_c}{L - d_c}\right) \qquad (3.36)$$

Equation (3.35) is based on visual observations and is admittedly a guess about the height of a mixing zone (see section 3.5.1).

The value of w has been calculated from equation (3.36) using dispersion coefficients calculated for the 15.2 and 30.5 cm columns. An empirical relationship was then found correlating w with u_{sg} and $u_{s\ell}$: a graph $\log_e \omega$ vs. $u_{sg} - a u_{s\ell}$ for a = 0.5 is given in Fig.3.23. Data from other sources were obtained and w was calculated in this way: Fig.3.23 shows they are in reasonable agreement with the present work. All the data used for Fig.3.23

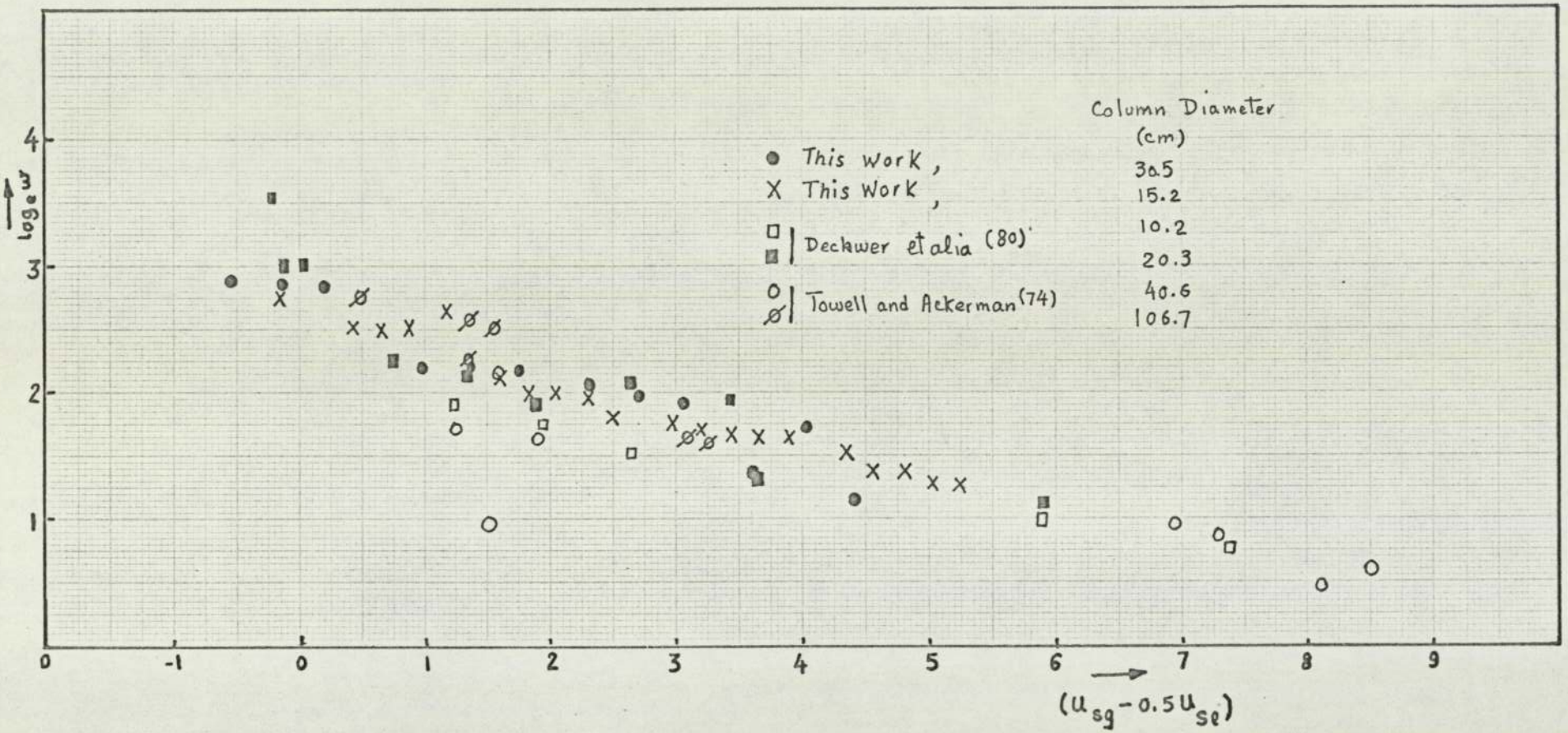

Fig 3.23. Correlation of w with $u_{sg} - a u_{sl}$.

are given in Table(9) of Appendix B.

Although the model is based on intuitive ideas, it may well provide a useful starting point for a more detailed model in the future. In its present form it can be used to estimate dispersion coefficients for first design purposes.

The back-mixing coefficient, f, could also be calculated from equation :

$$f = \exp\left(\frac{-u_{*\ell}}{D_\ell} \cdot \frac{L d_c}{L - d_c}\right) \qquad (3.37)$$

For $u_{*\ell}$ = 0.5 - 2.5 cm/s, the f-value varies between .97 - .87 for the 15.2 cm column and between 0.97 - 0.80 for the 30.5 cm column.

4. Final Comments and Suggestions for Further Work

Achievements

1. Reviews of previous work on factors affecting gas holdup and mixing in bubble columns have been undertaken.

2. A systematic experimental study of the effects of superficial gas velocity, superficial liquid velocity and column diameter on gas holdup and dispersion coefficient in air-water systems has been completed.

3. The effect of liquid phase properties on gas holdup has also been partly examined. A general correlation is not likely to be useful since actual experimental values can be readily obtained.

4. Consideration has been given to preliminary models of mixing in the liquid phase: experimental techniques for studying mixing have also been critically examined. Although mixing studies have been interpreted by means of the dispersed plug-flow model, an alternative model has been put forward based on back-mixing.

Gas Holdup Studies

The following points may be concluded from the gas holdup studies:

1) there is almost a linear increase of gas holdup with superficial gas velocity in the bubbly-flow regime;
2) superficial liquid velocity has little effect on gas holdup in the same regime;
3) the transitional region from bubbly flow to the coalesced bubble-slug flow regime is difficult to characterise;
4) the design of the gas distributor is of little importance provided distribution occurs uniformly;
5) the important effect of column diameter was confirmed;
6) end effects cannot be ignored;

7) physical properties of the liquid phase have an effect, but not a marked effect, on gas holdup in the bubbly flow regime at room temperature: temperature rise and antifoam addition are of most importance;

8) it is recommended that local gas holdup be measured in future work: perhaps overall values of gas holdup are of limited value.

Liquid Mixing Studies

From the mixing studies the following conclusions can be drawn:

1) superficial gas velocity is the most important variable: changes in dispersion coefficient values can readily be related to gas holdup values;

2) superficial liquid velocity has some effect, especially in the transition to the coalesced bubble-slug flow regime;

3) column diameter has an important effect - visual observations indicate changes in mixing patterns;

4) radial mixing cannot be ignored - this could be of the same order of magnitude as axial mixing;

5) the complexity of the mixing patterns highlights the need for measurement of local interstitial liquid velocities as well as gas holdup;

6) steady-state tracer methods are recommended.

Modelling of Mixing in the Liquid Phase

1) The axially dispersed plug-flow model provides a satisfactory description of mixing judged by plots of dispersion coefficient vs superficial gas velocity. In our present state of knowledge about hydrodynamics in bubble columns this one-parameter model has helped our understanding of the effects of operating conditions and design on mixing.

2) A Back-mixing Model provides an alternative description of mixing and can be related in an intuitive way to visual observations of mixing in larger columns. An empirical method of relating a mixing parameter, w, to changes in operating parameters has been briefly introduced.

3) Since radial mixing is important, a more detailed model based on both radial and axial dispersion would seem to be the next logical step.

4) More detailed information about point values of gas holdup and true liquid velocity should provide a sounder basis for modelling in the longer term.

APPENDIX A

Table 1. Gas holdup data for 7.5 cm column

Air-water System

Length of the column in operation 161.1 cm

Gas distributor : Porous plate

U_{sl} =.15 cm/s		U_{sl} =.55 cm/s		U_{sl} =1.01 cm/s		U_{sl} =1.83 cm/s		U_{sl} =2.93 cm/s		U_{sl} = 0	
U_{sg} cm/s	ε	U_{sg} cm/s	ε	U_{sg} cm/s	ε	U_{sg} cm/s	ε	U_{sg} cm/s	ε	U_{sg} cm/s	ε
1.03	0.046	1.03	.049	1.00	0.047	1.01	.044	.985	.0413	1.02	.041
1.52	0.076	1.53	.076	1.52	0.073	1.52	.073	1.52	.065	1.54	.068
2.02	0.104	2.03	.103	2.03	0.099	2.02	.095	2.03	.091	2.04	.098
2.58	0.137	2.55	.132	2.54	0.127	2.52	.121	2.53	.117	3.09	.160
3.05	0.158	3.05	.159	4.04	0.196	3.03	.146	3.04	.142	4.04	.204
4.05	0.202	5.09	.230	5.08	0.228	4.08	.199	4.05	.188	5.09	.240
5.07	0.230	6.09	.257	6.16	0.254	5.01	.227	5.03	.220	6.17	.267
6.07	0.270	7.09	.285	7.15	.275	6.15	.252	6.04	.245	7.19	.291
7.06	0.285	8.09	.296	8.12	,294	7.08	.261	7.11	.267	8.11	.312
8.12	0.315					8.12	.283	8.14	.291	8.89	.312

Table 2. Gas holdup data for 15.2 cm Column

1. Air-Water system
2. Length of the column in operation: 247 cm
3. Gas distributor : Porous Plate
4. Length of the column for no-liquid flow 177.5 cm

u_{sg} cm/s	ε						
	$u_{s\ell}$ cm/s						
	0.00	0.23	0.46	0.69	0.92	1.37	1.92
.816	.031	.032	.032	.032	.032	.030	.030
1.06	.042	.045	.042	.042	.042	.041	.046
1.33	.055	.057	.055	.054	.053	.051	.052
1.80	.080	.082	.071	.078	.075	.074	.072
2.21	.095	.097	.094	.093	.090	.089	.088
2.67	.116	.113	.110	.110	.109	.109	.105
3.55	.146	.147	.142	.144	.143	.143	.143
4.44	.174	.173	.169	.169	.167	.164	.167
5.33	.188	.193	.187	.177	.188	.194	.200
6.22	.183	.177	.177	.178	.180	.197	.224
8.00	.179	.181	.177	.175	.180	.195	.228

Table 3. Gas holdup data for 15.2 cm column

1. Air-water system
2. Length of column in operation : 247 cm
3. Length of column considered : 122.5 cm (middle section)
4. Gas distribution : perforated plate

u_{sg} cm/s	ε				ε
	$u_{s\ell}$ cm/s			u_{sg} cm/s	$u_{s\ell}$ cm/s = 2.29
	0.23	0.92	1.37		
1.10	0.042	.046	.045	1.09	.048
1.86	.075	.074	.078	1.84	.067
2.74	.104	.104	.106	2.72	.097
3.66	.139	.144	.145	3.62	.126
5.48	.188	.188	.196	5.43	.162
7.31	.180	.200	.204	7.24	.167
11.0	.196	.200	.200	8.80	.182
				10.6	.184

Table 4. Gas holdup Data for 30.5 cm Column

1. Air-water System
2. Length of Column in Operation 247 cm
3. Gas distributor : porous plate

u_{sg} cm/s	ε				u_{sg} cm/s	ε	
	$u_{s\ell}$ cm/s					$u_{s\ell} = 0$ Length cm	
	0.23	0.69	1.49	2.24		169.0	101.5
.330	.011	.010	.085	-	.339	.018	.015
.882	.033	.0325	.0313	.033	1.35	.063	0.64
2.20	.091	.0907	.0806	.087	2.25	.103	.103
3.75	.130	.130	.124	.138	3.61	.143	.150
5.29	.147	.147	.150	.158	4.96	.157	.172
7.05	.159	.153	.156	.172	6.31	.165	.182
9.37	.173	.166	.170	.172	7.66	.178	.187
12.50	.189	.192	.186	.186	9.24	.186	.207

Perforated Plate

u_{sg} cm/s	ε		
	$u_{s\ell}$ cm/s		
	0	0.23	0.69
.339	.012	.011	.011
1.35	.048	.052	.049
2.25	.092	.095	.091
3.61	.153	.147	.143
4.96	.188	.189	.187
6.31	.201	.187	.187
7.66	.216	.194	.197
9.24	.228	.209	.208

Table 5. Gas Holdup Data for 61.0 cm Column

1. Air-water system
2. Length of Column in operation 189 cm
3. Gas distributor : perforated plate

u_{sl} =0.086		u_{sl} =0.23		u_{sl} =.34		u_{sl} =0.56		u_{sl} = 0.85	
u_{sg}	ε	u_{sg}	ε	u_{sg}	ε	u_{sg}	ε	u_{sg}	ε
0.583	0.167	.725	.0292	0.583	.0185	.445	.017	.445	.0167
1.00	.035	.96	.350	1.00	.0392	1.78	.069	1.54	.063
1.41	.050	1.41	.525	1.41	.050	2.50	.083	2.79	.092
2.21	.079	2.21	.075	2.21	.079	4.10	.117	3.86	.113
3.09	.100	3.09	.100	3.09	.98	4.43	.124	4.49	.125
4.00	.113	4.00	.113	4.00	.108			6.75	.149
4.98	.125	4.98	0.125	4.98	.125				
6.73	0.150	6.73	.150	6.73	.142				

u_{sg} = [cm/s] u_{se} = [cm/s] ε = [-]

Table 6. Gas holdup distribution data for 15.2 cm Column

U_{sg} cm/s	Liquid level of manometer from column outlet (cm)					
	6	5	4	3	2	1*
			U_{sl} = 0.23 cm/s			
1.10	4.3	5.7	7.0	8.3	9.5	10.5
1.86	6.8	9.4	11.8	14.0	16.0	18.8
2.74	9.7	13.0	15.2	19.5	22.4	27.0
3.66	12.5	16.8	21.5	25.5	29.5	35.0
5.48	17.0	23.0	28.5	35.0	40.0	48.0
7.31	16.0	21.0	27.0	33.0	38.5	47.5
11.0	18.0	24.0	30.0	35.0	42.0	52.5
			U_{sl} =0.92 cm/s			
1.10	3.2	4.6	6.0	7.3	8.8	9.6
1.86	5.8	7.8	10.5	12.7	14.8	17.7
2.74	8.2	11.3	14.7	18.0	21.0	25.0
3.66	10.8	15.0	19.6	24.2	28.5	34.0
5.48	15.0	21.0	26.0	32.5	38.0	46.0
7.31	13.0	19.0	25.0	31.5	37.5	47.0
11.0	14.0	19.5	26 0	32.5	38.5	49.0
			U_{sl} =1.92 cm/s			
1.10	2.5	4.0	5.5	6.7	8.0	9.0
1.86	5.0	7.5	10.2	12.2	14.5	17.5
2.74	7.5	10.5	14.3	17.5	20.5	25.0
3.66	10.2	14.4	19.5	23.6	28.0	33.5
5.48	12.5	18.5	25.0	31.0	36.5	45.0
7.31	10.0	16.5	23.5	30.0	37.0	46.5
11.0	10.5	16.0	22.5	29.0	35.0	46.0

* Numbers from 1 - 6 refer to manometer location (Fig.211)

Table 7. Gas holdup distribution data for 30.5 cm Column

U_{sg} cm/s	Liquid level of manometer from column outlet (cm)							
	8	7	6	5	4	3	2	1
			$U_{s\ell}$ = .69 cm/s					
.88	+1.2*	+0.2	.8	1.8	2.8	3.8	4.8	5.8
2.20	+0.5	2.5	5.5	8.0	10.5	13.5	16.4	19.0
3.75	0.5	5.5	10.0	14.0	18.0	22.0	25.5	30.5
5.29	1.5	7.0	11.5	16.0	21.0	25.5	29.5	35.5
9.24	3.0	9.5	15.0	20.0	25.0	30.0	35.0	42.0
			$U_{s\ell}$ = 1.49 cm/s					
.88	+3.0	+2.0	+1.0	0	0.8	1.8	2.8	3.6
2.20	+2.0	0.8	3.4	6.0	8.5	11.0	14.0	16.5
3.75	+1.0	4.0	8.5	12.0	16.0	19.0	23.0	28.5
5.29	+0.2	5.0	9.5	14.0	18.5	23.0	28.0	33.0
9.24	1.0	7.0	13.0	18.0	23.0	28.0	33.0	39.5
			$U_{s\ell}$ =2.24 cm/s					
.88	+4.2	+3.1	-	-	0	1.0	1.9	2.7
2.20	+3.5	+0.4	2.5	4.9	7.6	10.2	13.0	16.0
3.75	+2.0	2.8	7.5	11.5	16.0	20.0	24.0	28.8
5.29	+1.3	4.5	9.5	14.5	19.5	24.0	28.8	34.7
9.24	+0.5	5.5	11.0	16.0	21.0	27.0	32.0	39.0

* Sign (+) indicates that manometer level was above column outlet

Table 8. Gas holdup distribution data for 61.0 cm Column

U_{sg} cm/s	Liquid level of manometer from column outlet (cm)						
	7	6	5	4	3	2	1
			U_{sl} = 0.09 cm/s				
0.583	1.3	-	-	-	-	-	3.3
1.00	2.1	3.1	3.8	4.3	4.8	5.8	6.3
1.41	2.8	3.8	4.8	6.3	7.3	8.3	8.8
2.21	3.8	5.3	7.1	9.3	10.8	11.8	13.3
3.09	4.8	7.3	9.3	11.8	13.6	15.3	16.8
4.00	6.3	8.3	11.1	13.8	15.8	18.3	19.8
4.98	6.8	9.8	12.8	15.8	18.3	19.8	21.8
6.73	8.3	12.3	15.3	18.3	20.8	23.8	26.3
			U_{sl}=0.56 cm/s				
.445	*+3.6	+3.0	-	-	-	-	+1.6
1.78	+2.5	+1.0	.3	1.7	3.0	4.5	5.8
3.49	+2.5	0	2.5	4.5	7.0	9.5	10.7
4.10	+2.0	0.5	3.0	5.5	8.0	11.0	12.0
4.43	+2.5	0.5	3.5	6.0	8.5	10.5	12.5
			U_{sl}=0.85 cm/s				
.445	+2.5	+2.0	-	-	-	-	+0.5
1.54	+1.0	.5	1.9	3.0	4.2	5.5	6.5
2.79	.8	2.3	4.5	6.5	8.5	10.5	11.8
3.86	.7	2.9	5.7	8.0	10.4	12.8	14.2
4.49	1.0	4.5	6.5	9.0	11.5	14.0	16.0

* above outlet

Table 9. Effect of liquid-phase temperature on gas holdup

Column diameter = 15.2 cm

9.1 $U_{sl} = 0$ (Length of the column in operation 147.2 cm)

15.8°C		26°C		29.7°C	
U_{sg}	ε	U_{sg}	ε	U_{sg}	ε
1.09	.0441	1.10	.0484	1.12	.0458
1.84	.0778	1.87	.0825	1.89	.0754
2.71	.109	2.76	.115	2.80	0964
3.62	.143	3.69	.143	3.73	.114
5.43	.211	5.53	.179	5.60	.142
7.24	.211	7.36	.187	7.47	.171
10.75	.220	11.0	.214	11.2	0.210

U_{sg} = [cm/s]

9,2 u_{sl} =0.23 cm/s

15.8°C		26.0°C		29.7°C		34.0°C		45°C	
u_{sg}	ε	u_{sg}	ε	u_{sg}	ε	u_{sg}	ε	u_{sg}	ε
1.09	.0405	1.10	.0474	1.12	.0458	1.12	.045	1.19	.0535
1.84	.0722	1.87	.0810	1.89	.0802	1.89	075	2.01	.0850
2.71	.104	2.76	.113	2.80	.112	2.80	.964	2.97	.104
3.62	.138	3.69	.147	3.73	.130	3.73	.115	3.96	.123
5.43	.193	5.53	.178	5.60	.151	5.59	.147	5.95	.156
7.24	.208	7.36	.182	7.47	.170	7.45	.170	7.93	.182
10.75	.200	11.0	.206	11.2	.204	11.2	.212	11.9	.225

u_{sg} = [cm/s]

(Effect of liquid-phase temperature on gas holdup-continued)

9.3 $u_{s\ell} = 0.92$ cm/s

15.8°C		26.0° C		29.7°C		34.0°C		45.0° C	
u_{sg}	ε	u_{sg}	ε	u_{sg}	ε	u_{sg}	ε	u_{sg}	ε
1.09	.0420	1.10	.0492	1.12	.0508	1.12	.0524	1.19	.657
1.84	.0718	1.87	.0817	1.89	.0835	1.89	.0775	2.01	.100
2.71	.104	2.76	.114	2.80	.100	2.80	.0990	2.97	.112
3.62	.137	3.69	.144	3.73	.116	3.73	.116	3.96	.128
5.43	.198	5.53	.157	.5.60	.143	5.59	.142	5.95	150
7.24	.208	7.36	.170	7.47	.166	7.45	.168	7.93	.180
10.75	.204	11.0	.200	11.2	.200	11.2	.208	11.9	.219

9.4 $u_{s\ell} = 1.37$ cm/s

15.8°C		26.0°C		29.7°C		34.0°C	
u_{sg}	ε	u_{sg}	ε	u_{sg}	ε	u_{sg}	ε
1.09	0.0420	1.10	.0523	1.12	.0576	1.12	.0602
1.84	.0738	1.87	.0884	1.89	.0918	1.89	.0962
2.71	.107	2.76	.120	2.80	.123	2.80	.122
3.62	.140	3.69	.154	3.73	.138	3.73	.137
5.43	.207	5.53	.169	5.60	.152	5.59	.158
7.24	.227	7.36	.182	7.47	.169	7.45	.174
10.75	.212	11.0	.207	11.2	.209	11.2	.212

$u_{sg} = [cm/s]$

Table 10. Superficial gas velocity and gas holdup for 1% and 4% wt/wt KCl solutions (15.2 cm column)

U_{sg} cm/s	ε					
	1% KCl			4% KCl		
	$U_{s\ell}$ (cm/s)			$U_{s\ell}$ (cm/s)		
	0.23	0.92	1.87	0.23	.92	1.87
1.10	.050	0.515	.0540	.049	.047	.047
1.86	.083	.089	.093	.078	.076	.077
2.74	.120	.122	.131	.113	.118	.112
3.66	.165	.180	.188	.159	.155	.150
5.48	.224	.249	.265	.261	.229	.224
7.31	.216	.245	.265	.212	.212	.204
11.0	.220	.229	.257	.229	.224	.216

Table 11. Superficial gas velocity and gas holdup for 2,3,4,5,7 and 10% wt/wt sugar solutions

u_{sl} = 0.92 cm/s Column diameter 15.2 cm

u_{sg} cm/s	ε Sugar concentration %					
	2	3	4	5	7	10
1.10	.0457	.0351	.0465	.0449	.0392	.0465
1.86	.0686	.0653	.0792	.0760	.0702	.0776
2.74	.102	.0988	.111	.109	.109	.110
3.66	.147	.140	.161	.159	.151	.158
5.48	.207	.212	.240	.237	.234	.240
7.31	.204	.212	.233	.229	.237	.245
11.0	.208	.212	.220	.224	.220	.233

Table 12. Superficial gas velocity and gas holdup for 3% (wt/wt) malt extract* at different u_{sl}'s in 15.2 cm column

u_{sg} cm/s	ε		
	u_{sl} cm/s		
	0.23	0.92	1.87
1.12	.0449	.0424	.0410
1.89	.0734	.0735	.0776
2.80	.106	.108	.106
3.73	.147	.143	.139
5.60	.278	.224	.233
7.47	-	.331	.318
9.4	-	.371	.343

* Brewers' malt extract is produced by hot water extraction of malted barley.

The product supplied by E.D.M.E. is a concentrated extract produced by vacuum evaporation and has the following approximate composition:

70 - 75% carbohydrate

5 - 6% protein

1 - 1.5% mineral matter

18 - 24% water

Table 13. Superficial gas velocity and gas holdup for charging wort* at different U_{sl}'s in 15.2 cm column

25°C				30°C	
U_{sg} cm/s	ε			U_{sg} cm/s	ε
	U_{sl} cm/s				U_{sl} = .92 cm/s
	.23	.92	1.87		
1.10	.0465	.0490	.0514	1.12	.0440
1.87	.0833	.0841	.0849	1.89	.0800
2.76	.119	.115	.118	2.80	.113
3.69	.159	.157	.158	3.73	.158
5.53	-	19.2	20.0	5.60	.196
7.36	-	22.1	.214	7.47	.223
9.2	-	26.4	.258	9.4	.257

*Charging wort is the product of alcoholic fermentation of a sweet wort. The sweet wort is produced by extracting malted barley with warm water.

Charging wort contains approximately 6% alcohol and numerous by-products of yeast metabolism. The latter compounds may be present in quantities of only a few p.p.m.

Table 14. Physical properties of suspensions of brewers' yeast

Physical Properties	Dry weight % .0584	1.599	2.872	3.724	5.561
Density 25°C (g/cm^3)	1.0005	1.0041	1.0086	1.0103	1.0135
Surface Tension (25°C) (dyn/cm)	55.2	51.0	53.8	52.0	49.8
Viscosity 25°C (C.P)	1.26	1.52	1.79	4.15	8.90

Table 15. Superficial gas velocity and gas holdup for different yeast suspensions at 25°C

U_{sl} = 0.92 cm/s

U_{sg} cm/s	ε				
	dry weight % wt/wt				
	.584	1.56	2.87	3.72	5.56
1.06	0514	0423	.0449	.0473	.0530
1.79	.0776	.0759	.0824	.0865	.0920
2.64	.117	.109	.118	.130	.139
3.52	.155	.156	.163	.177	.175
5.29	.191	.187	.208	.241	.220
7.05	.215	.220	.229	.274	.265
8.8	.237	.251	.267	.284	.303

U_{sg} cm/s	ε					
	U_{sl} =0.23 cm/s			U_{sl} =2.87 cm/s		
	dry yeast % wt/wt					
	.584	1.56	2.87	.584	1.56	2.87
1.06	.0450	.0408	.0408	.0450	.0423	.0449
1.79	.0735	.0751	.0776	.0735	.0735	.0792
2.64	.112	.111	.122	.113	.113	.115
3.52	.148	.147	.163	.147	.151	.163
5.29	.180	.184	.186	.182	.182	.198
7.05	.191	.212	.220	.205	.208	.229
8.8	.220	.223	.248	.235	.233	.247

Table 16. Superficial gas velocity and gas holdup for different mould suspensions at 29 - 30°C

Dilute molasses* solution (10%) was used as medium

u_{sg} cm/s	ε			
	mould dried wt. %			
	0.085	0.170	0.30	0.51
1.12	.0365	.0319	.0378	.0273
1.89	.056	.0526	.0566	.0468
2.80	.0834	.0709	.0748	.0632
3.73	.0994	.0872	.0904	.0847
5.6	.119	.119	12.1	.107
7.47	.141	.145	.150	.138
9.36	.170	.171	.171	.161

* Beet molasses was supplied by British Sugar Refinery, Kidderminster Worcs. and has the following approximate concentration:

Reducing sugar	55% (wt/wt)
Mineral and organic materials	23%
Nitrogen	1.5%
Water	20%

Table 17. Superficial gas velocity and holdup for air-water system with and without antifoam (5.0 c.c. of 2.5% silicone : see Section 2.4.3)

u_{sg} cm/s	ε	
	with antifoam	without antifoam
1.10	0.018	0.045
2.2	0.036	0.093
2.65	0.046	0.115
3.65	0.059	0.143
5.4	0.083	0.180

Table 18. Superficial gas velocity and holdup at different stages of vinegar production

u_{sg} cm/s	ε (-)		
	Time (h)		
	0	24	48
1.12	0.046	.044	.43
1.89	0.08	.078	.72
2.80	0.113	.112	.107
3.73	15.9	.162	.153

Table 19. Variation of ε by time in vinegar production

u_{sg} = 1.89 cm/s

Time (h)	0	24	28	32	44	48	57
ε (-)	.08	-07.80	-07.73	-07.73	-07.25	-07.24	.07.5
	68		70	75	78	81	92
	.07.24		.07.17	.07.17	.07.10	.07.04	.07.00

Table 20. Physical properties of the medium during the course of vinegar fermentation.

Physical Properties (18 - 20°C)	Time (h) 0	24	2 x 24	3 x 24	4 x 24
Acid content (g/l)	8.18	10.94	13.13	28.11	42.20
Alcohol content (%)	6	4.6	3.2	-	<0.1
Surface tension (dyn/cm)	45.9	49.2	45.9	44.6	43.2
Density (g/cm^3)	.9976	.9983	.9811	.9799	.9797

APPENDIX B

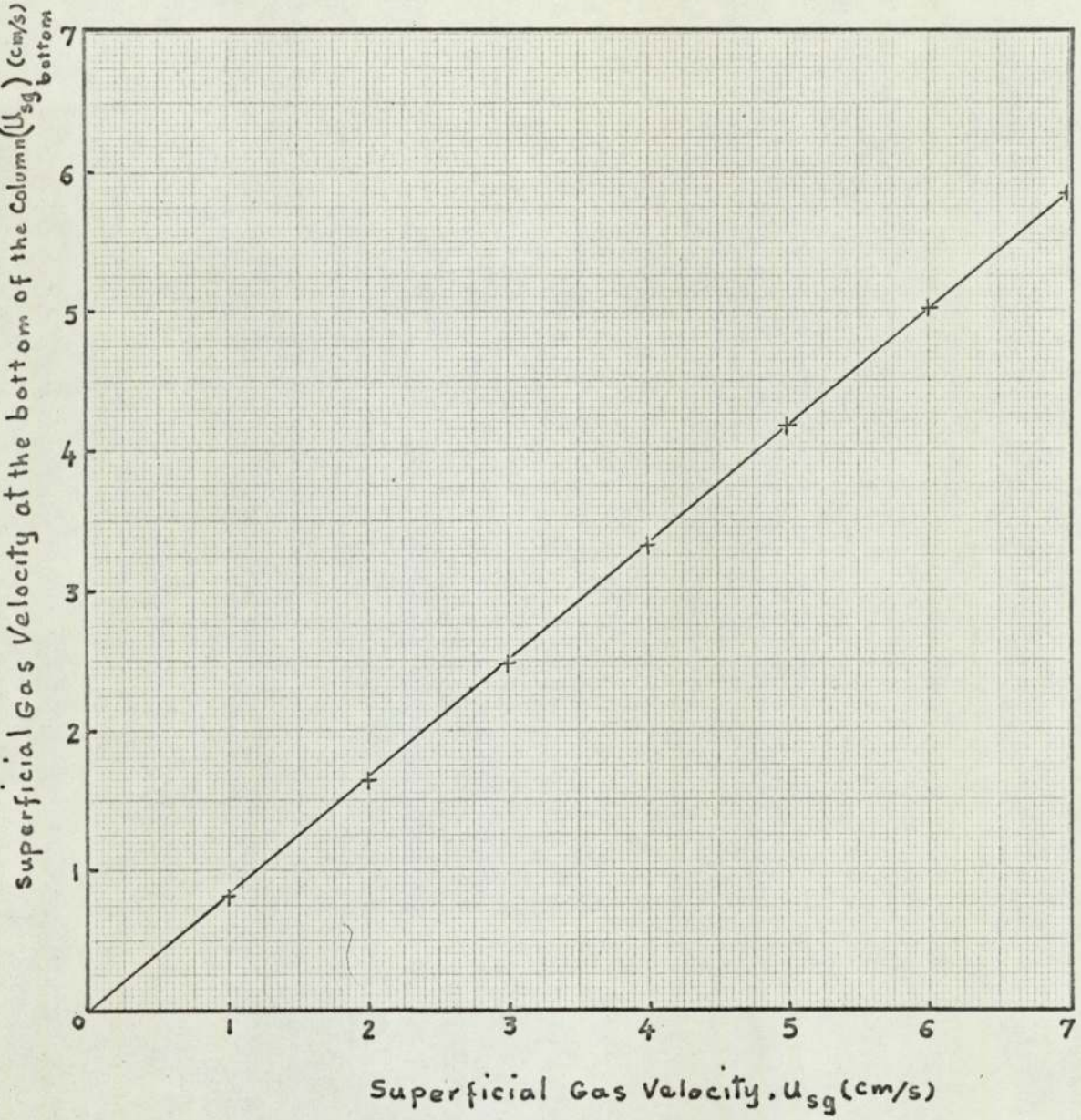

Fig 1. The Relationship between U_{sg} and u_{sg}. U_{sg} computed from values of u_{sg} and $(u_{sg})_{bottom}$ Taken from plot using

$$U_{sg} = \frac{u_{sg} + (u_{sg})_{bottom}}{2}$$

Table 1. Tracer concentrations over the length of the 15.2 cm column for different gas and liquid flow-rates

Liquid Flow : 0.46 cm/s

Distance from outlet (cm)	C/Co (-)						
	U_{sg} (cm/s)						
	1.10	2.74	4.11	5.48	7.31	9.13	11.9
54.0	0.857	.851	.841	.872	.905	.920	.924
84.8	0.800	.820	807	.830	.851	.867	.869
116.1	.753	.782	.772	.782	.802	.818	.818
146.6	.708	.747	.741	.745	.755	.772	.777
177.3	.664	.709	.707	.712	.716	.730	.751
223.8	.593	.613	.650	.648	.654	.665	.673
Liquid Flow: 0.91 cm/s							
54.0	.721	.737	.727	.837	.844	.860	.866
84.8	.642	.683	.673	.735	.748	.757	.776
116.1	.562	.625	.617	.655	.699	.671	.697
146.6	.493	.569	.571	.585	.597	.601	.621
177.3	.443	.515	.525	.525	.537	.537	.562
223.8	.347	.430	.445	.442	.460	.453	.478
Liquid Flow: 1.38 cm/s							
54.0	.637	.655	.649	.696	.757	.779	.815
84.8	.548	.572	.581	.594	.633	.657	.686
116.1	.453	.510	.511	.519	.526	.558	.584
146.6	.382	.447	.454	.458	.450	.470	.492
177.3	.318	.388	..396	.399	.387	.409	.424
223.8	.223	.303	.311	.314	.306	.321	.333

Distance from outlet (cm)	C/C_o (–)						
	u_{sg} (cm/s)						
	1.10	2.74	4.11	5.48	7.31	9.11	11.9
Liquid Flow: 1.83 cm/s							
54.0	.505	.557	.561	.635	.683	.735	.748
84.8	.421	.487	.485	.525	.548	.581	.601
116.1	.324	.403	.399	.423	.438	.468	.488
146.6	.271	.340	.342	.361	.362	.379	.404
177.3	.217	.280	.290	.302	.304	.310	.338
223.8	.153	.208	.215	.224	.223	.233	.256
Liquid Flow: 2.28 cm/s							
54.0	.483	.509	.490	.557	.655	.678	.708
84.8	.389	.419	.397	.430	.497	.518	.536
116.1	.290	.334	.321	.353	.379	.398	.414
146.6	.232	.285	.265	.292	.297	.311	.321
177.3	.183	.238	.219	.239	.238	.246	.255
223.8	.127	.166	.159	.180	.175	.184	.181

Table 2. Dispersion coefficients for different liquid and gas superficial velocities (15.2 cm diameter column)

u_{sl}	D_l (cm^2/s)						
	u_{sg} (cm/s)						
cm/s)	1.01	2.52	3.77	5.03	6.71	8.38	10.44
0.46	225	274	354	324	293	295	311
0.91	224	319	361	325	303	299	326
1.38	235	337	370	362	314	323	325
1.83	270	345	378	365	330	343	363
2.28	299	390	403	422	358	362	357

Table 3. Dispersion coefficients for different liquid and gas superficial velocities (30.5 cm diameter column)

u_{sl}	D_l (cm^2/s)					
	u_{sg} (cm/s)					
cm/s	0.38	1.66	2.77	3.87	5.54	7.20
0.51	2.84	617	798	839	683	677
1.25	303	647	859	940	810	776
2.03	322	657	932	1042	924	787

Table 4. Tracer concentrations over the length of the 30.5 cm column for different gas and liquid flow rates

Liquid Flow : 0.51 cm/s

Distance from outlet (cm)	C/Co (-)					
	u_{sg} (cm/s)					
	0.46	1.99	3.32	4.65	6.65	8.64
57.9	.901	.896	.898	.899	.920	.928
88.6	.854	.883	.884	.877	.888	.904
119.7	.817	.870	.868	.863	.877	.886
149.9	.765	.845	.850	.837	.851	.862
180.5	.731	.826	.839	.823	.831	.840
211.5	.700	.778	.804	.789	.797	.812
Liquid Flow : 1.25 (cm/s)						
57.9	.778	.773	.754	.788	.832	.875
88.6	.670	.730	.719	.753	.788	.837
119.7	.576	.695	.688	.718	.743	.800
149.9	.513	.635	.653	.680	.705	.756
180.5	.490	.597	.618	.660	.673	.710
211.5	.440	.547	.573	.617	.619	.655
Liquid Flow : 2.03 (cm/s)						
57.9	.580	.644	.651	.713	.772	.792
88.6	.525	.592	.599	.641	.707	.736
119.7	.475	.554	.567	.607	.658	.688
149.9	.433	.492	.528	.560	.606	.623
180.5	.382	.448	.483	.533	.566	.576
211.5	.337	.398	.447	.482	.508	.523

Table 5. Tracer concentrations over the length of the 61.0 cm column for different gas and liquid flow-rates

Liquid Flow : 0.25 cm/s

Distance from outlet (cm)	C/C_o (−)			
	u_{sg} (cm/s)			
	2.01	3.42	4.52	
53.4	.965	.953	.969	
73.5	.954	.949	.963	
94.5	.955	.944	.956	
112.1	.951	.944	.952	
132.6	.955	.941	.947	
153.0	.954	.940	.942	

Liquid Flow : 0.51 (cm/s)

	0.5	2.01	2.26	4.0
53.4	.877	.964	.971	.953
73.5	.866	.942	.966	.943
94.5	.859	.936	.954	.930
112.1	.859	.935	.944	.926
132.6	.858	.928	.948	.921
153.0	.859	.917	.933	.916

Liquid Flow : 0.82 (cm/s)

	0.5	3.42		
53.4	.970	.904		
73.5	.965	.886		
94.5	.949	.881		
112.1	.942	.874		
132.6	.936	.864		
153.0	.908	.841		

Table 6. Tracer concentrations at various radial positions for 15•2 cm diameter column

Distance from Gas Distributor (cm) = A

Distance from the Wall (cm) = B

Tracer Concentration

(Conductivity of the Solution (μmho)= C

u_{sl} (cm/s)	u_{sg} (cm/s)	A	B 1.0	2.5	3.95	5.35	7.35
					C		
1.0	1.10	70.	1086	985	1021	968	928
		100.9	1241	1265	1141	1114	1106
		131.4	1400	1371	1323	1298	1267
		162.7	1542	1554	1483	1495	1397
1.0	2.74	70.2	1221	1185	1127	1120	1089
		100.9	1347	1326	1291	1274	1230
		131.4	1515	1468	1438	1399	1355
		162.7	1654	1596	1545	1492	1476
1.0	5.30	70.2	1192	1187	1132	1129	1127
		100.9	1315	1337	1305	1270	1244
		131.4	1478	1450	1433	1436	1396
		162.7	1674	1634	1649	1586	1599
1.0	2.74	70.2	297.5	290.8	270.7	263.6	256.8
		100.9	373	358.3	343.0	310.9	313.8
		131.4	443.8	417.9	386.1	383.9	371.8
		162.7	528.7	526.9	484.3	460.3	444.8

Table 7. Tracer concentrations at various radial positions for 30.5 cm diameter column

Distance from Gas Distributor (cm) = A

Distance from the Wall (cm) = B

Tracer Concentration (conductivity of the solution) = C

u_{sl} = 1.25 cm/s

u_{sg} = 2.0 cm/s

A = 43.5

B	1.5	4.5	8.0	11.5	15.0
C	399.1	403.5	396.0	401.9	390.2

A = 74.4

B	1.5	4.5	8.0	11.5	15.0
C	459.5	452.5	438.4	427.4	415.3

A = 104.8

B	1.5	4 5	8.0	11.5	15.0
C	499.5	488.4	466.3	465.0	455.1

A = 135.9

B	1.5	4.5	8.0	11.5	15.0
C	534.2	509.8	505.1	492.9	497.7

A = 166.2

B	1.5	4.5	8.0	11.5	15.0
C	535.8	541.9	529.4	518.1	523.0

Table 8. Tracer concentrations at various radial positions for 61.0 cm diameter column

Distance from the Gas Distributor = 90.0 cm

Distance from the Wall (cm) = B

Tracer Concentration (conductivity of the solution) = C

$U_{sl} = 0.25$ (cm/s)

$U_{sg} = 4.52$ (cm/s)

B	0	5.1	10.2	15.2	20.3	25.4	30.5
C	572.7	569.9	568.4	566.1	563.0	561.7	561.4

$U_{sl} = 0.51$ (cm/s)

$U_{sg} = 0.50$ (cm/s)

B	0	5.1	10.2	15.2	20.3	25.4	30.5
C	329.6	329.0	327.1	325	322.1	319.6	320.3

$U_{sl} = 0.51$ (cm/s)

$U_{sg} = 2.26$ (cm/s)

B	0	5.1	10.2	15.2	23.3	25.4	30.5
C	311.1	308.0	308.2	308.1	305.8	303.9	304.6

$U_{sl} = 0.51$ (cm/s)

U_{sg} 4.0 (cm/s)

B	0	5.1	10.2	15.2	23.3	25.4	30.5
C	311.3	309.6	308.7	306.9	305.8	304.9	304.3

$U_{sl} = 0.82$ (cm/s)

$U_{sg} = 3.42$ (cm/s)

B	0	5.1	10.2	15.2	23.3	25.4	30.5
C	210.8	207.5	206.0	203.8	201.2	199.9	199.6

Table 9. Corresponding values of ω for different conditions.

	u_{sg}	u_{se}	D_ℓ	ω
This work	1.1	0.46	225	12.39
L = 250 cm	2.74	"	274	6.07
d_c=15.25 cm	4.11	"	354	5.25
	5.48	"	324	3.60
	1.1	0.91	225	12.19
	2.74	"	319	7.00
	4.11	"	361	5.30
	5.48	"	325	3.57
	1.1	1.37	235	12.54
	2.74	"	337	7.33
	4.11	"	370	5.38
	5.48	"	362	3.94
	1.1	1.83	270	14.30
	2.74	"	345	7.42
	4.11	"	378	5.44
	5.48	"	365	3.94
	1.1	2.28	299	15.72
	2.74	"	390	8.35
	4.11	"	403	5.76
	5.48	"	422	4.54
This work				
L = 250	0.46	0.51	284	17.22
d_c = 30.5	1.99	"	617	8.80
	3.32	"	798	6.84
	4.65	"	839	5.14
	0.46	1.25	202	17.64
	1.99	"	647	9.05

Table 9 continued

	3.32	"	859	7.26
	4.65	"	940	5.69
	0.46	2.03	322	18.02
	1.99	"	657	9.00
	3.32	"	932	7.80
	4.65	"	1042	6.23
Towell & Ackerman (74)				
L = 150 d_c = 40.6	2.20	0.678	672	5.33
	8.85	0.678	930	1.85
	2.20	1.356	362	2.66
	8.85	1.356	826	1.60
L = 284 d_c = 40.6	1.92	0.678	801	8.63
	7.62	0.678	878	2.39
	1.92	1.356	542	5.61
	7.62	1.356	956	2.56
L = 510 d_c = 106.8	1.74	.373	2895	12.21
	3.45	.373	2320	4.92
	.854	.745	1885	15.91
	1.74	.745	3255	13.63
	3.45	.745	2480	5.21
	1.74	.745	2245	9.34

Table 9 continued

Deckwer et alia[80]	1.4	0.34	104 *	6.87
L = 256	2.1	"	129 *	5.70
d_c = 10.2	2.8	"	138 *	4.58
	3.8	"	146 *	3.57
	6.0	"	173	2.69
	7.5	"	175	2.17
	1.4	-0.17+	85 *	5.78
	2.6	"	154 *	5.61
	3.8	"	230 *	5.72
L = 222	0.15	0.74	123	34.89
d_c = 20	0.24	"	118	20.86
	0.40	"	190 *	20.70
	1.1	"	244 *	9.76
	1.7	"	340 *	8.88
	2.2	"	340 *	6.86
	3.0	"	550 *	8.22
	3.8	"	604 *	7.13
	6.2	"	426	3.07

* Upper Region of Column + Counter-current flow

Nomenclature

A	area
A_o	orifice cross-sectional area
A_c	column cross-sectional area
C	concentration
C_o	*
d	diameter
d_b	bubble diameter
d_c	column diameter
d_o	orifice diameter
D	dispersion coefficient
D_ℓ	axial dispersion coefficient
D_r	radial dispersion coefficient
f	back-mix coefficient
f_w	wake fraction, volume of wake/volume of bubble
F	probability distribution of displacements of a solid particle within a fixed short time interval, t.
g	gravity
G	mass flow rate
h	manometric height
K_1	constant
K	Bankoff flow parameter
K_2	flow parameter for slug flow
l	length
l	distance from column outlet
L	bubble bed height
l_m	length of measuring section
L'	height of gas-free liquid in the column
MRT	mean residence time
*	exprimental tracer concentration of exit stream leaving the column.

n	number of tanks
n	number of holes
N_{Re}	Reynolds number
N_{Bo}	Bond number
N_{Fr}	Fronde number
N_{Ga}	Galileo number
N_{Pe}	Peclet number
N_{Pr}	Prandt number
ΔP	Pressure drop
ΔP_f	Pressure drop due to the friction and contraction of gas flow through the gas distributor.
ΔP_o	maximum bubble-pressure required for the formation of the bubbles at the surface of the gas distributor.
ΔP_D	$\Delta P_f + \Delta P_o$
Q	volumetric flow rate
Q_B	bubble phase flow rate
Q_i	interstitial flow rate
R	column radius
r	distance from the centre of the column
r_c	rate of chemical reaction, (moles/time-volume)
S	source term
t	time
t_r	reduced time
u	velocity
u_{bs}	bubble swarm velocity, bubble rise velocity
U_{sg}	Average superficial gas velocity
u_{sg}	superficial gas velocity
u_{sl}	superficial liquid velocity

u_{tg}	true gas velocity
u_{tl}	true liquid velocity (See page 105)
u_s	slip velocity or relative velocity
u_∞	rise velocity of a single bubble in an infinite media
u_{slc}	superficial liquid velocity at the centre of the column
u_{slw}	superficial liquid velocity near the wall
u_d	downward liquid velocity
V	volume
V_b	bubble volume
x	position of measuring point
x	longitudinal distance
X	dimensionless Lockhart-Martinelli parameter
Z	length of Column
α	factor accounting for departure from vertical rise of bubbles
γ	surface tension
$\delta(t)$	Dirac's delta function
Δ	difference
ε	fractional gas holdup
η	slip ratio
μ	viscosity
ρ	density
σ	variance
τ	residence time
ϕ	Lockhart-Martinelli parameter

superscripts

l	liquid phase
g	gas phase

REFERENCES

1. Nicklin, D.J. , Chem. Engng Sci., 19, 693 (1962).

2. Hughmark, G.A. and Pressburg, B.S., A.I.Ch.E. Jl 7, 677 (1961).

3. Wallis, G.B., Trans. Am. Soc. mech. Engrs. Heat Trans.Conference, 319 (1961/2).

4. Kim, D.S., Baker, C.G.J. and Bergougnon, Can. J. Chem. Engng, 50, 695, (1972).

5. Reith, T., Renken, S. and Israël, B.A., Chem. Engng Sci., 23, 619, (1968).

6. Towell, G.D., Strand, C.P. and Ackerman, G.H., A.I. Ch.E. – I. Chem. E.Symposium series No.10 (1965).

7. Downie, J. McC., Ph.D. thesis, University of Aston (1972).

8. Perkins, N.C., Yusuf, M. and Leppert, G., Nucl.Sci.Engng., 1, 525 (1960).

9. Neal, L.G. and Bankoff, S.G., A.I.Ch.E.Jl 9, 490 (1963).

10. Lockhart, R.W. and R.C. Martinelli, Chem. Engng. Prog., 45, 39, (1949).

11. Chisholm, D. and Laird, A.D.K., Trans. Am. Soc. mech.Engrs, 80, 276 (1958).

12. Scott, D.S., Adv. chem. Engng, 4, 199 (1963).

13. Bankoff, S.G., Trans. Am. Soc. mech. Engrs., C82, 265 (1960).

14. Bankoff, S.G. and Nassos, G.P., Chem. Engng Sci., 22, 661 (1967).

15. Nicklin, D.J., Wilkes, J.O. and Davidson, J. F., Trans. Instn. chem. Engrs., 40, 61 (1962).

16. Hughmark, G.A., Chem. Engng. Prog. 58, 62 (1962).

17. Brown, R.W., Gomezplata, A. and Price, J.D., Chem. Engng Sci., 24, 1483 (1969).

18. Fair, J.R., Chem. Engng., 74, 67 (1967).

19. Turner, J.C.R., Chem. Engng Sci., 21, 971 (1966).

20. Lehrer, I.H., Ind. Engng. Chem., Process Design Develop. 10, 37, (1971).

21. Freedman, W. and Davidson, J.F., Trans. Instn. chem. Engrs., 47, T251 (1969).

22. Gomezplata, A. and Nichols, C.R., Chem. Engng., 74, 182 (1967).

23. Mashelkar, R.A., Br. chem. Engng., 15, 1297 (1970).

24. Hughmark, G.A., Ind. Engng. Chem., Process Design Develop., 6, 218 (1967).

25. Bhaga, D. and Weber, M.E., Can. J. chem. Engng., 50, 323 (1972).

26. Akita, K. and Yoshida, F., Ind. Engng. Chem., Process Design Develop., 12, 76 (1973).

27. Kunugita, E., Ikura, M. and Otake, T., J. Chem. Eng. Jap., 3, 24, (1970).

28. Argo, W.B. and Cova, D.R., Ind. Engng. Chem., Process Design Develop., 4, 352 (1965).

29. Fair, J.R., Lambright, A.J. and Andersen, J.W., Ind. Engng. Chem., Process Design Develop., 1, 34 (1962).

30. Bischoff, K.B. and Phillips, J.B., Ind. Engng. Chem. Process Design Develop., 5, 416 (1966).

31. Yoshida, F. and Akita, K., A.I.Ch.E. Jl , 11, 9 (1965).

32. Ellis, J.E. and Jones, E.L., Two-phase Flow Symp., Exeter, 2, B102 (1965).

33. Kato, Y. and Nishiwaki, A., Int. Chem. Eng., 12, 182 (1972).

34. Østergaard, K. and Michelsen, M.L., Symp. on Fundamental and Applied Fluidization, Tampa, Florida, May (1968).

35. Shulman, H.L. and Molstad, M.C., Ind. Engng. Chem., 42, 1058 (1950).

36. Aoyama, Y., Ogushi, K., and Kubota, H., J. chem. Eng. Jap., 1, 158 (1968).

37. Braulick, W.J., Fair, J.R. and Lehrer, B.J., A.I.Ch.E. Jl., 11, 73 (1965).

38. Kato, Y., Nishiwaki, A. Fukuda, T. and Tanaka, S., J. chem.Eng. Jap., 5, 112 (1972).

39. Imafuki, K., Want, T., Koide, K. and Kubota, H., J. chem. Eng. Jap., 1, 153 (1968).

40. Morris, G.G., Ph.D. thesis, University of Aston (1972).

41. Akita, K. and Yoshida, F., Ind. Engng. Chem., Process Design Develop., 13, 84 (1974).

42. Valentin, F.H.H., Absorption in Gas-Liquid Dispersions, E & F.N. Spon Ltd. (1967).

43. Kutateladze, S.S. and Slyrikovich, M.A., Hydraulics of Gas-Liquid systems, Liaison Office, Technical Information Center, Wright-Patterson Air Force Bases, Ohio (1960).

44. Hobbs, S.Y. and Pratt, C.F., A.I.Ch.E. Jl , 20, 178 (1974).

45. Calderbank, P.H., Chem. Engr., 203, CE209 (1967).

46. De Nevers, N., A.I.Ch. E. Jl , 14, 222 (1968).

47. Rietema, K. and Ottengraf, S.P.P., Trans. Instn. chem. Engrs. 48, T54 (1970).

48. Donders, A.J.M., Wijffels, J.B. and Rietema, K., Proceedings of the Fourth European Symposium on Chemical Reaction Engineering, Brussels, 159 (1968).

49. Wijffels, J.B. and Rietema, K., Trans. Instn. chem. Engrs., 50 224, (1972).

50. Handley, D., Doraismy, A., Butcher, K.L. and Franklin, N.L., Trans. Instn. chem. Engrs., 44, T.260 (1966).

51. Whitehead, A.B. and Young, A.D. In Drinkenburg, A.A.H. (Ed). Proceedings of the International Symposium on Fluidization, Netherland, University Press, Amsterdam (1967).

52. Crabtree, J.R. and Bridgewater, J., Chem. Engng Sci., 24, 1755, (1969).

53. Rowe, P.N., Fluidization, Edited by Davidson, J.F. and Harrison, D., Academic Press (1971).

54. Letan, R. and Kehat, E., A.I.Ch. E. Jl , 14, 398 (1968).

55. Letan, R. and Kehat, E., A.I.Ch.E. Jl , 16, 955, (1970).

56. Kehat, E. and Letan, R., A.I.Ch.E. Jl , 17, 984 (1971).

57. Yeheskel, J. and Kehat, E., Chem. Engng Sci., 26, 1223 (1971).

58. Yeheskel, J. and Kehat, E., A.I.Ch.E. Jl , 19, 720 (1973).

59. Grace, J.R., A.I.Ch.E. Jl , Symp. Series No.116, 67, 159, (1971).

60. Toei, R., A.I.Ch.E.J. Symp.Series No.128, 69, 18 (1973).

61. Rowe, P.N., Proceedings of the Fifth European/Second International Symposium on Chemical Reaction Engineering, Amsterdam, A 9 - 1 (1972).

62. Hills, J.H., Trans. Instn. chem. Engrs., 52, 1 (1974).

63. Levenspiel, O. and Bischoff, K.B., Adv. chem. Engng , 4, 95 (1963).

64. Levenspiel, O. and Smith, W.K., Chem. Engng Sci., 6, 227 (1957).

65. Bischoff, K.B., Chem. Engng Sci., 12, 69 (1960).

66. Bischoff, K.B. and Levenspiel, O., Chem. Engng Sci., 17, 257, (1962).

67. Mixon, F.O., Whitaker, D.R. and Orcutt, J.C., A.I.Ch.E.Jl,13, 21 (1967).

69. Østergaard, K. and Michelsen, M.L., Can. J. chem. Engng. 47, 107 (1969).

70. Michelsen, M.L. and Østergaard, K., Chem. Eng. Jl, 1, 37 (1970).

72. Michelsen, M.L. and Østergaard, K., Chem. Engng Sci.,25, 583 (1970).

73. Boyadzhiev, L. and Atarasova, E., Theo. Found. chem. Eng., 3, 326 (1969).

74. Towell, G.D. and Ackerman,, Proceedings of the Fifth European/ Second International Symposium on Chemical Reaction Engineering, Amsterdam B3-1 (1972).

75. Ohki, Y. and Inoue, H., Chem. Engng Sci., 25, 1 (1970).

76. Siemes, W. and Weiss, W., Chemie-Ingr-Tech, 29, 727 (1957).

77. Tadaki, T. and Maeda, S.,Chem. Engng. Tokyo, 2, 195 (1964).

78. Eissa, S.H and El-halwagi, M.M., Ind. Engng. Chem. Process Design Develop., 10, 311 (1971).

79. Eissa, S.H. and El-halwagi, M.M., Genie chim., 104, 2080 (1971).

80. Deckwer, W., Graeser, U., Langemann, H. and Serpemen, Y., Chem. Engng Sci., 28, 1223, (1973).

81. Fidgett, M., Ph.D. thesis, University of Aston (to be published).